

THE REACTIONS OF $O(2^1D)$ and $OH(X^2\Pi)$
WITH HALOGEN CONTAINING MOLECULES

JOHN GARRAWAY

Ph.D.
University of Edinburgh
1981



To
J.A. and S.P. Garraway

DECLARATION

Except where due reference is made, the material presented in this thesis is my original work. Certain aspects of this work have been published

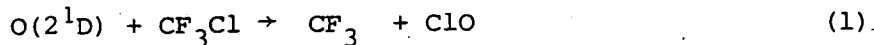
Date...7/12/80.....

Signed
John Garraway

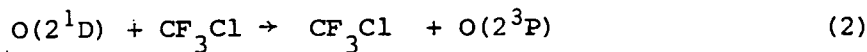
SUMMARY

The reactions of O(2¹D) with CFCl₃, CF₂Cl₂, CF₃Cl and CF₂HCl have been investigated using flash photolysis and time resolved kinetic spectroscopy.

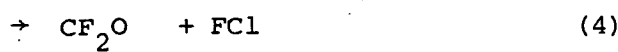
The dominant reaction (~ 50%) is Cl atom abstraction



while quenching of O(2¹D) to O(2³P) accounts for about 25% of the reaction cross section



Reactions (3) and (4) were found to be minor channels

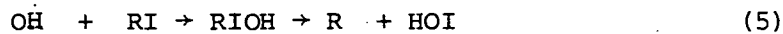


The branching ratios into reaction (1) to (4) were similar for all the molecules investigated.

The reaction mechanism is discussed in terms of a singlet CF₃ClO species which may fragment to give either reaction (1) or (2).

The reactions of OH were investigated using flash photolysis with resonance absorption. New data are reported for the reaction of OH with CD₂Cl₂ and CDCl₃.

Rate data for the novel reactions of OH with CF₃I, C₂F₅I, C₃F₇I and Cl₂ are presented. This reaction is thought to proceed via a RIOH (Cl₂OH) complex to yield R and HOI (Cl and HOCl).



Evidence is presented to indicate a rapid reaction between OH and ClO, $k \approx 3.5 \times 10^{-12} \frac{cm^3}{molec \cdot s}$. This reaction displays a pressure dependency and is considered to proceed by reaction (6) or (7) or both.



V

ACKNOWLEDGEMENTS

I should like to thank Professor R.J. Donovan for his advice, interest and encouragement during the course of my research.

I thank Dr.H.Gillespie and Dr.G.Black who contributed to the work on the reactions of O(2¹D) with chlorofluorocarbons, and also Mr.M.Addison for his useful advice on the setting up of the OH resonance absorption apparatus.

I thank Professor C.Kemball for his support and provision of laboratory facilities and the Science Research Council for financial support.

C O N T E N T S

	<u>Page</u>
Abstract	
Chapter 1. Introduction	
1.1 Introduction	2
1.2 Experimental techniques	2
1.3 Properties of O(2 ¹ D)	3
1.4 The reaction of O(2 ¹ D) with CH ₄	4
1.5 Effect of translational energy on the reactions of O(2 ¹ D)	6
1.6 Reactions of OH	7
Chapter 2. Experimental techniques	
2.1 Introduction	9
2.2 Flash photolysis with time resolved kinetic spectroscopy	9
2.3 Detection and processing results	12
2.4 Computer modelling of flash profile	14
2.5 Flash photolysis with kinetic spectroscopy	16
2.6 OH emission lamp and detection of OH	16
2.7 Analysis of results	20
2.8 Gas handling	22
Chapter 3. Reaction of O(2 ¹ D) with CF ₃ Cl, CF ₂ Cl ₂ and CFC1 ₃	
3.1 Introduction	25
3.2 Experimental	27
3.3 Reaction of O(2 ¹ D) with CF ₂ Cl ₂ and CFC1 ₃	29
3.4 Secondary growth of ClO	40
3.5 O ₃ depletion	41
3.6 Reaction of O(2 ¹ D) with CF ₃ Cl	42
3.7 Decay of ClO and formation of OClO	44

	<u>Page</u>
Chapter 4. Reaction of O(2 ¹ D) with CF ₂ HCl	
4.1 Introduction	52
4.2 Experimental	52
4.3 Results and discussion	53
4.4 Effect of translational energy of O(2 ¹ D) on the CF ₂ yield	59
4.5 Decay of CF ₂	60
4.6 Decay of CF ₂ in the presence of O ₂	62
4.7 Reaction of CF ₂ with O ₃ , O ₂ (¹ Δ) and O(2 ³ P)	65
Chapter 5. Reaction of O(2 ¹ D) with CF ₂ ClBr and CF ₃ Br and discussion on the reaction of O(2 ¹ D) with halomethanes	
5.1 Reaction of O(2 ¹ D) with CF ₂ ClBr and CF ₃ Br	67
5.2 Discussion	72
5.3 Conclusion	78
Chapter 6. Reaction of OH with CHCl ₃ , CH ₂ Cl ₂ , CD ₂ Cl ₂ and NH ₃	
6.1 Introduction	80
6.2 Experimental	80
6.3 Results and discussion	83
6.4 Isotope effects in the reactions of OH with CHCl ₃ /CDCl ₃ and CH ₂ Cl ₂ /CD ₂ Cl ₂	92
6.5 Correlation of H donor dipole moment with rate of reaction with OH	94
6.6 Yield of OH from the reaction of O(2 ¹ D) with NH ₃	96
6.7 Conclusion	98
Chapter 7. Reaction of OH with CH ₃ I, CF ₃ I, C ₂ F ₅ I, C ₃ F ₇ I and Cl ₂	
7.1 Introduction	100
7.2 Reaction of OH with CH ₃ I, CF ₃ I, C ₂ F ₅ I and C ₃ F ₇ I	101
7.3 Nature of reaction products	106
7.4 Reaction of OH with Cl ₂	109
7.5 Conclusion	111

	<u>Page</u>
Chapter 8. Reaction of OH with ClO	
8.1 Introduction	113
8.2 Results	114
8.3 Nature of reaction of OH with ClO	120
8.4 Discussion	126
8.5 Conclusion	128
Appendix 1	129
Appendix 2	130
Appendix 3	131
References	133
Addendum	143
Published work	144

LIST OF FIGURES

	<u>Page</u>	
Figure 2.1	Apparatus for flash photolysis with time resolved kinetic spectroscopy	10
Figure 2.2	Simulation of O ₃ removal profile	15
Figure 2.3	Apparatus for monitoring the OH emission	17
Figure 2.4	Arrangement of flow lamp	18
Figure 2.5	OH emission spectrum	19
Figure 2.6	Photomultiplier circuit diagram	21
Figure 3.1	Formation of ClO following the reaction of O(2 ¹ D) with CF ₂ Cl ₂	30
Figure 3.2	Temporal development of ClO following the reaction of O(2 ¹ D) with CFCl ₃	31
Figure 3.3	Temporal development of ClO in the O ₃ /CF ₂ Cl ₂ /C ₂ H ₆ system	32
Figure 3.4	Temporal development of ClO in the O ₃ /CFCl ₃ /C ₂ H ₆ system	33
Figure 3.5	Extrapolation of ClO decay to estimate amount of ClO removed	35
Figure 3.6	Evaluation of amount of ClO removed in Figure 3.6	36
Figure 3.7	Temporal development of ClO and OClO in the O ₃ /CF ₃ Cl system	42
Figure 3.8	Temporal development of ClO in the O ₃ /CF ₃ Cl/C ₂ H ₆ system	43
Figure 3.9	Temporal development of ClO and OClO in the O ₃ /CF ₃ Cl system	46
Figure 4.1	Temporal development of CF ₂ in the O ₃ /CF ₂ HCl system	54
Figure 4.2	Temporal development of ClO in the O ₃ /CF ₂ HCl system	55
Figure 4.3	Decay of CF ₂ in the presence of ClO	61
Figure 4.4	Decay of CF ₂ in the presence of O ₂	64

	<u>Page</u>	
Figure 5.1	Temporal development of BrO and OClO in the O_3/CF_2HCl system	68
Figure 5.2	Temporal development of BrO in the O_3/CF_3Br system	71
Figure 5.3	Potential energy diagram for the reaction of $O(2^1D) + RCl$	76
Figure 5.4	Potential energy diagram for the reaction of $O(2^1D)$ and $O(2^3P)$ with RI	76
Figure 6.1	Plot of $\log(I_0/I)$ against $P(O_3)$	82
Figure 6.2	Trace of OH decay in the presence of NH_3	84
Figure 6.3	First order plots of the decay of OH in the presence of NH_3	85
Figure 6.4	Plot of first order decay constants of OH against NH_3 pressure	86
Figure 6.5	Plot of first order OH decay rates against CCl_3X pressure	87
Figure 6.6	Plot of first order OH decay rates against CCl_2X_2 pressure	88
Figure 6.7	Plot of \log (rate of reaction of OH with X) against dipole moment of X	95
Figure 6.8	Yield of OH from $O(2^1D) + H_2O$, and $O(2^1D)$ $+ NH_3$	97
Figure 7.1	Decay of OH in the presence of C_2F_5I	102
Figure 7.2	Plot of rate of OH decay against CF_3I , and CH_3I pressure	103
Figure 7.3	Plot of rate of OH decay against C_2F_5I and C_3F_7I pressure	104
Figure 7.4	Plot of \log of rate of reaction of OH with RI against $D(R-I)$	108
Figure 7.5	Plot of rate of OH decay against Cl_2 pressure	110
Figure 8.1	Trace of OH decay in the presence of ClO	115
Figure 8.2	Plot of first order decay of OH against O_3 in the $O_3/CF_2Cl_2/H_2O$ system	116
Figure 8.3	Plot of first order decay of OH against O_3 in the O_3/H_2O system	119
Figure 8.4	Plot of experimental and simulated first order decay of OH against O_3 pressure	122
Figure 8.5	Plot of second order rate constant for OH $+ ClO$ versus pressure of He or SF_6	124
Figure 8.6	Plot of second order rate constant for OH + ClO versus pressure of He or SF_6	125

LIST OF TABLES

	<u>Page</u>	
Table 3.1	Best fit computer simulation of the reaction of $O(2^1D)$ with CF_2Cl_2	38
Table 3.2	Best fit computer simulation of the reaction of $O(2^1D)$ with $CFCl_3$	38
Table 3.3	Product branching ratios for the reactions of $O(2^1D)$ with CF_3Cl , CF_2Cl_2 and $CFCl_3$	
Table 3.4.	Best fit computer simulation of $O(2^1D)$ with CF_3Cl	45
Table 3.5	Literature values for the reaction of $ClO + ClO + M \rightarrow Cl_2O_2 + M$	47
Table 4.1	List of branching ratios for the reaction of $O(2^1D) + CF_2HCl$	56
Table 4.2	First order rate constants of CF_2 decay and ClO concentration	63
Table 5.1	Best fit computer simulation of the reaction of $O(2^1D)$ with CF_2ClBr	70
Table 5.2	Branching ratios for the reaction of $O(2^1D)$ with CF_3Cl , CF_2Cl_2 , $CFCl_3$, CF_2HCl , CH_3Cl and CCl_4	73
Table 6.1	Rate of reaction of OH with NH_3 , $CHCl_3$, $CDCl_3$, CH_2Cl_2 and CD_2Cl_2	89
Table 6.2	Equations used in the simulation of the $OH + NH_3$ reaction	91
Table 7.1	Rate constants for $OH + RI$ and $OH + Cl_2$	105
Table 7.2	Rate of reaction of $O(2^3P)$ and OH with CH_3X and CF_3X	107
Table 7.3	Calculated activation energies for $OH + RI$	107
Table 8.1	Rates of reaction of $O(2^1D)$ with H_2O and CF_2Cl_2 , and yields of ClO	118
Table 8.2	Rates of reaction of $OH + ClO$	123

CHAPTER ONE

INTRODUCTION

1.1 Introduction:

The reactions of electronically excited oxygen atoms, $O(2^1D)$, and of $OH(X^2\Pi)$ have been the subject of a great many experimental studies. This has been stimulated by the importance of these species to atmospheric chemistry. The reactions of $O(2^1D)$ have been well reviewed^{1,2,3,4,5}, and only certain aspects of $O(2^1D)$ chemistry relevant to the work presented here will be discussed. In particular the reactions of $O(2^1D)$ with methane and the alkanes will be surveyed in detail, and will serve as a basis for the discussion of the reaction of $O(2^1D)$ with chlorofluorocarbons and hydrogen containing chlorofluorocarbons.

In the latter part of this chapter certain aspects of OH chemistry will be presented.

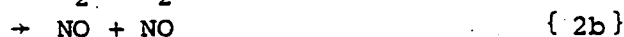
1.2 Experimental techniques

Absolute rate data for the deactivation of $O(2^1D)$ by a wide range of compounds have been obtained by Davidson *et al*^{6,7,8}, who monitored the weak $O(2^1D \rightarrow 2^3P)$ emission at 630 nm following the photolysis of O_3 . Husain⁹⁻¹¹ obtained absolute rate data by following the absorption of the $O(3^1D \leftarrow 2^1D)$ line at 115 nm, also after the photolysis of O_3 .

Relative rate data have been obtained from competitive experiments.

The first detailed work of this kind was done by Cvetanovic and Yamazaki^{12a}, who photolysed N_2O to obtain $O(2^1D)$.

In the absence of any quenching {2} rapidly follows {1}



where $k_{\{2a\}} / k_{\{2b\}}$ is close to unity (section 5).

The yield of N_2 , ϕ_{N_2} , per quantum of light absorbed is then 1.5.

In the presence of some quencher of $O(2^1D)$ {2a} and {2b} do not occur, and ϕ_{N_2} is 1.0, and hence by varying the pressure of the quencher relative rate data have been obtained. Such rate data are normally expressed relative to CO_2 ^{12b}.

Reference 3 contains a compilation of such data.

1.2 cont'd

These techniques only provide information on the overall rate of $O(2^1D)$ deactivation and are complemented by studies of the reaction products. Steady state photolysis with gas-liquid chromatography and mass spectrometric analysis has been extensively used, for example, by Cvetanovic and Yamazaki^{12c} in the study of $O(2^1D)$ reacting with alkanes.

Much information on the reaction products has been provided by flash photolysis of a suitable $O(2^1D)$ precursor coupled to suitable detection methods, for example plate photometry¹³, or the study of chemical laser emission^{14,15}.

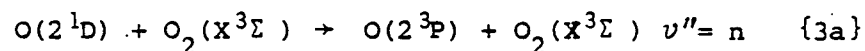
The rates of removal of $OH(X^2\Pi)$ radicals have been studied in discharge flow systems, where OH was monitored by laser magnetic resonance¹⁶, or by resonance fluorescence ($OH(A^2\Sigma \rightarrow X^2\Pi)$) near 308 nm^{17,18,19}. Rate data have also been obtained from flash photolysis with resonance fluorescence²⁰ or resonance absorption detection of OH ^{21,22}.

Pulse radiolysis of water vapour with resonance absorption detection of OH has been utilised by Gordon and Mulac²³.

1.3 Reactions of $O(2^1D)$

$O(2^1D)$ is the first excited state of the oxygen atom lying some $15,868 \text{ cm}^{-1}$ ²⁴ above the ground state $O(2^3P)$. The long radiative lifetime ($t_{\lambda} = 100 \text{ s}$) of the $O(2^1D \rightarrow 2^3P)$ transition indicates that radiative decay will be of little significance compared to collisional removal under laboratory conditions.

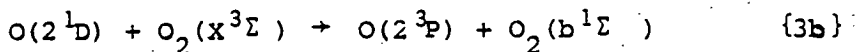
The reactions of $O(2^1D)$ with the noble gases, O_2 , N_2 , N_2O and CO_2 have been reviewed¹. These reactions generally proceed via complex formation, viz



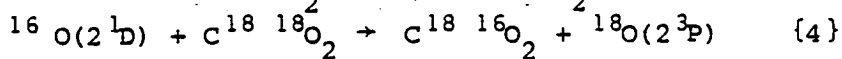
with formation of O_2 in $v'' = 13, 14, 15$. The electronic excitation energy of $O(2^1D)$ is only sufficient to populate up to $v'' = 10$, and it has been postulated that the translational energy of $O(2^1D)$ is also transferred. This would require a long lived complex (O_3) with triplet-singlet crossing occurring many times.

1.3 cont'd

Reaction {3b} competes with {3a}



Evidence for complex formation in these reactions is found in the isotopic scrambling of O atoms observed in the reaction of O(2¹D) with CO^{12b,25,26} and O₂²⁶.

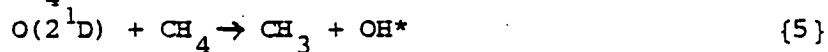


Reaction of O(2¹D) with H₂ has been shown to proceed via a HOH* complex²⁷, that is by insertion, although abstraction is an allowed process.

The overall rate constants for O(2¹D) removal⁶⁻¹¹, are generally close to gas kinetic collision frequency; this and the experimentally observed lack of significant temperature dependence indicate that there is no early barrier to reaction. Tully²⁸ has calculated rate constants, product branching ratios and temperature dependencies, which are generally in good agreement with the experimental results.

1.4 The reaction of O(2¹D) with methane and the higher alkanes

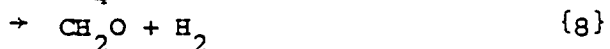
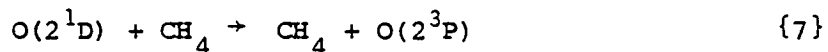
The reaction of O(2¹D) with CH₄ was first studied by Basco and Norrish¹³, who observed OH (v < 2) formation following the flash photolysis of O₃ in the presence of CH₄. They suggested the major reaction was



De More and Raper²⁹ photolysed O₃ / CH₄ mixtures at liquid Ar temperatures, and proposed that insertion {6a} was the major process accounting for about 37% of the reaction cross section.



They also found evidence for quenching {7} (30%) molecular elimination {8} (5%) and OH formation (28%)



and suggested that {5} may occur, in part at least, through the fragmentation of the excited methanol.

1.4 cont'd

Cvetanovic *et al* studied the reactions of $O(2^1D)$ with propane^{12c}, isobutane^{30a}, neopentane^{30b} and cyclopentane³¹. In this study N_2O was photolysed to yield $O(2^1D)$, and the products detected by gas-liquid chromatography and mass spectrometry. The branching ratios into {5} to {8} were found to be approximately constant for the different alkanes. Insertion into a C-H bond to form an excited alcohol was observed to be the dominant channel ($\approx 60\%$). Insertion occurred in a statistical manner, showing no preference for tertiary, secondary or primary bonds. The alcohols formed in {6} could be stabilised if the pressure was sufficiently high. The lifetimes of these excited alcohols were measured as ranging from 10^{-12} s for methanol to 10^{-9} s for neopentanol, the increase being due to the greater number of degrees of freedom in the higher alcohols. The alcohols fragmented to yield R and OH. OH formation was observed at pressures sufficiently high to completely stabilise the excited alcohols indicating the occurrence of {5}, that is H atom abstraction. This was estimated to have a branching ratio of 20 - 30%.

Butene³² was used to scavenge $O(2^3P)$, and from measurements of the products of this reaction, quenching of $O(2^1D)$ by alkanes was estimated at $< 2\%$. Reaction {8} was found to occur to a small extent, $< 3\%$ (but 9% for neopentane). Cvetanovic also observed a correlation between the rate of removal of $O(2^1D)$ by an alkane and the number of C-H bonds possessed by that alkane.

Lin and De More³³ in a similar study of the reaction of $O(2^1D)$ with CH_4 and C_2H_6 , obtained essentially similar results, and showed that {8} was an independent pathway and not a break up product of the excited alcohol.

1.4 cont'd

OH formation may occur at long range interactions of $O(2^1D)$ and RH and should occur with all alkanes with approximately constant probability. . The large rate constant for overall removal of $O(2^1D)$ by CH_4 and the approximately constant branching ratios found by Cvetanovic support this contention . At smaller impact parameter collisions insertion to give ROH (corresponding to a minimum on the potential surface) will occur, but the complex will have enough energy to fragment unless it is stabilised by collision . It is likely that {8} occurs at very small impact parameter collisions , where the energy of the incoming $O(2^1D)$ is channeled directly into C-H motion, and leads to concerted elimination of H_2 .

The mechanism of the reaction of $O(2^1D)$ with alkanes has recently been investigated in some detail by Luntz and this work is discussed on page 143.

1.5 Effect of translational energy on the reactions of $O(2^1D)$

There is considerable interest in whether the translational energy of $O(2^1D)$ has any effect on the reaction dynamics .

Most of the work in this field has been done on the reaction of $O(2^1D)$ with N_2O , which can proceed by two pathways .



Quenching is insignificant (< 2 %) . The ratio of $k_{\{2a\}}$ to $k_{\{2b\}}$ has been the subject of several determinations and is about unity ³⁴ . Although some authors claim to have found that the ratio is dependent on the translational energy of $O(2^1D)$ ³⁴ , the balance of the evidence tends to suggest otherwise . The experimental results have been reviewed by Marx , Bahe and Schurath ³⁴ .

Overend *et al* ³⁵ extended their studies to the reactions of $O(2^1D)$ with CO_2 , Xe , CO and N_2 and again found no evidence that the reaction products were affected by the translational energy of $O(2^1D)$.

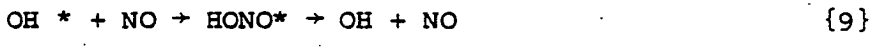
1.6 OH reactions

The rates of reaction of OH with methane and chlorofluorobromomethanes have been measured by Howard ¹⁶ and by Clyne ¹⁹ . These reactions have been shown to proceed by H atom abstraction , and no reaction is observed with fully halogenated methanes . Howard ^{16b} has observed a correlation between the rate of H atom abstraction by OH from a halomethane and halomethane C-H bond strength .

Deuterium isotope effects have been reported by Smith and Zellner ³⁶ for the reaction of OH with H₂/D₂ and HCl/DCl , and by Gordon and Mulac ²³ for the reaction of OH with CH₄ , CH₃D , CH₂D₂ , CHD₃ and CD₄ .

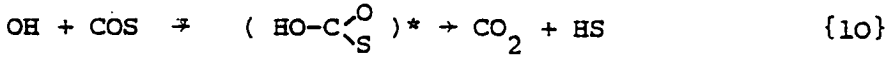
The reaction of OH with alkenes proceeds by addition to the alkene .

The reactions of OH with radical species have not been extensively investigated due to the experimental problems , but combination of OH with OH , NO and NO₂ ³⁸ to yield H₂O₂ , HONO and HNO₃ has been shown to occur . Smith ³⁹ has recently shown that quenching of OH (v = 1) by NO and NO₂ proceeds by an intermediate complex e.g.



The rate of quenching of OH (v = 1) by NO and NO₂ is similar to the high pressure limiting value for the combination of OH with these species .

Complex formation has been invoked to explain the reaction of OH with COS and CS₂ ⁴¹



Evidence for such complex formation has been obtained by Kurylo who observed isotopic scrambling in the reaction of ¹⁸OH with CO₂ . A similar mechanism has been postulated for the reaction of OH with CO , this will be discussed in chapter 8 ⁴⁰

CHAPTER TWO

EXPERIMENTAL TECHNIQUES

2.1 Introduction.

Flash photolysis, originally developed by Porter and Norrish⁴³ has become one of the most useful and versatile techniques for the study of excited states. In this study two adaptations of flash photolysis have been used, flash photolysis with time resolved kinetic spectroscopy and flash photolysis with kinetic spectrophotometry. The first is useful when investigating a reaction for the first time, as it provides information on the nature of the reaction products. This technique was used to study the reaction of $O(2^1D)$ with chlorofluorocarbons. For kinetic work, it has the disadvantage that many experiments must be done, to build up a complete concentration profile.

Flash photolysis with kinetic spectrophotometry, wherein the concentration of a species is followed by its absorption of light at some characteristic wavelength, has the advantage for kinetic studies of providing information over the whole decay in one experiment. This technique was used to study the reactions of OH radicals.

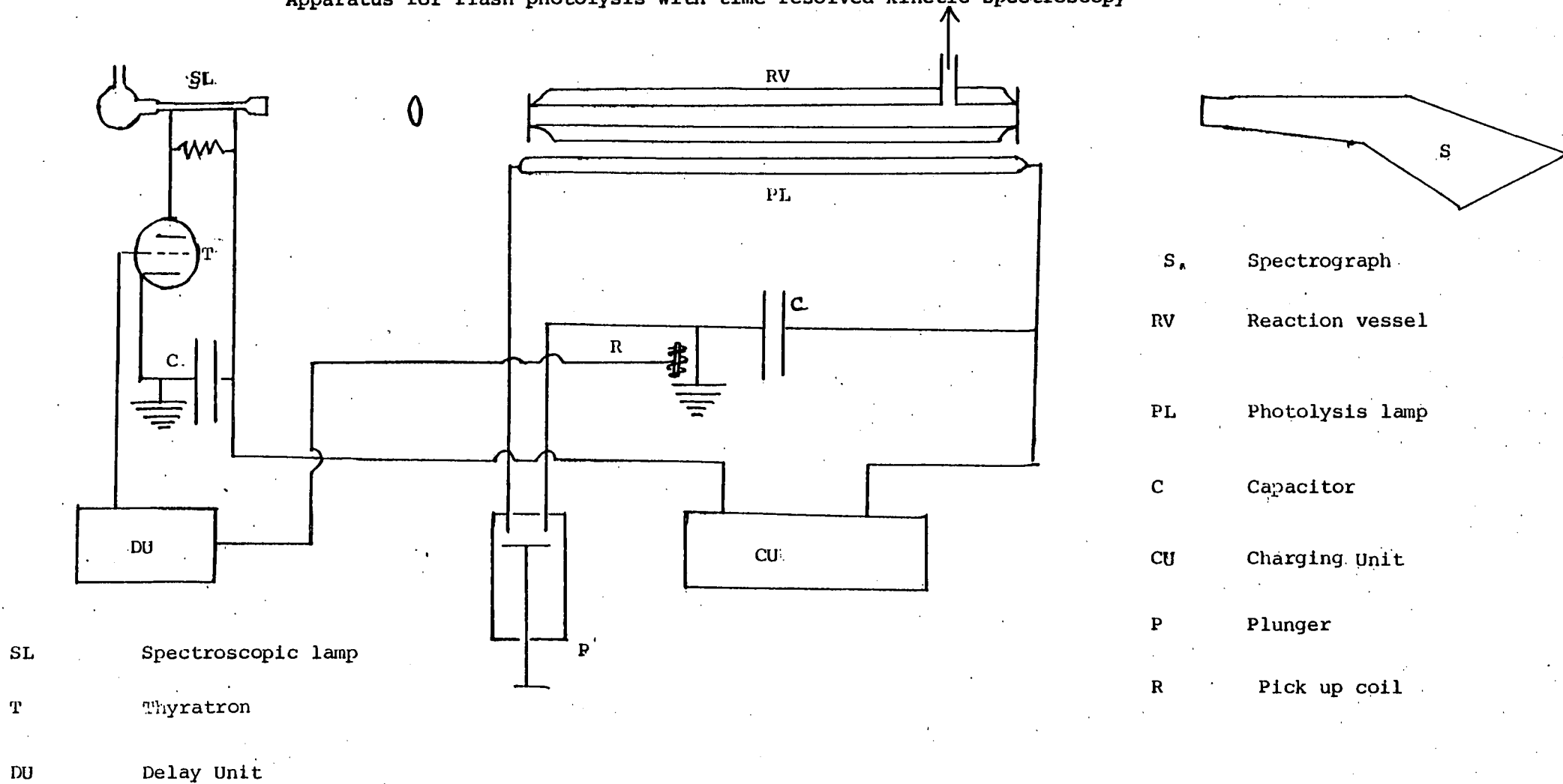
2.2 Flash photolysis with time resolved kinetic spectroscopy.

This technique has been well reviewed⁴⁴ and only a brief description will be given here. A diagram of the apparatus is shown in figure 2.1.

Reaction vessel.

Two reaction vessels were used in this study. The first was of quartz (length 1m, o.d. 2 cm), thus limiting photolysis to $\lambda > 200$ nm. Spectrosil windows were attached by epoxy resin.

Figure 2.1
Apparatus for flash photolysis with time resolved kinetic spectroscopy



2.2 cont'd.

The second was similar to the first, but had an outer quartz jacket (o.d. 5 cm) constructed such that the outer wall of the reaction vessel formed the inner wall of the jacket. This outer vessel could be filled with filter solutions or gases.

Flash lamp.

This was a 1m quartz flash lamp (o.d. 1.5 cm) filled with Kr to about 800 N m^{-2} . The flash lamp was discharged at 12 kV from a 10 μf capacitor dissipating 720 J. The lamp was fired by means of a low impedance mechanical plunger. Aluminium foil, wrapped around the flash lamp and reaction vessel, acted as a condenser to increase photolysis and to reduce scattered light.

Spectroscopic lamp.

This was a conventional quartz capillary tube. The discharge between the tungsten electrodes is mechanically pinched by a narrow quartz capillary (i.d. 1mm) resulting in a hot plasma and a good continuum emission. Continued flashing gradually increased the capillary diameter with a resultant loss in continuum emission. This necessitated replacing the capillary at regular intervals.

The spectroscopic lamp was fired in a similar manner to that of the photolysis lamp, except that electronic switching was used. When the capacitor was charged a 165 M Ω resistor in parallel with the lamp allowed both electrodes to go to a high potential.

The delay unit was triggered by a Regowski induction coil which picked up the current of the discharging photolysis lamp and after the pre-set delay sent a 100 V spike to the grid of the hydrogen thyatron. This allowed the thyatron to conduct, and the lamp to fire. The 1 μf capacitor was charged to 10 kV and dissipated 50 J. The delay and triggering circuit is shown in figure 2.1.

2.2 cont'd.

A second Regowski coil, coupled to a Tektronix type 549 oscilloscope, was used to check the time delay between the photolysis and spectroscopic flashes.

2.3 Detection and processing of results.

Spectra were dispersed on a Hilger Watts medium quartz spectrograph (slits $60 \mu\text{m} \times 3 \text{mm}$) and recorded on Kodak Panchro Royal film. Plates were developed for five minutes at 20°C in Ilford Contract FF developer, diluted 1 + 3.

A single quartz lens was used to focus the light from the spectroscopic lamp on to the slits of the spectrograph. Initial alignment of the reaction vessel, spectroscopic lamp and spectrograph was achieved with the aid of a helium neon laser.

Processing results.

The characteristic curve, or $D-\log(E)$ is a plot of optical density versus the logarithm of the exposure. For quantitative work, it is necessary to be in the linear region of the curve, scattered light from the photolysis flash normally being sufficient to take images into this region. At high optical densities plate saturation and non linearity occurs.

Plates were microdensitometered on a Joyce Loebel double beam recording microdensitometer mark 3. The absorbance is related to concentration by the relationship.

$$A = \gamma \cdot \log(I_0/I) = \gamma \cdot \log(E_0/E) = D - D_0, \text{ where}$$

A = absorbance

γ = slope of the linear part of the $D-\log E$ curve.

I and I_0 are the light intensities incident on the plate at some wavelength, with and without some absorbing species present. E and E_0 , D and D_0 are respectively the exposures and optical densities under the same conditions.

2.3 cont'd

If the Beer Lambert law is obeyed then ,

$$\log(I_0/I) = \epsilon.c.l , \text{ and thus}$$

$$D - D_0 = \gamma.\epsilon.c.l , \text{ where}$$

- c = concentration of absorber
- l = length over which absorption occurs
- ε = extinction coefficient

Hence optical density on the microdensitometer trace is proportional to concentration . γ was measured by the method of Basco⁴⁵ wherein the photographic plate is subjected to a series of exposures, each greater by a constant factor than that of the preceeding one ; and the resultant optical densities measured .

Beer Lambert law

The Beer Lambert law relates absorption and concentration of absorber by the expression

$$I = I_0.\exp(-\epsilon.c.l) \quad \text{or}$$

$$\log(I_0/I) = \epsilon.c.l$$

This may be more generally written as

$$\log(I_0/I) = (\epsilon.c.l)^\beta$$

where β is the Beer Lambert exponent and can vary from zero to one , the latter being the optimum value . Factors which affect β are the resolving power of the spectrograph or monochromator , and in kinetic spectrophotometry , doppler broadening and reversal of the emission line . β can be determined by masking off half of the reaction vessel and so halving l . β was so determined by Donovan and Gillespie⁴⁶ for ClO to be 1.01 ± 0.06 and so the Beer Lambert law was used without modification .

2.4 Computer modelling

The chemical kinetics simulation program CHEK , developed by Curtis and Chance ⁴² , is extensively used in this work to analyse the experimental results .

Input data are in natural free format language . Integration steps are taken by Gear's (1971) predictor corrector , which is suitable for stiff sets of differential equations . Data are printed out in tabular and graphical form . The program was run on an IBM system/360 or 370 computer .

As a considerable portion of the reaction occurs during and immediately after the flash , it was necessary to simulate accurately the photolysis flash profile . A subroutine , PatchD , using the following expression , simulated the flash intensity and profile .

$$I = A.t.\exp(-B.t)$$

where , I is the flash intensity at time t

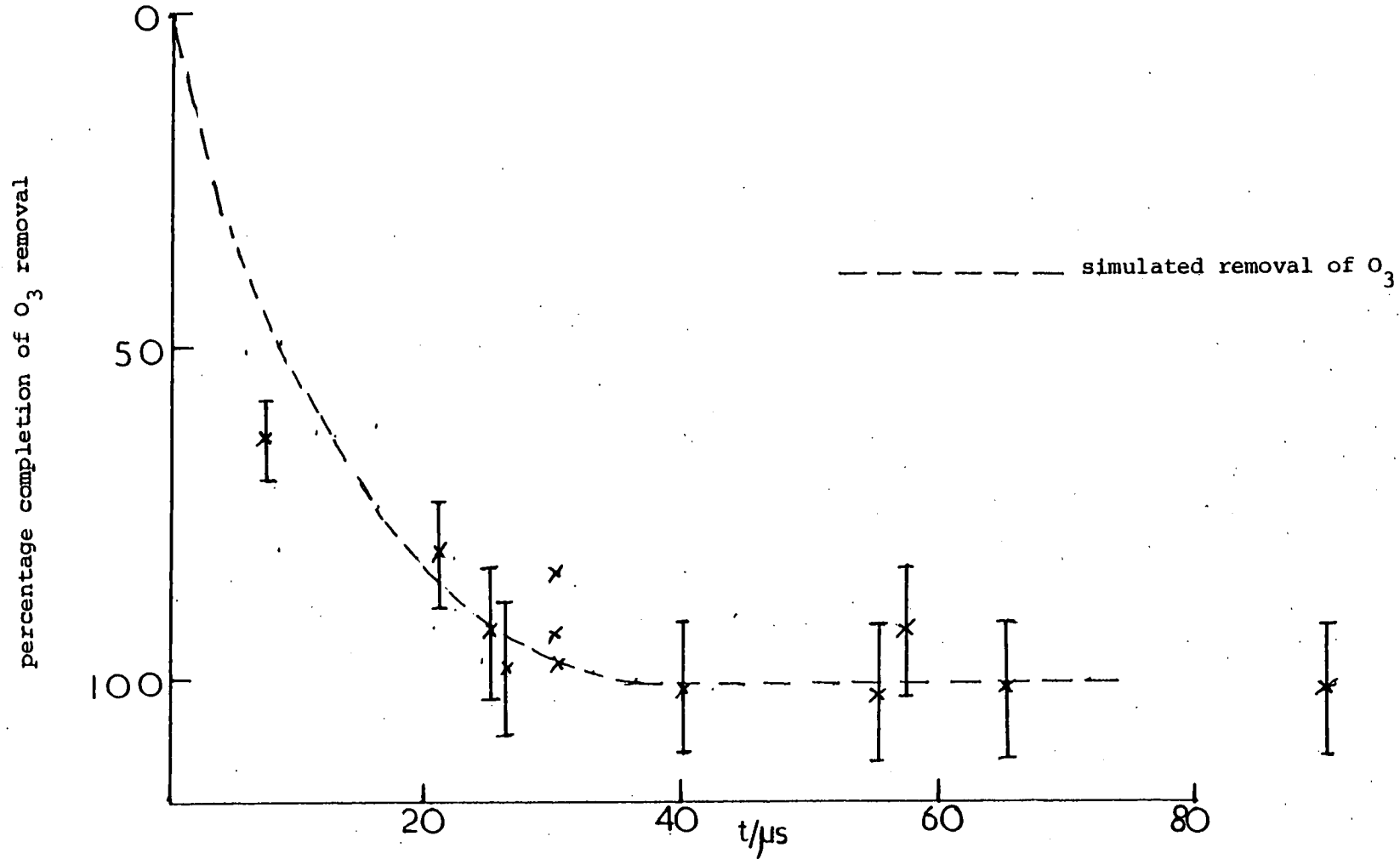
A is a constant

B is inversely proportional to the time at which the flash intensity is at a maximum .

The photolysis flash profile may be measured using a photomultiplier to record the light output . However a different approach was used here . It was assumed that the removal profile of O₃ during the flash photolysis of O₃/CO₂ (where removal is by photolysis alone) mirrors the flash intensity profile . The percentage completion of O₃ removal during the photolysis of O₃/CO₂ mixtures was plotted against time (figure 2.2) and A and B varied until the program simulated accurately the experimental results . The dotted line (figure 2.2) is the computer fit to the experimental data .

Figure 2.2

Simulation of the O_3 removal profile = flash profile in the O_3/CO_2 system



2.5 Flash photolysis with kinetic spectrophotometry

The experimental apparatus is essentially similar to that described by Smith and Morley²¹. A diagram of the apparatus is shown in figure 2.3.

The reaction vessel/photolysis lamp arrangement is identical to that described above (section 2). A 50 cm quartz reaction vessel (o.d. 2 cm) with spectrosil windows attached by epoxy resin was used. A coaxial outer quartz jacket (o.d. 5 cm) was filled to an atmosphere of Cl₂ to absorb scattered light in the region of the OH absorption. Parallel to the reaction vessel was a 50 cm quartz flash lamp (o.d. 1 cm) filled with Kr to about 800 N m⁻². The lamp was fired at 9 kV from a 2.5 μf capacitor by a plunger and dissipated 100 J. The capacitor was charged by an Applied Photophysics Ltd. power supply.

2.6 OH emission lamp and detection of OH

The kinetics of OH were followed by measuring the extent of absorption of the Q₁(3) line at 308.15 nm emitted by an OH flow lamp.

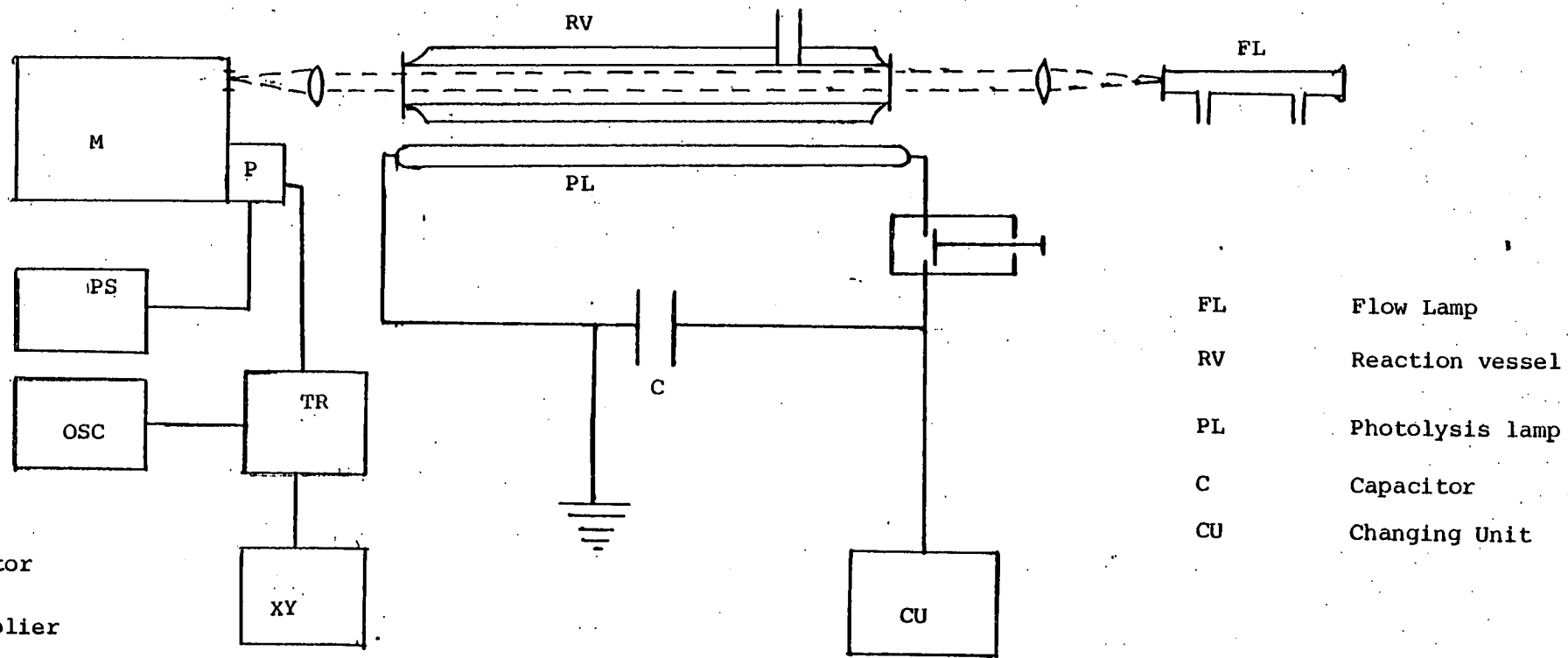
Resonance lamp

A strong OH (A²Σ → X²Π) emission was produced by passing argon containing a small percentage of water vapour through a microwave discharge. The flow system is shown in figure 2.4. The flow lamp (length 22 cm , o.d. 2 cm) was made of quartz and fitted with spectrosil windows. The lamp was powered by a Microtron 200 mk 2 microwave generator working at 70 watts incident power. The cavity was tuned to give the minimum reflected power, and the resulting discharge filled the entire tube. The emission spectrum is shown in figure 2.5, with an assignment of the various features, it is essentially similar to that reported by Carrington and Broida⁴⁷.

The monochromator was a McKee Pederson mp 1081B grating monochromator operated with a slit width of 60 μm.

Figure 2.3.

Apparatus for monitoring the OH ($A^2\Sigma + X^2\Pi$) absorption;



M, Monochromator
P Photomultiplier
TR Transient Recorder
PS Photomultiplier power supply
OSC Oscilloscope
XY XY Plotter

FL Flow Lamp
RV Reaction vessel
PL Photolysis lamp
C Capacitor
CU Changing Unit

Fig 2.4.

Arrangement of flow lamp

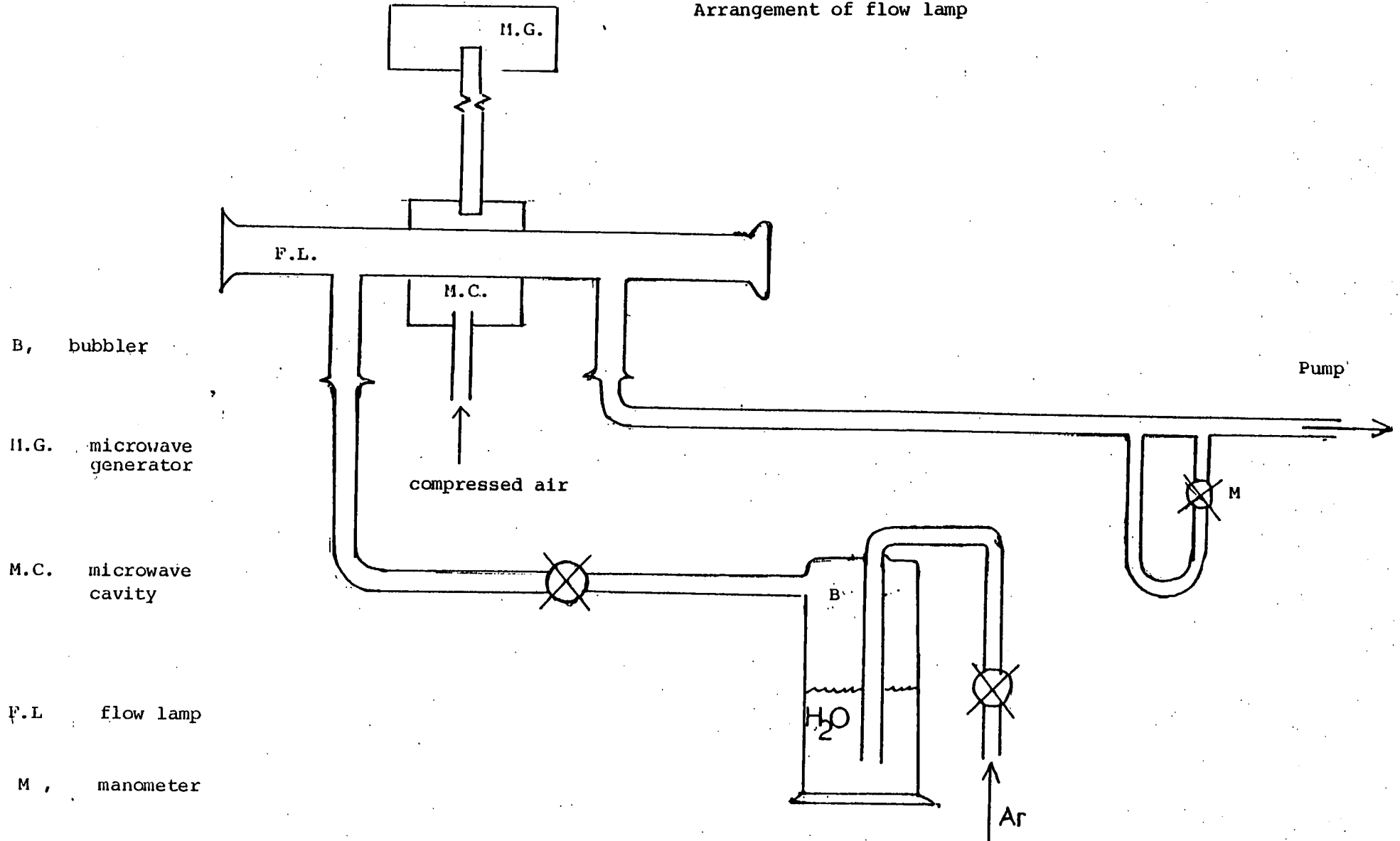
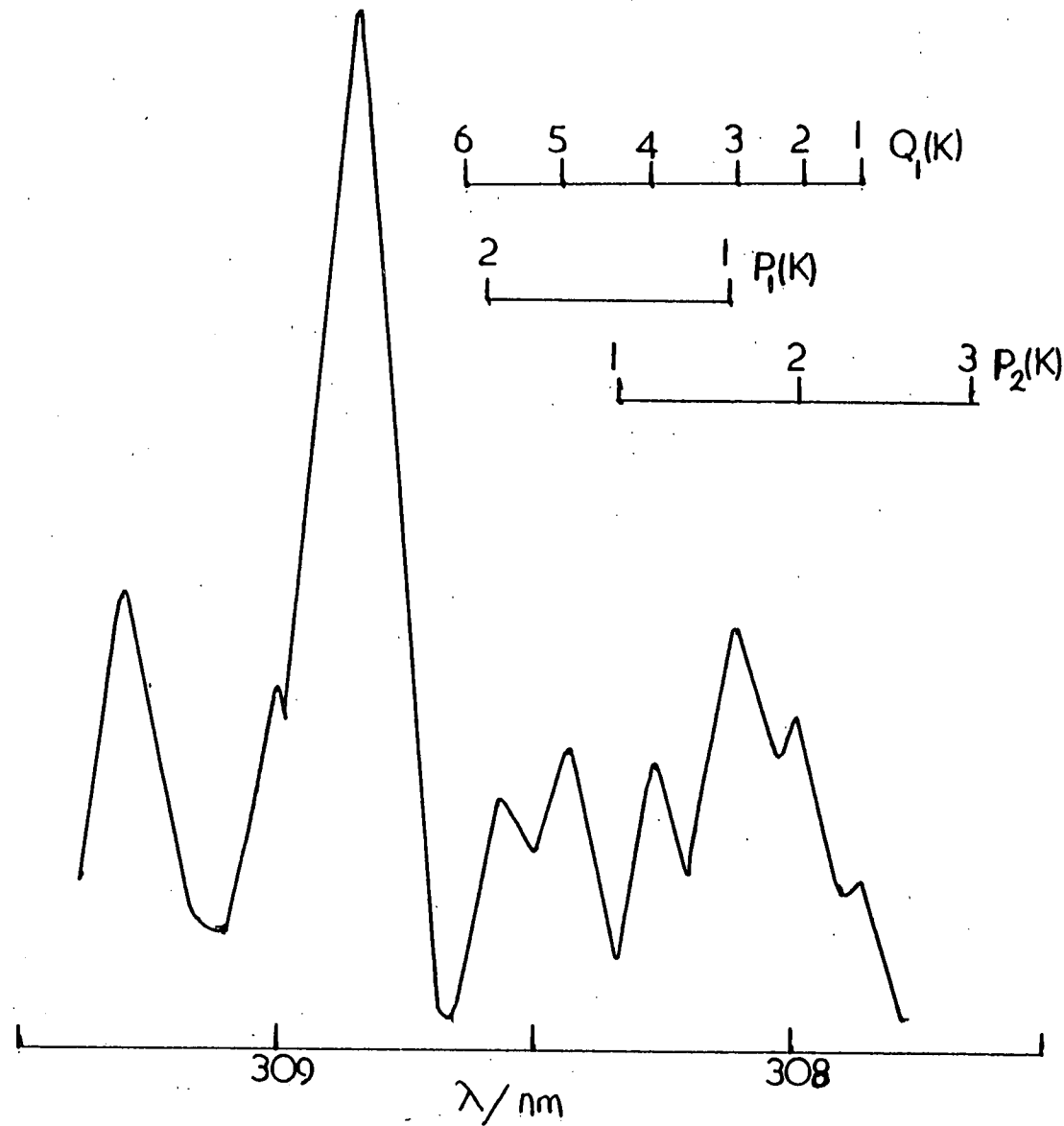


Figure 2.5.
Part of the $\text{OH}(A^2\Sigma \rightarrow X^2\Pi)$ spectrum



2.6 cont'd.

Absorption signals were detected by means of an EMI S5 9661B photomultiplier tube, mounted at the exit slit of the monochromator. This photomultiplier was a 9 stage side window tube, with a Corning 9741 glass window, which transmitted down to 200 nm, with a maximum sensitivity from 300 to 400 nm. The circuit diagram is shown (figure 2.6). The photomultiplier was run at 670 to 730 V (Brandenburg 472R Power Supply) with the output developed across a $10k\Omega$ resistor before being fed to a fast analogue to digital converter (Datalab DL 905) in parallel to a $100k\Omega$ resistor. The analogue to digital converter had an 8 bit x 1024 word integral memory. Signals were displayed on a Telequipment DM 64 oscilloscope and recorded on a Bryans 26000 X-Y plotter.

2.7 Analysis of results.

The decay of OH reacting with some species is given by the expression-

$$-\frac{d\{OH\}}{dt} = k\{OH\}\{S\} \quad \{1\}$$

where k is the second order rate constant. If $\{S\} \gg \{OH\}$ such that $\{S\}$ does not significantly change during the reaction, then {1} may be rewritten as -

$$-\frac{d\{OH\}}{dt} = k^1\{OH\}, \text{ where } k^1 = k\{S\} \quad \{2\}$$

The decay of OH is then 'pseudo first order' and k^1 is the pseudo first order rate constant. The integrated form of {2} is

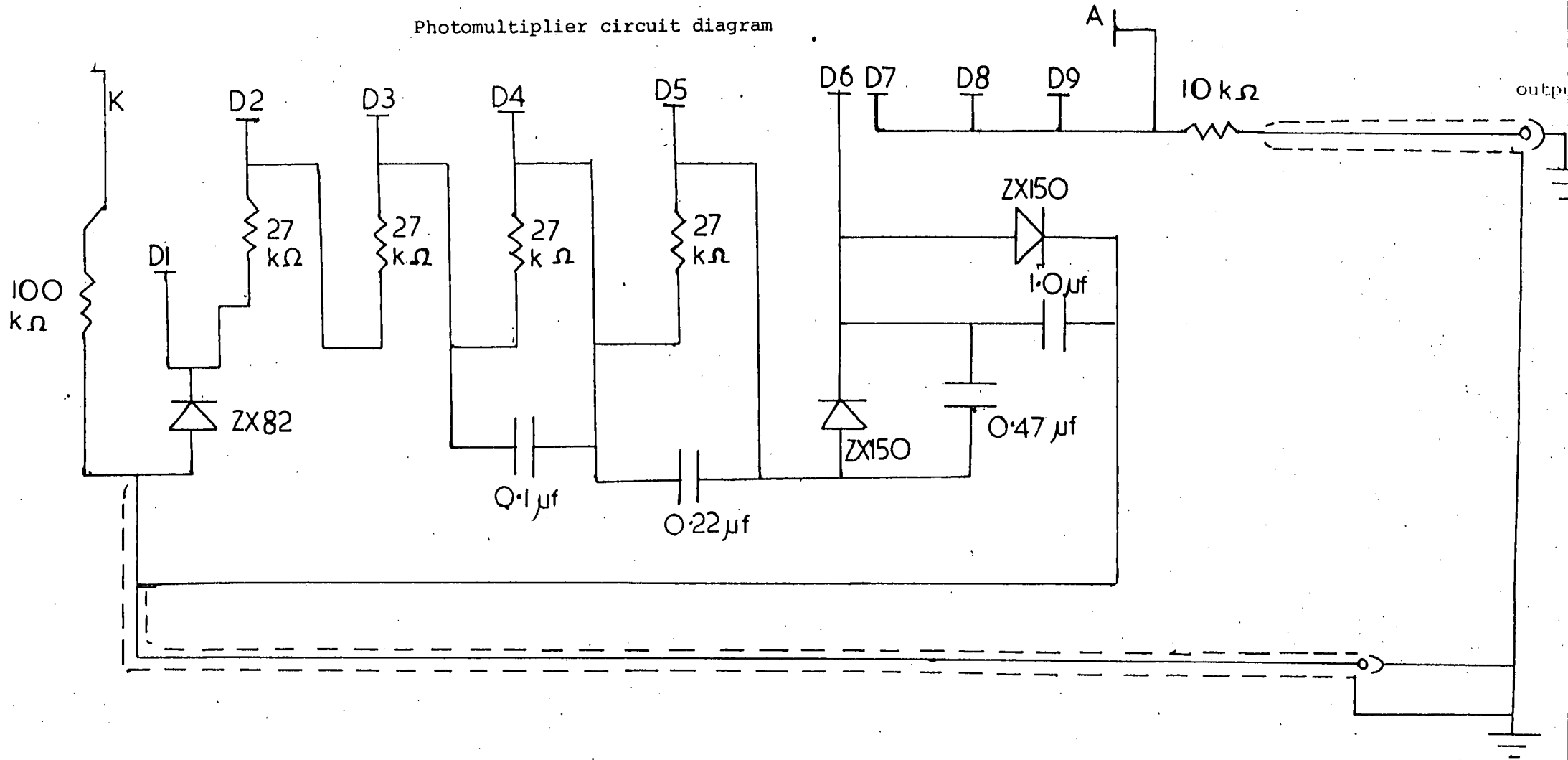
$$\ln \frac{\{OH\}_0}{\{OH\}} = k^1 t + C \quad \{3\}$$

where $\{OH\}_0$ is the initial OH concentration and $\{OH\}$ is the concentration at some time t on the decay. From the Beer Lambert law discussed above,

$$\{OH\} \propto \log(I_0/I)$$

where $\{OH\}$ is expressed in units of absorbance. It is not necessary to know the absolute OH concentration here as only ratios are required in {3}.

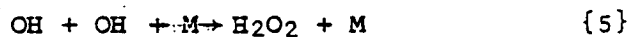
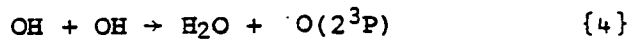
Figure 2.6
Photomultiplier circuit diagram



2.7 cont'd.

Pseudo first order rate constants, k^1 , at various concentrations of S are calculated from {3} and plotted against the concentration of S. The gradient of this plot gives k, the second order rate constant.

However, there are other removal processes of OH in addition to {1}, namely,



These are generally considered to be insignificant, in this work, however, because of the relatively high OH concentrations a small correction for {4} and {5} was required. This will be discussed in detail in Chapter 6.

2.8. Gas handling.

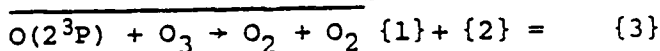
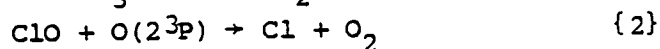
Gases were handled on conventional glass vacuum lines.

Pressures were measured by glass spiral gauges backed by mercury manometers. Appendix 1 lists the preparations and purifications of the gases used in this work.

CHAPTER THREEREACTION OF O(2¹D) WITH CF₃Cl, CF₂Cl₂ AND CFCI₃

3.1 Introduction.

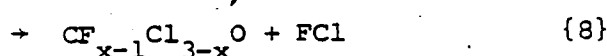
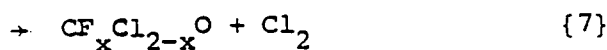
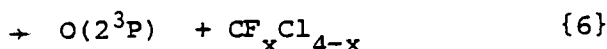
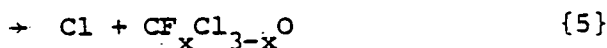
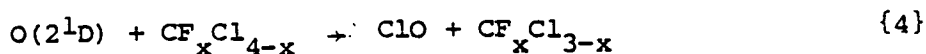
In 1974 Rowland and Molina⁴⁸ proposed that release of man made chlorofluorocarbons (CFCs) into the atmosphere could have long term deleterious effects on the Earth's ozone shield. There are detectable concentrations of these molecules in the atmosphere, particularly CF_2Cl_2 and CFCl_3 . CFCs are inert in the troposphere, and are transported into the stratosphere, where photodissociation in the atmospheric window between 190 and 210 nm, and reaction with $\text{O}(2^1\text{D})$ atoms produce Cl atoms and ClO. This could eventually lead to a depletion of ozone in the stratosphere by way of the ClO_x cycle.



There have been several studies of the photolysis products of CFCs.^{50,51}

Although the absolute rate constants for the reactions of $\text{O}(2^1\text{D})$ atoms with a large number of CFCs are now well established, little is known about the reaction mechanism and products.

The reaction of $\text{O}(2^1\text{D})$ with CH_4 has been discussed above (Chapter 1) and by analogy, the following reactions bear consideration.



Employing flash photolysis of O_3 with time resolved kinetic spectroscopy, Donovan, Gillespie and Garraway reported lower limits into {4} for the reaction of $\text{O}(2^1\text{D})$ with CF_3Cl , CF_2Cl_2 , CFCl_3 , CF_2HCl and CFHCl_2 ^{46,52}.

3.1 cont'd.

Under their experimental conditions, however, the half-life of Cl atom removal by {1} is only a few μs , and formation of ClO by reactions {5} and {1} would be indistinguishable from formation by {4}. {5} is more exothermic than {4}, for CF_3Cl , $\Delta H_{298}^{\circ}\{5\} = -239 \text{ kJ mole}^{-1}$ and $\Delta H_{298}^{\circ}\{4\} = -198 \text{ kJ mole}^{-1}$ ⁵³. If insertion occurs, a major pathway in the reaction of $\text{O}(2^1\text{D})$ with CH_4 , then an excited hypochlorite ROCl^* would be formed, which might be stabilised at high pressures. CF_3OCl is a well characterised molecule ⁵⁴, which on thermolysis or pyrolysis is thought to yield CF_3O and Cl, indicating that {5} could be an important pathway, if the primary step is insertion. Direct abstraction would, however, favour {4}.

Prior to this work no direct measurement of the branching ratio into {6} had been reported. As a result of this and other work ⁵⁵ Addison, Donovan and Garraway have recently reported the occurrence of, and branching ratios into {6} in the reaction of $\text{O}(2^1\text{D})$ with CF_2HCl and CF_3Cl ⁵⁶. In earlier experiments, however, Heicklen and co-workers ⁵⁶ concluded that quenching of $\text{O}(2^1\text{D})$ to $\text{O}(2^3\text{P})$ by CCl_4 , CFCl_3 and CF_2Cl_2 was negligible. Pitts et al ⁵⁷ came to a similar conclusion.

Evidence for reactions of the type {7} and {8} was obtained by Kaufmann, Donovan and Wolfrum ⁵⁸, who employed flash photolysis in a fast flow system with nozzle beam mass spectrometric sampling and detected species such as FCl , CFClO (from CFCl_3) and CF_2O (from CF_2Cl_2). Unfortunately, no quantitative values have been reported.

Studies of HF and HCl chemical laser emission following the reaction of $\text{O}(2^1\text{D})$ with hydrogen containing CFCs were explained by Lin ^{59,60} as occurring through an insertion elimination process, analogous to {7} and {8}.

In this chapter the branching ratios obtained for the reaction of $\text{O}(2^1\text{D})$ with CF_3Cl , CF_2Cl_2 and CFCl_3 will be presented, and in the succeeding chapter for the reaction of $\text{O}(2^1\text{D})$ with CF_2HCl .

3.1 cont'd

In chapter 5 the reaction of $O(2^1D)$ with CF_2ClBr will be presented and the results obtained in chapters 3-5 discussed .

3.2 Experimental

The apparatus for flash photolysis with time resolved kinetic spectroscopy has been described above (chapter 2) . To prevent photolysis of CF_2Cl_2 and $CFC1_3$, both of which absorb appreciably between 210 and 230 nm , photolysis was restricted to $\lambda > 245$ nm by means of a filter solution , (aqueous KI , 0.3 g l^{-1}).

$O(2^1D)$ was produced by the photolysis of O_3 in the Hartley continuum ($\lambda = 210 - 310 \text{ nm}$) . The concentration of O_3 in a mixture was measured by recording the UV absorption around 250 nm on a spectrophotometer (Perkin Elmer model 402) .

Extinction coefficients were taken from the work of Griggs ⁶¹ .

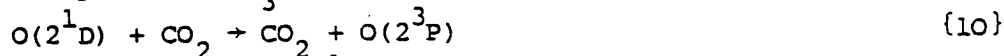
In order to determine branching ratios , it was necessary to measure the yield of $O(2^1D)$ atoms arising from the photolysis of O_3 . This was done by measuring the change in O_3 continuum absorption on photolysis of O_3 in the presence of an excess of CO_2 (2.7 kN m^{-2}) or He (2.7 kN m^{-2}) . There is some controversy surrounding the quantum efficiency of the $O(2^1D)$ yield from {9} .

$$h\nu , \lambda = 210 - 310 \text{ nm}$$



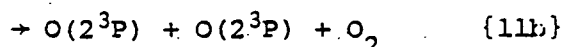
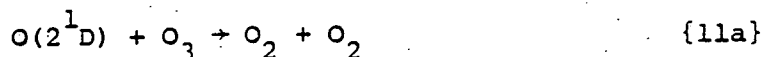
while it has generally been accepted as unity ^{62 - 65} ,

Lawrence *et al* have claimed to have shown that the yield of $O(2^1D)$ decreases steadily from 0.93 to 0.87 in the wavelength region 300 to 274 nm ⁶⁶ . In this work the quantum efficiency of the photolysis of O_3 in the wavelength region 210 - 310 nm to produce $O(2^1D)$ was taken as unity . In the O_3/CO_2 system $O(2^1D)$ is rapidly quenched by {10} , and the initial quantum yield for O_3 removal is 1.0 .



In the O_3/He system $O(2^1D)$ is not quenched efficiently and reacts with O_3 , so that the initial quantum yield is 2.0 .

3.2 cont'd.



Removal of O_3 by O_2 ($^1\Delta$) and $O(2^3P)$ is insignificant at times $< 50 \mu s$. The depletion in the presence of CO_2 was found to be $11.8 \pm 0.9 \%$ and in He was $24.3 \pm 1.2 \%$, and suggests that $O(2^3P)$ production from the photolysis of O_3 in the Hartley continuum is negligible.*

Quantitative determination of ClO concentrations.

The ($A^2\Pi_{3/2} \leftarrow X^2\Pi_{3/2}$) spectrum of ClO consists of a series of bands in the region 273 to 312 nm. The concentration of ClO was determined from (5,0) band at 295.4 nm. Extinction coefficients (base 10) at 298K for the (11,0) band have been determined by Clyne and Coxon⁶⁷ as $\epsilon = 3.15 \pm 0.10 \times 10^{-18} \text{ cm}^2 \text{ molec}^{-1}$ and by Basco and Dogra⁶⁸ as $\epsilon = 2.82 \times 10^{-18} \text{ cm}^2 \text{ molec}^{-1}$. The ratio of the (11,0) to (5,0) band was measured from good quality ClO spectra obtained by the flash photolysis of $CFCl_3/O_2$ mixtures. The ratio was found to be 2.10 ± 0.13 . Taking an average of $3.00 \pm 0.20 \times 10^{-18} \text{ cm}^2 \text{ molec}^{-1}$ for the (11,0) band, then ϵ (5,0) is calculated to be $1.43 \pm 0.13 \times 10^{-18} \text{ cm}^2 \text{ molec}^{-1}$. These values for the (11,0) and (5,0) bands are in good agreement with recent determinations^{69, 70}.

No appreciable dependence upon slit width of intensity of absorption by ClO was observed by Clyne and Coxon.

Quantitative determination of OClO concentrations.

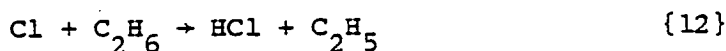
The ($^2A_2 \leftarrow ^2B_1$) spectrum of OClO consists of a series of regularly spaced bands extending from 320 to 370 nm, with a maximum intensity at the band at 351.5 nm. The extinction coefficient (base 10) was measured by Clyne and Coxon as $5.0 \times 10^{-18} \text{ cm}^2 \text{ molec}^{-1}$ and by Basco and Dogra⁶⁸ as $5.13 \times 10^{-18} \text{ cm}^2 \text{ molec}^{-1}$. No dependency of intensity of absorption upon slit width was observed by Clyne and Coxon⁷¹.

* Recently however Lee et al¹⁷⁵ appear to have shown conclusively that there is about a 10% yield of $O(2^3P)$ from the photolysis of O_3 . This is discussed in more detail on page 39.

3.3. The reaction of $O(2^1D)$ with CF_2Cl_2 and $CFC1_3$.

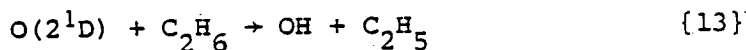
When O_3 (27 N m^{-2}) was photolysed in an excess of CF_2Cl_2 or $CFC1_3$ (2.7 kN m^{-2}) a strong spectrum of ClO was observed. No ClO was observed when N_2 or CO_2 was added to quench $O(2^1D)$ indicating that ClO arises from reaction between $O(2^1D)$ and the CFC. The growth of ClO continued for several hundred μs after the completion of the flash indicating the occurrence of secondary ClO formation reactions (see figures 3.1, 3.2).

To distinguish between initial ClO formation by {4} and by {5} followed by {1}, a small pressure of C_2H_6 (66 to 266 N m^{-2}) was added to remove Cl atoms by {12}, $k_{\{12\}} = 6.7 \pm 0.7 \times 10^{-11} \text{ cm}^3 \text{ molec}^{-1} \text{ s}^{-1}$,⁷²



Under the conditions used $> 95 \%$ of the Cl atoms were removed by {12}

Some $O(2^1D)$ reacted with C_2H_6 , {13}, in competition with {4} to {8}, $k_{\{13\}} = 3.1 \times 10^{-10} \text{ cm}^3 \text{ molec}^{-1} \text{ s}^{-1}$ ⁹



and a small correction to the branching ratios into {4} and {6} calculated by the graphical method described below is required. OH is assumed to be rapidly removed by {14}

$$k_{\{14\}} = 3.0 \times 10^{-13} \text{ cm}^3 \text{ molec}^{-1} \text{ s}^{-1}$$
⁷³



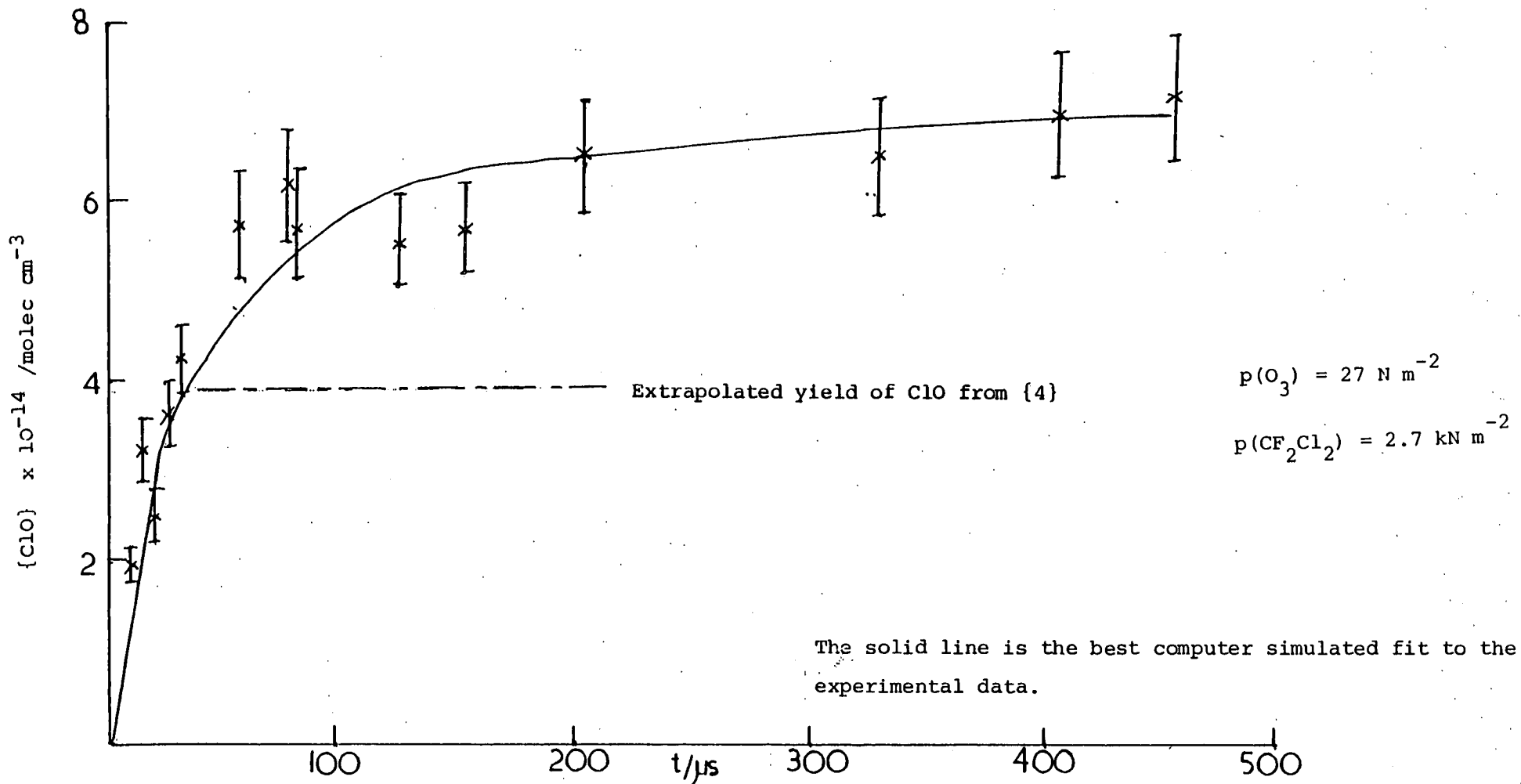
and to have no effect on ClO kinetics.

Similarly, C_2H_5 is assumed to have no effect.

The result of the addition of C_2H_6 is shown in figures 3.3 and 3.4. Note that there is now no secondary growth of ClO , indicating that C_2H_6 has reacted with some intermediate in the secondary formation scheme. The decay of ClO after $150 \mu\text{s}$ is extremely slow, and is ascribed to the disproportionation reactions of ClO . These are discussed in detail in Section 7.

Figure 3.1

Formation of ClO following the reaction of $O(^1D)$ with CF_2Cl_2



The solid line is the best computer simulated fit to the experimental data.

Figure 3.2

Temporal development of ClO following the reaction of $O(^1D)$ with $CFCl_3$

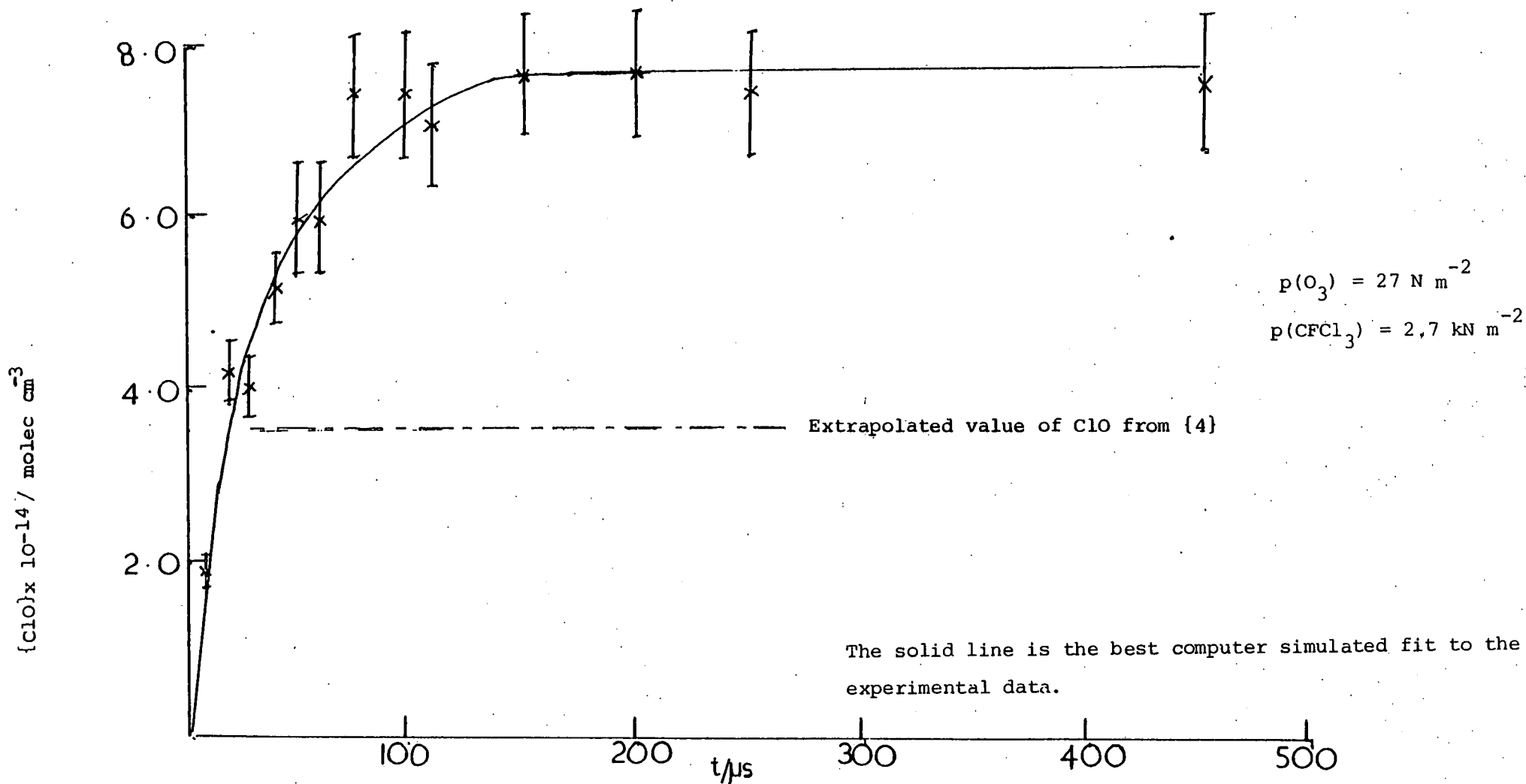


Figure 3.3

Temporal development of ClO in the $O_3/CF_2Cl_2/C_2H_6$ system

pressure $O_3 = 27 \text{ N m}^{-2}$
 $CF_2Cl_2 = 2.3 \text{ kN m}^{-2}$
 $C_2H_6 = 66 \text{ N m}^{-2}$

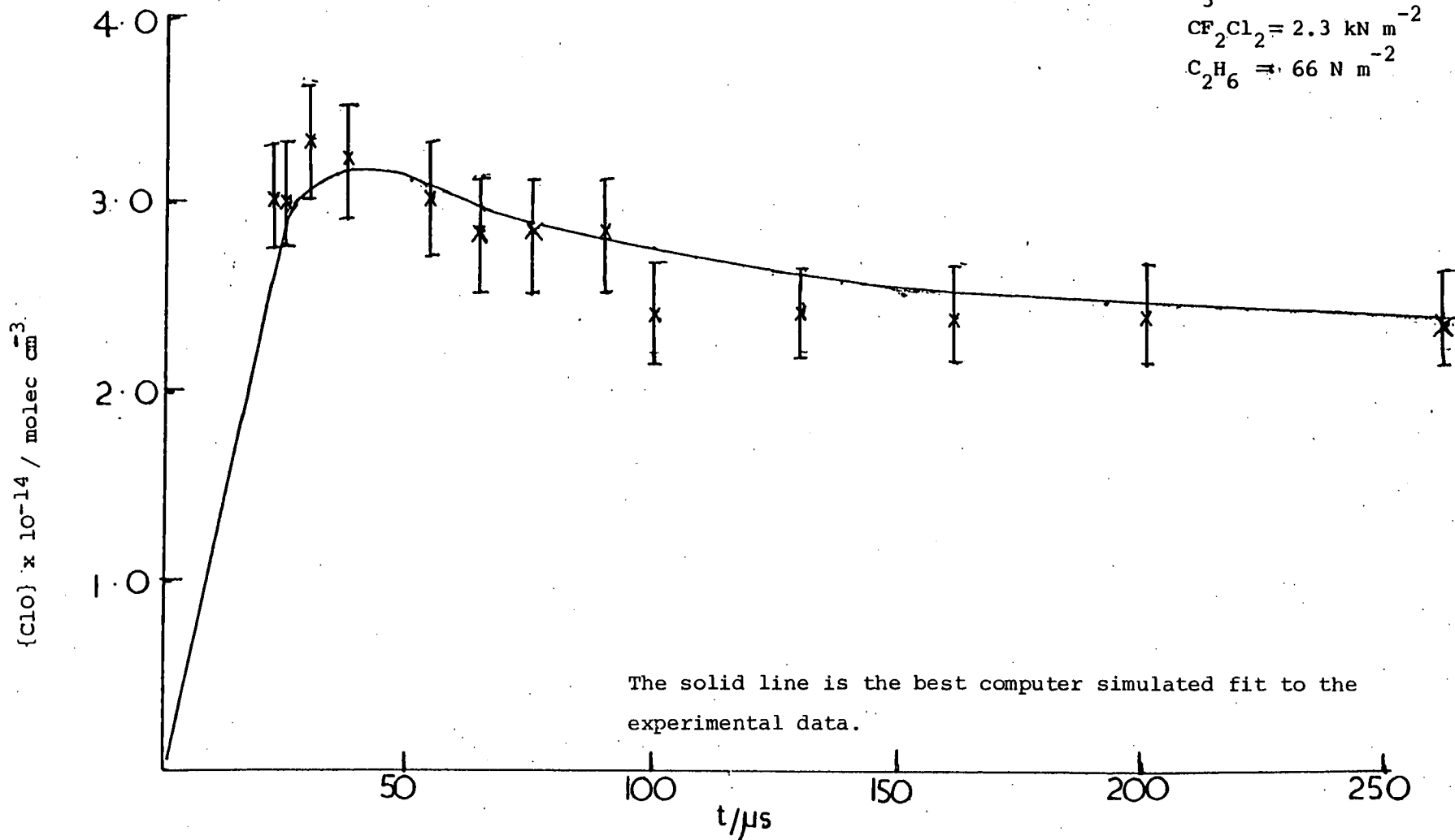
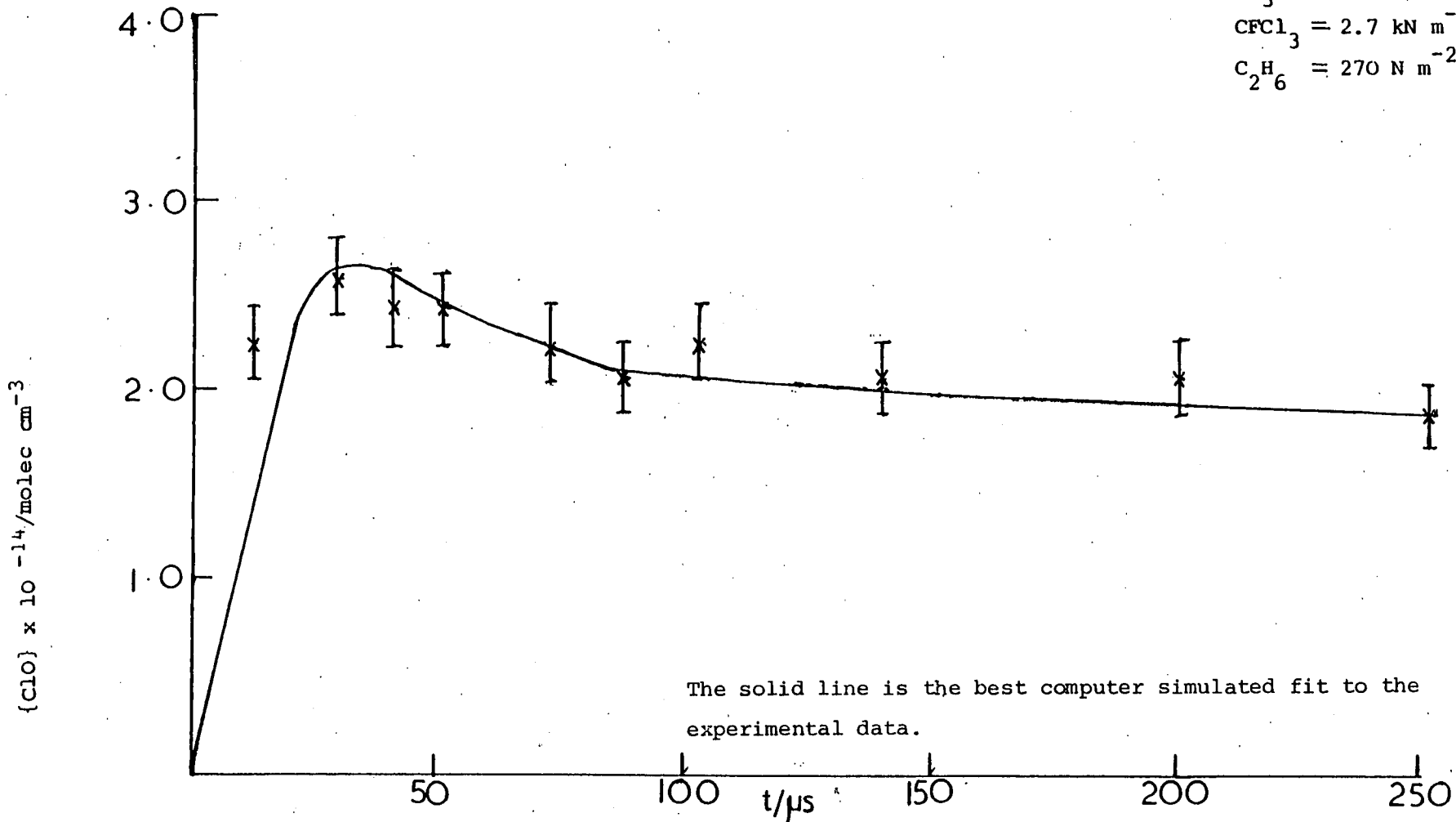


Figure 3.4

Temporal development of ClO in the $O_3/CFC1_3/C_2H_6$ system

pressure $O_3 = 27 \text{ N m}^{-2}$
 $CFC1_3 = 2.7 \text{ kN m}^{-2}$
 $C_2H_6 = 270 \text{ N m}^{-2}$



3.3 cont'd.

The initial rapid decay of ClO could be due to either

- (a) quenching of O(2¹D) to O(2³P) by CF₂Cl₂ or CFC1₃ followed by {2} and {12} or

- (b) recombination with CF₂Cl, CF₂ClO or CFC1₂, CFC1₂O.

Alternative (b) is unlikely in that it would require an extremely efficient recombination reaction, $k \sim 5 \times 10^{-11} \text{ cm}^3 \text{ molec}^{-1} \text{ s}^{-1}$. And there is evidence to suggest that the major reactions of these radicals are combination, and reaction with O₃ (see Section 4).

Alternative (a) was shown to be the correct one by M.C. Addison who was able to detect the formation of, and measure the yield of O(2³P) following the reaction of O(2¹D) with CFCs.

The apparatus for flash photolysis with resonance absorption of O(2³P) at 130 nm has been described⁵⁵. The experimental approach was to measure the O(2³P) absorbance when a given concentration of O₃ was photolysed in an excess of N₂, such that all the O(2¹D) was quenched to O(2³P). The same O₃ concentration was then photolysed in an excess of CFC.

The fractional branching ratio into {6} was found by comparing the O(2³P) absorbance in the latter experiment with the absorbance in the former.

Because of problems of absorption by CFCs in the region of the O(2³P) absorption, Addison was only able to measure O(2³P) yields for CF₃Cl and CF₂HCl. However, it is reasonable to assume that quenching also occurs in the reaction of O(2¹D) with CF₂Cl₂ and CFC1₃.

To determine the branching ratios into {4} and {6} it was necessary to measure the amount of ClO removed in the decay. A first approximation was obtained by a graphical method. Tangents (figure 3.5) were drawn to the ClO decay at 10 μs intervals and the gradient plotted against time (figure 3.6). The area under the curve up to time t was taken as the amount of ClO removed by then, and was added on to the experimental concentration of ClO at that time.

Figure 3.5.

Extrapolation of ClO decay to estimate amount of ClO removed.

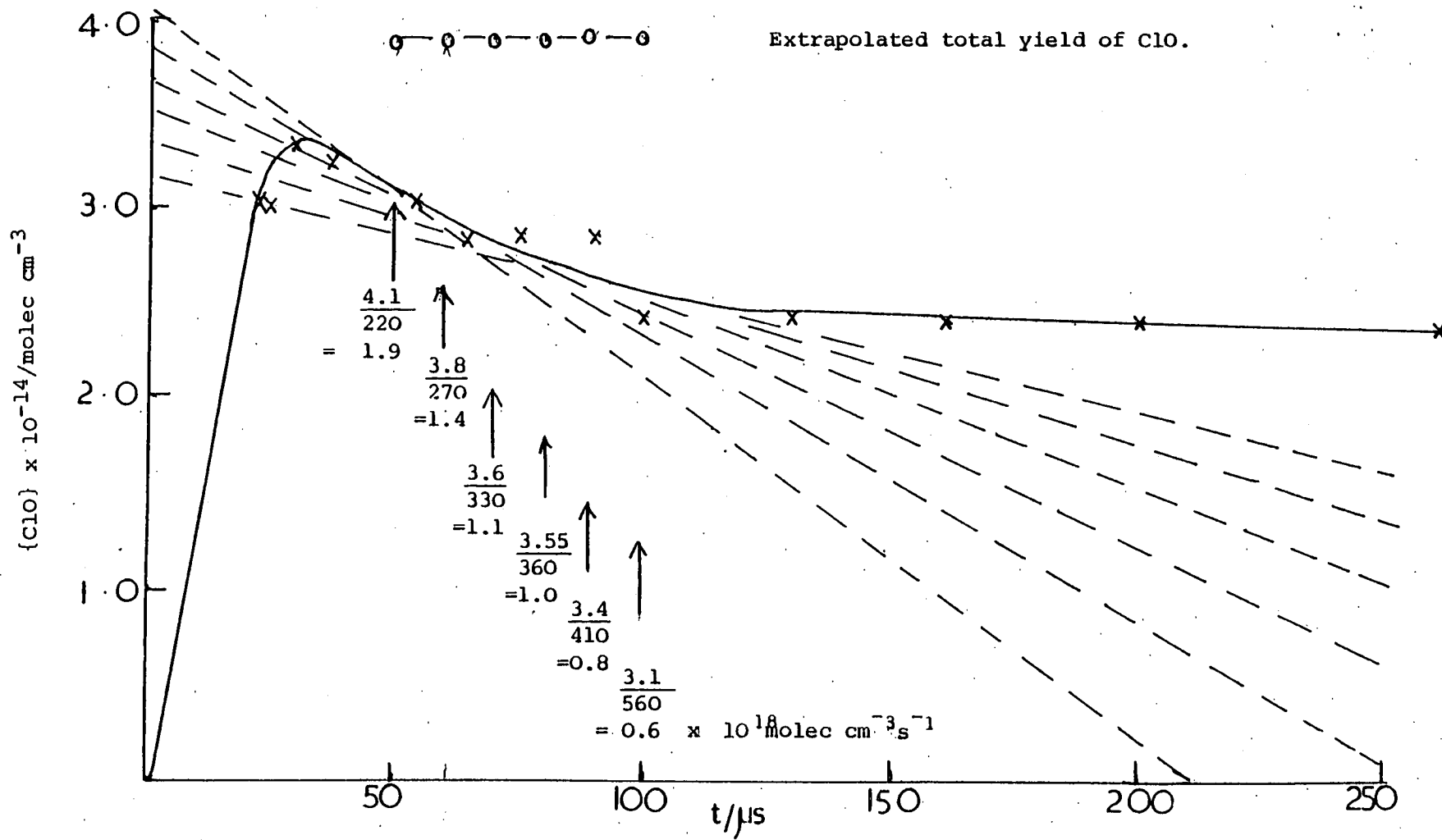
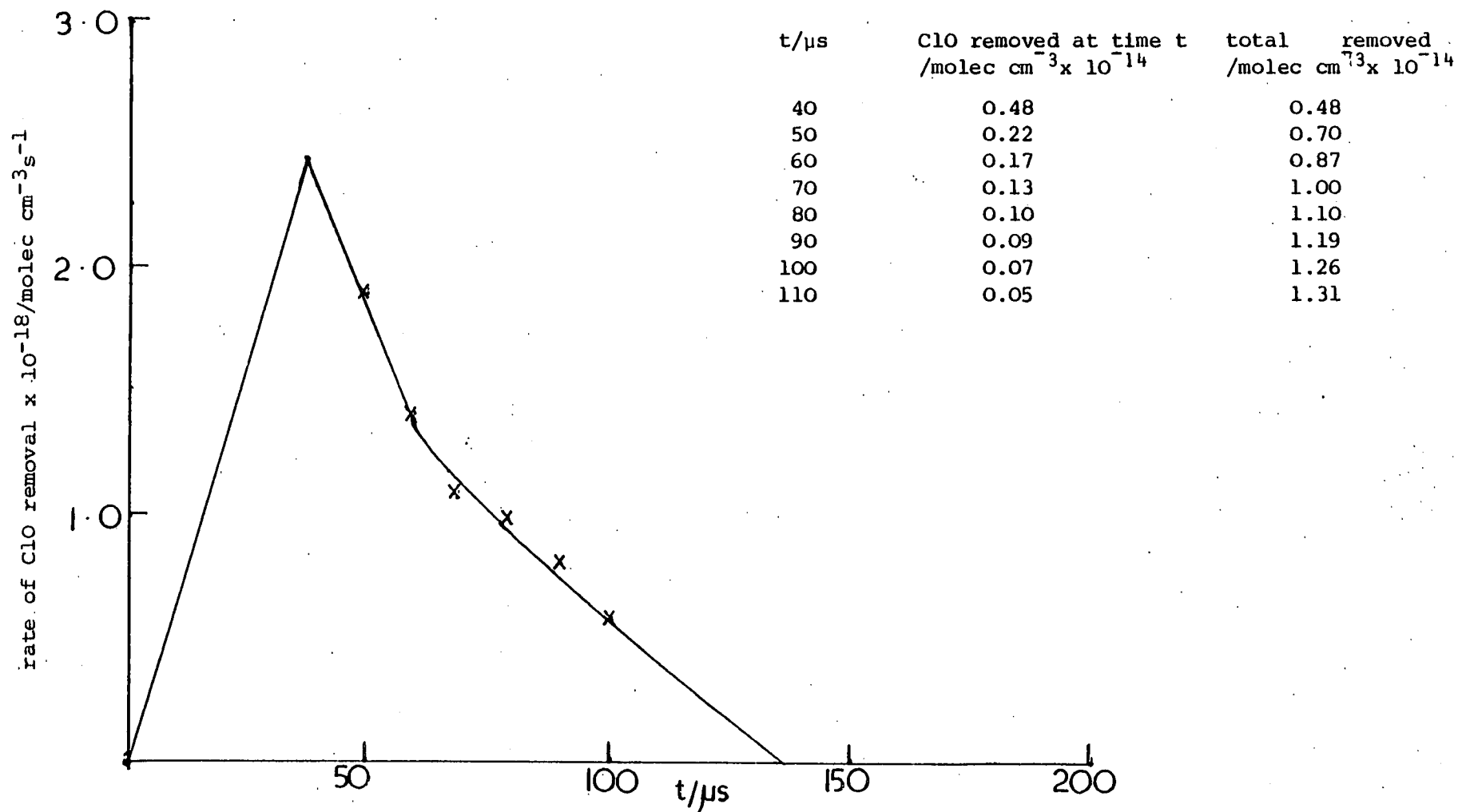


Figure 3.6.

Evaluation of amount of ClO removed in Figure 3.6



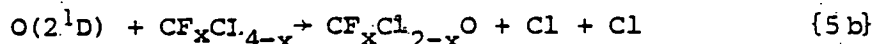
3.3 cont'd.

The ClO decay and estimate of total ClO yield is shown in figure 3.5. (This method has been illustrated for the $O_3/CF_2Cl_2/C_2H_6$ system shown in figure 3.3). The difference between the estimated value of total ClO production and experimental value at the end of the decay is a measure of the $O(2^3P)$ yield. These values (corrected for loss of $O(2^1D)$ by {13}) were taken as initial values in a computer simulation (using the Harwell 'CHEK' program, Chapter 2) of the ClO decay. Rate constants for the reaction of $O(2^1D)$ with CF_2Cl_2 , $CFCl_3$ ¹⁰ and C_2H_6 ⁹ were taken from the work of Fletcher and Husain. These authors reported two values for the rates of removal of $O(2^1D)$ depending on whether the Beer Lambert exponent β was 0.41 or 1.0. Although Fletcher and Husain preferred $\beta = 0.41$, their values of rate constants are only in agreement with other determinations if $\beta = 1.0$. And there are theoretical reasons supporting $\beta = 1.0$ ⁷⁶. Thus the rate constants used in the simulation are Fletcher and Husain's values when $\beta = 1.0$.

The best fits for the decay of ClO for CF_2Cl_2 and $CFCl_3$ are shown in figure 3.3 and 3.4. Tables 3.1 and 3.2 list the equations used in the simulation for CF_2Cl_2 and $CFCl_3$. Table 3.3 lists the branching ratios. (See note on page 45)

Branching ratios into {5}, {7} and {8}

The CX_3O species formed in {5} have enough energy to dissociate into CX_2O and X. Thus it was assumed that {5} was on a μs time-scale effectively,



$$\Delta H_{298}^{\circ} = -336 \text{ kJ mole}^{-1} \text{ for } CF_2Cl_2$$

$$\text{and } = -29 \text{ kJ mole}^{-1} \text{ for } CFCl_3$$

An upper limit into {5.b} may be obtained from the difference between the experimental ClO concentration at the end of the flash ($t \sim 40 \mu s$) and the calculated ClO yield from {4}, (illustrated in figures 3.1 and 3.2). This is an upper limit as there will be some contribution to the ClO concentration from secondary formation reactions.

Table 3.1

Best fit computer simulation of the reaction of $O(^1D)$ with CF_2Cl_2

No.	Equation	$k/cm^3molec^{-1}s^{-1}$	Ref.
9	$O_3 \rightarrow O_2(^1\Delta) + O(^1D)$		61-65
5b	$O(^1D) + CF_2Cl_2 \rightarrow CF_2O + Cl + Cl$	$1.0 E -11$	calc.
4	$O(^1D) + CF_2Cl_2 \rightarrow CF_2Cl + ClO$	$1.0 E -10$	calc.
6	$O(^1D) + CF_2Cl_2 \rightarrow CF_2Cl_2 + O(^3P)$	$4.0 E -11$	calc.
7	$O(^1D) + CF_2Cl_2 \rightarrow CF_2O + Cl_2$	$5.0 E -11$	calc.
1	$Cl + O_3 \rightarrow ClO + O_2$	$1.2 E -11$	74
17	$CF_2Cl + CF_2Cl \rightarrow C_2F_4Cl_2$	$2.0 E -11$	78
15a	$CF_2Cl + O_3 \rightarrow CF_2O + Cl + O_2$	$2.0 E -12$	calc.
2	$O(^3P) + ClO \rightarrow Cl + O_2$	$5.3 E -11$	75
13	$O(^1D) + C_2H_6 \rightarrow C_2H_5 + OH$	$3.0 E -10$	9
12	$Cl + C_2H_6 \rightarrow HCl + C_2H_5$	$6.7 E -11$	72

The equations above the line simulate the O_3/CF_2Cl_2 system, inclusion of the equations below the line simulates the $O_3/CF_2Cl_2/C_2H_6$ system. Two experiments with C_2H_6 (270 and $66 N m^{-2}$) were done.

Table 3.2

Best fit computer simulation of the reaction of $O(^1D)$ with $CFCl_3$

9	$O_3 \rightarrow O_2(^1\Delta) + O(^1D)$		61-65
5b	$O(^1D) + CFCl_3 \rightarrow CFClO + Cl + Cl$	$2.3 E -11$	calc.
4	$O(^1D) + CFCl_3 \rightarrow CFCl_2 + ClO$	$1.0 E -10$	calc.
6	$O(^1D) + CFCl_3 \rightarrow CFCl_3 + O(^3P)$	$4.5 E -11$	calc.
7	$O(^1D) + CFCl_3 \rightarrow CFClO + Cl_2$	$5.6 E -11$	calc.
1	$Cl + O_3 \rightarrow ClO + O_2$	$1.2 E -11$	74
17	$CFCl_2 + CFCl_2 \rightarrow C_2F_2Cl_4$	$2.0 E -11$	est. *
15a	$CFCl_2 + O_3 \rightarrow CFClO + ClO + O_2$	$5.0 E -12$	calc.
2	$O(^3P) + ClO \rightarrow Cl + O_2$	$5.3 E -11$	75
13	$O(^1D) + C_2H_6 \rightarrow C_2H_5 + OH$	$3.0 E -10$	9
12	$Cl + C_2H_6 \rightarrow HCl + C_2H_5$	$6.7 E -11$	72

The equations above the line simulate the $O_3/CFCl_3$ system, inclusion of the equations below the line simulates the $O_3/CFCl_3/C_2H_6$ system.

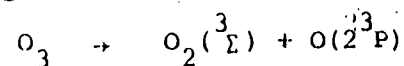
One experiment with C_2H_6 ($270 N m^{-2}$) was done.

* The rate of combination of $CFCl_2$ was assumed to be the same as that of CF_2Cl .

Table 3.3 Product branching ratios for the reactions of $O(2^1D)$ with CF_3Cl , CF_2Cl_2 and $CFC1_3$

Reaction No	{4}	{5}	{7} + {8}	{6}	{8} (Addison)
reaction products	$ClO + CX_3$	$CX_2O + 2X$	$CX_2O + X_2$	$O(2^3P)$	$O(2^3P)$
CF_3Cl	0.55 ± 0.10	0.23 ± 0.10	< 0.10	0.27 ± 0.10	0.30 ± 0.10 0.15
CF_2Cl_2	0.50 ± 0.10	0.05 ± 0.10 0.05	< 0.25	0.20 ± 0.10	-
$CFC1_3$	0.45 ± 0.10	0.10 ± 0.10	< 0.25	0.20 ± 0.10	-

Lee et al ¹⁷⁵ photolysed O_3 in a supersonic molecular beam and measured the translational energy of the primary products. They detected five peaks corresponding to centre of mass translational energies of ~ 250 , 55.2, 42.8, 26.4, and 9.9 kJ mol^{-1} . The only reaction capable of giving products with translational energies around 250 kJ mol^{-1} is



and was estimated to have a branching ratio of 0.10.

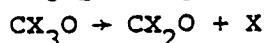
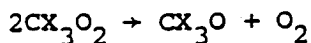
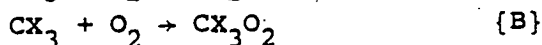
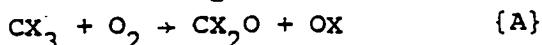
An $O(2^1D)$ yield of 0.9 rather than unity does not greatly alter the branching ratios shown in figure 3.3 except for the yield into $O(2^3P)$. The revised figures for CF_3Cl for example are now 0.61, 0.25 and 0.11 for reactions 4,5, (7 + 8), respectively, but now only 0.19 for reaction 6.

3.3 cont'd.

These upper limits were taken as initial values in the computer simulation of the secondary growth(section 4). The best fit values are given in table 3. Branching ratios into {7} and {8} were estimated from mass balance calculations ,i.e. as the difference between 1.0 and the sum of the branching ratios into {5} ,{4} and {6}.

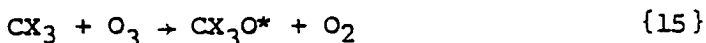
3.4 Secondary growth of ClO

From the branching ratios obtained above , the only species which could react to give secondary ClO formation is CX₃ , formed in {4}. The oxidation of CX₃ radicals is not well understood , but two mechanisms have been postulated for reaction with O₂⁷⁶ (some O₂ is always present with O₃).



With, in Heicklen's opinion, the balance of evidence favouring {A}. However, the suppression of secondary growth by C₂H₆ indicates that reaction proceeds via Cl atom release, since removal of CX₃ by reaction with C₂H₆ is too slow to be significant⁷⁷. Thus {A} must be ruled out. While secondary growth can occur by {B} a more likely reaction scheme has been proposed by Kaufmann et al⁵⁸, who similarly observed secondary ClO formation following the reaction of O(2¹D) with CCl₄.

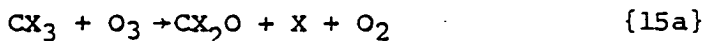
They suggested



The overall reaction is exothermic for CF₂Cl and CFC₂Cl₂.

The secondary growth of ClO in CF₂Cl₂, and CFC₂Cl₃ was simulated assuming that

- a) CX₃O* disintegrated immediately, so that {15} and {16} could be written as



3.4 cont'd.

b) {15a} competes with the combination of
 CX_3 radicals, {17} .

The best fits are shown in figures 3.1 and 3.2.

Tables 3.1 and 3.2. list the equations and rate constants used in the best fit simulations.

3.5 O₃ depletion.

The amount of O₃ removal following the photolysis of O₃ in the presence of CF₂Cl₂, CFC1₃ and CF₃Cl (Section 6) was measured. The experimental values were in good agreement with the values predicted by the best fit simulations. The amount of O₃ removed was approximately twice that photolysed even at short times, and explained the low values into ClO branching ratios obtained by Donovan et al,^{46,52} who monitored the amount of O₃ removed at 10 μs following photolysis of the O₃/CFC system, and assumed that the O(2¹D) yield was equal to the amount of O₃ removed.

3.6 The reaction of O(2¹D) with CF₃Cl

The temporal development of ClO following the flash photolysis of O₃ in the presence of an excess of CF₃Cl (2.7 kN m⁻²) is shown in figure 3.7 . In contrast to the behaviour observed in the reaction of O(2¹D) with CF₂Cl₂ and CFC1₃ , here the concentration of ClO was observed to decay rapidly after about 50 μs , with a contemporaneous formation of OC1O . This decay will be discussed later .

Branching ratios into {4} and {6} were obtained in the manner described above for CF₂Cl₂ and CFC1₃ . The effect of addition of C₂H₆ (66 to 270 N m⁻²) is shown in figure 3.8 . No OC1O formation is now observed , and the fast decay of ClO is complete by about 150 μs . This fast decay is similar to that observed in the O₃/ CFC1₃/ C₂H₆ and O₃/ CF₂Cl₂/ C₂H₆ systems and is ascribed to the effects of {2} and {12} .

Figure 3.7.

Temporal development of ClO and OCIO in the O_3/CF_3Cl system

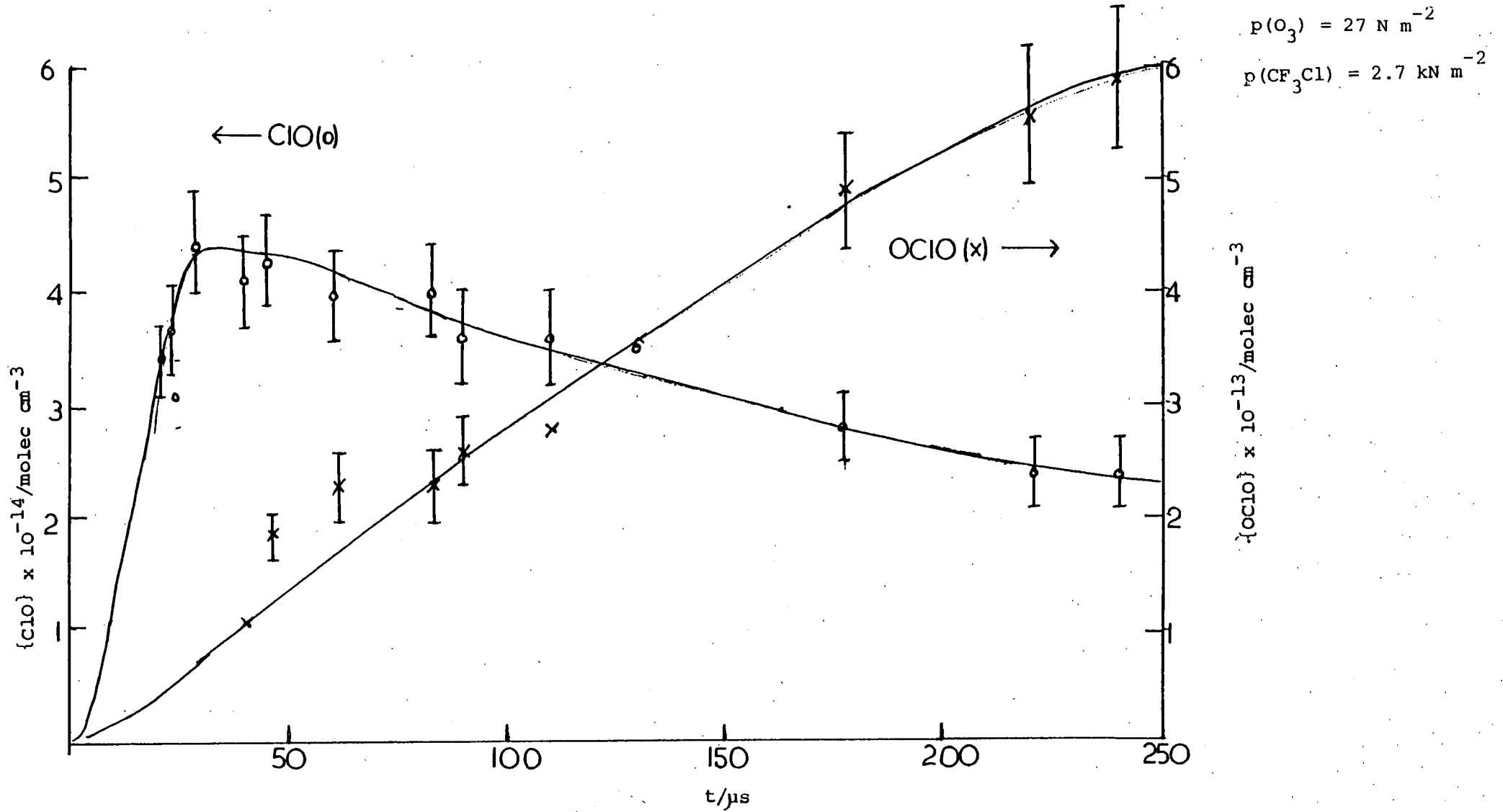
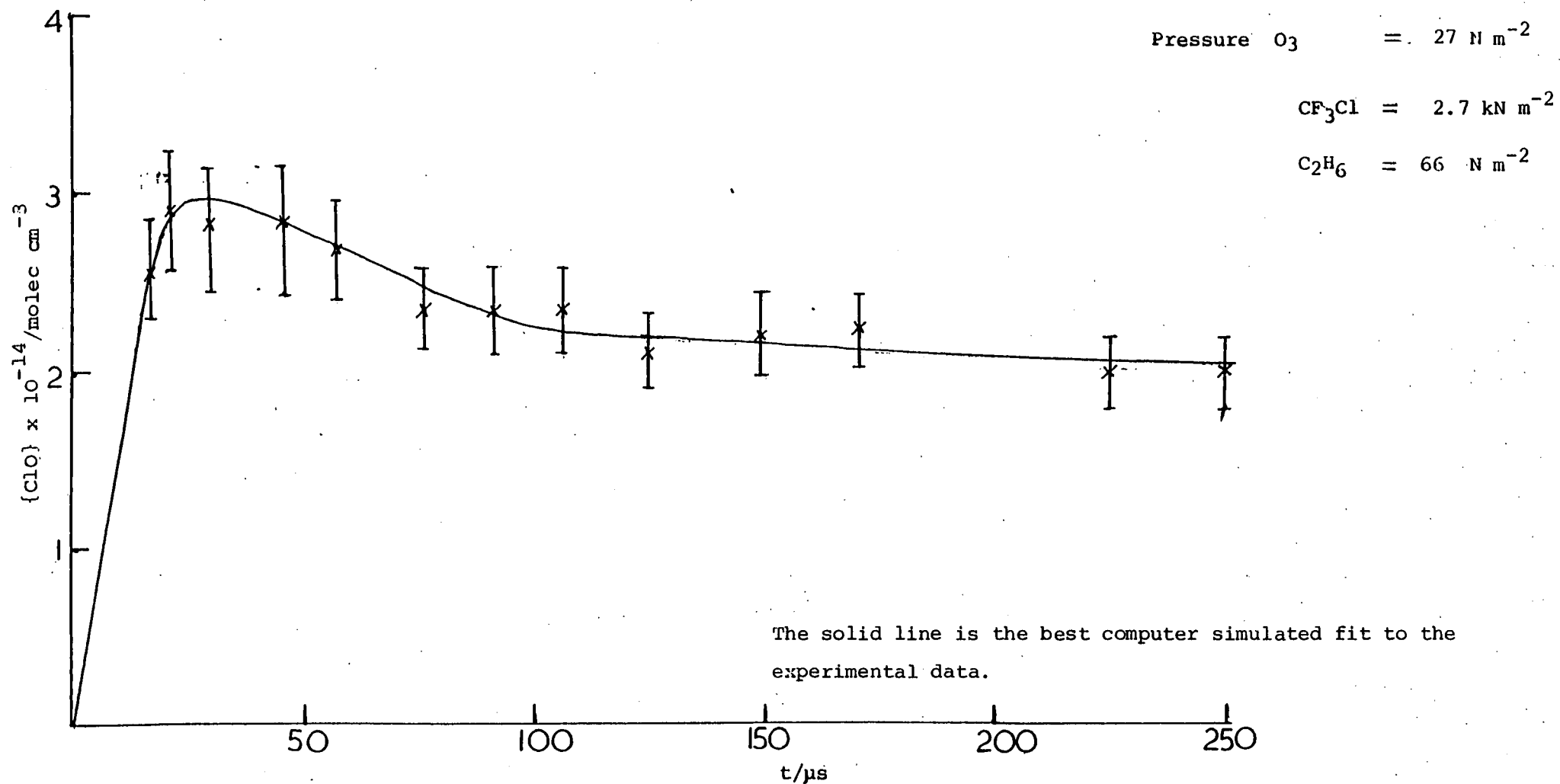


Figure 3.8

Temporal development of ClO in the $O_3/CF_3Cl/C_2H_6$ system



3.6 cont'd

The lack of continued fast ClO decay after 150 μ s indicates that the decay process observed in figure 3.7 has been suppressed in the presence of C_2H_6 . Figure 3.9 shows the best fit simulation of the ClO decay in the presence of C_2H_6 and table 3.4 lists the best fit equations. Table 3.3 lists the branching ratios into reactions {4} and {6}. The value of the $O(2^3P)$ branching ratio determined directly by Addison is in good agreement with the indirect determination.

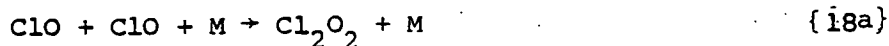
Branching ratio into {5} and {8}.

The difference between the total yield of ClO and the yield calculated for {4} is an estimate of the branching ratio into reaction {5}. The total yield of ClO ({4} + {5}) was obtained by graphical extrapolation of the decay in figure 3.7. The branching ratio into {8} was calculated by mass balance. Branching ratios for these reactions are shown in table 3.3.

3.7 The decay of ClO and the formation of OClO

The concentration profiles of ClO and OClO over 10 milliseconds are shown in figure 3.9. (It should be noted that in order to improve sensitivity, no filter solution was used in this experiment allowing higher percentage photolysis of O_3 , (CF_3Cl is not photolysed at $\lambda > 200$ nm, the reaction vessel cut-off)). At long times the disproportionation reactions of ClO must be considered. There has been considerable dispute about these reactions, but the situation now seems reasonably well resolved.

Recent studies by Basco and Hunt⁷⁹ using flash photolysis with photographic and photometric detection, and by Johnston *et al*⁸⁰ and Cox *et al*⁸¹, both groups using molecular modulation spectroscopy have indicated that there is a third order combination reaction.



Basco⁷⁹ observed a new absorption spectrum in the ultraviolet and which he ascribed to Cl_2O_2 . Determinations of $k_{\{18a\}}$ are listed in table 3.5.

Table 3.4

Best fit computer simulation of the reaction of $O(^1D)$ with CF_3Cl

No.	Equation	$k/cm^3 molec^{-1} s^{-1}$	Ref.
9	$O_3 \rightarrow O_2(^1\Delta) + O(^1D)$		61-65
5b	$O(^1D) + CF_3Cl \rightarrow CF_2O + F + Cl$	$2.3 E^{-11}$	calc.
4	$O(^1D) + CF_3Cl \rightarrow CF_3 + ClO$	$5.4 E^{-11}$	calc.
6	$O(^1D) + CF_3Cl \rightarrow CF_3Cl + O(^3P)$	$2.6 E^{-11}$	calc.
1	$Cl + O_3 \rightarrow ClO + O_2$	$1.2 E^{-11}$	74
2	$O(^3P) + ClO \rightarrow Cl + O_2$	$5.3 E^{-11}$	75
17	$CF_3 + CF_3 \rightarrow C_2F_6$	$9.0 E^{-12}$	91
19	$CF_3 + O_3 \rightarrow CF_2O + O_2 + F$	$3.0 E^{-13}$	calc.
20	$F + O_3 \rightarrow FO + O_2$	$1.3 E^{-11}$	83
21a	$FO + ClO \rightarrow FClO_2$	$8.1 E^{-12}$	calc.
21b	$FO + ClO \rightarrow F + OClO$	$3.2 E^{-11}$	calc.
	$O_2(^1\Delta) + O_3 \rightarrow O_2 + O_2 + O(^2^3P)$	$4.0 E^{-15}$	169
	$F + C_2H_6 \rightarrow HF + C_2H_5$	$5.2 E^{-11}$	84
13	$O(^1D) + C_2H_6 \rightarrow C_2H_5 + OH$	$3.0 E^{-10}$	9
14	$Cl + C_2H_6 \rightarrow HCl + C_2H_5$	$6.7 E^{-11}$	72

The equations above the line simulate the O_3/CF_3Cl system, inclusion of the equations below the line simulates the $O_3/CF_3Cl/C_2H_6$ system. Three experiments with C_2H_6 (270, 67 and 27 $N m^{-2}$) were done.

Note from page 37

The $O_3/CFC/C_2H_6$ experiments were simulated first. There were two variables in these simulations, the ClO and the $O(^2^3P)$ yield. Small changes (0.05) in the $O(^2^3P)$ branching ratios had significant effects on the slope of the simulated ClO decay over the period 40 to 150 μs . Similar changes in the ClO yield had much smaller effects on the slope of the ClO decay but did of course increase or decrease the simulated ClO concentration. Thus, unique values for the branching ratios into $O(^2^3P)$ and ClO could be determined.

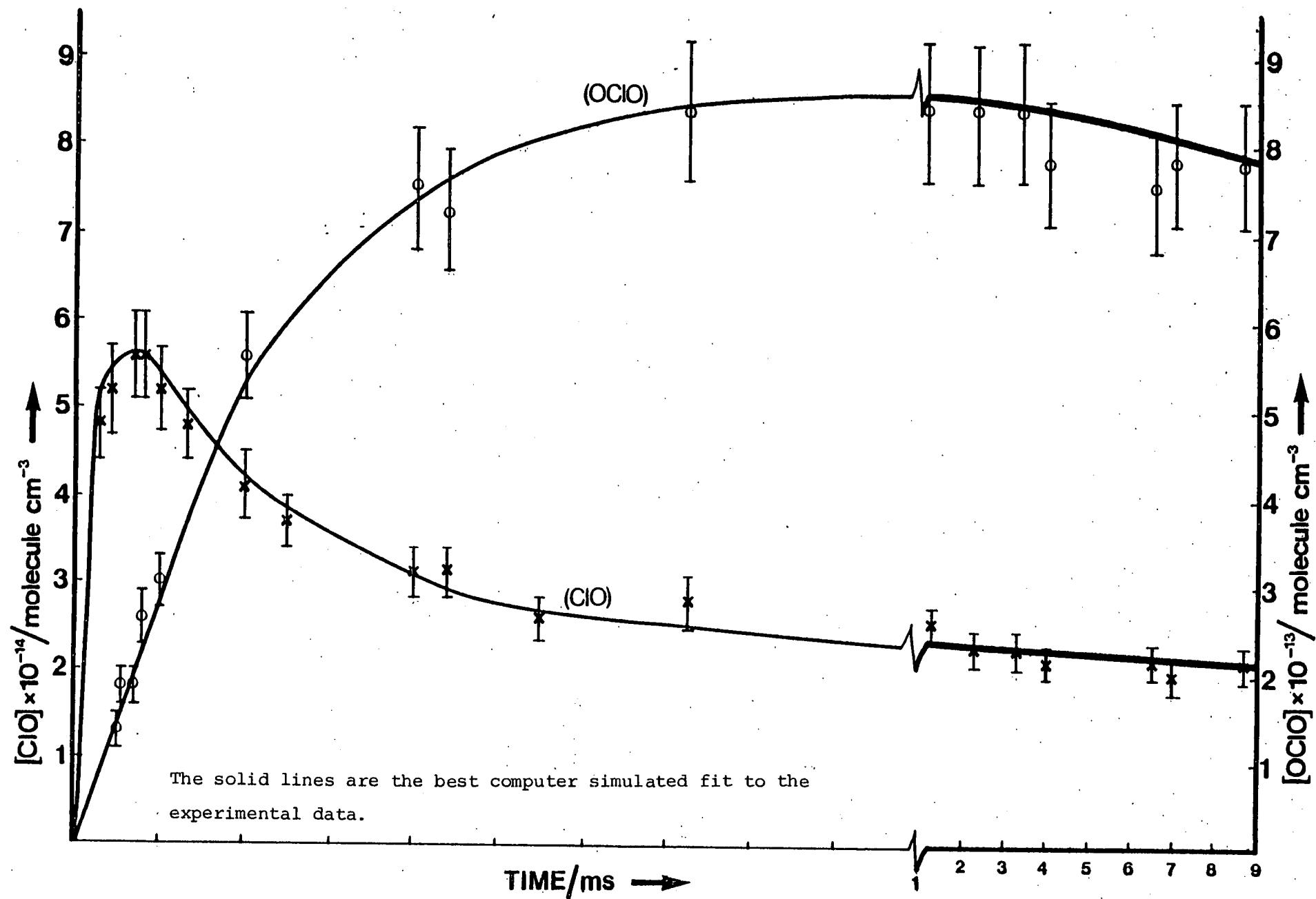


Figure 3.9 . Decay of ClO and formation of OCIO following the reaction of O(¹D) with CF₃Cl
 (P_{O₂} = 27 Nm⁻²; P_{CF₃Cl} = 2.7 k Nm⁻²).

Table 3.5

Literature values for the reaction, $\text{ClO} + \text{ClO} + \text{M} \rightleftharpoons \text{Cl}_2\text{O}_2 + \text{M}$

Ref.	$(k / \text{cm}^6 \text{molec}^{-2} \text{s}^{-1}) \times 10^{-33}$	remarks
79	9.7 ± 0.4	M = Ar
79	7.7	M = He
79	22	M = O ₂
81a	30 ± 5	M = N ₂ + O ₂
80	50 ± 5	M = O ₂

3.7 cont'd

Basco⁷⁹ found evidence for an independent second order reaction , but was unable to distinguish between {18b} - {18d}



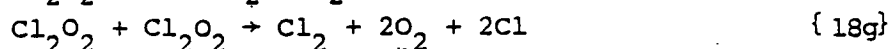
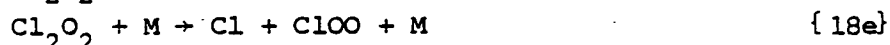
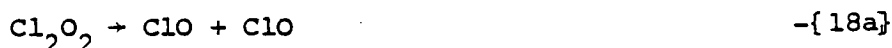
However , Cox⁸¹ was able to determine , by computer analysis , rates into {18b} - {18d} . His total second order rate constant , $k_{\{18bcd\}} = 1.0 \times 10^{-14} \text{ cm}^3 \text{ molec}^{-1} \text{ s}^{-1}$ is in good agreement with the value of $k_{\{18bcd\}} = 1.3 \times 10^{-14} \text{ cm}^3 \text{ molec}^{-1} \text{ s}^{-1}$ obtained by Basco⁷⁹ . These results are in disagreement with those of Clyne⁸² who monitored the decay of ClO mass spectrometrically in a flow system . They determined $k_{\{18bcd\}} = 2.3 \times 10^{-14} \text{ cm}^3 \text{ molec}^{-1} \text{ s}^{-1}$, and considered that {18c} was the major reaction at low pressures with {18d} as a minor (5%) reaction , but were unable to determine the extent of {18b} .

Cl_2O_2 is estimated to be a fairly stable molecule .

$\Delta H_{298}^{\circ} \{ \text{Cl}_2\text{O}_2 \} = -136 \pm 3 \text{ kJ mole}^{-1}$ and a bond strength of

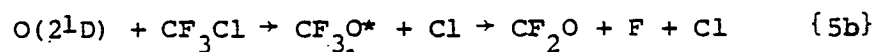
$D \{ \text{ClOO-Cl} \} = 79 \pm 5 \text{ kJ mole}^{-1}$ have been estimated by Basco⁷⁹ .

Subsequent removal of Cl_2O_2 is likely to be complicated , and the following reactions , in addition to -{18a} , have been suggested .



The decay of ClO and the formation of OClO over the first millisecond are thus too fast to be due to {18a} - {18d} . It is proposed

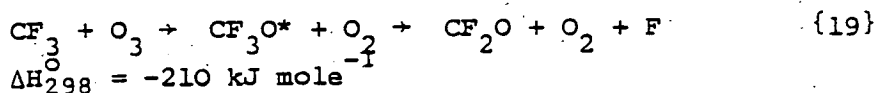
here that rapid reaction of ClO with FO leads to the observed ClO removal and OClO formation . F atoms may be formed by two reactions . Initially by {5b} ,



$\Delta H_{298}^{\circ} = -165 \text{ kJ mole}^{-1}$

3.7 cont'd

and secondly by {19} .

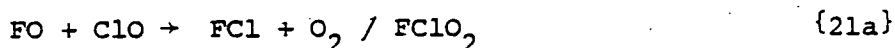


F atoms are rapidly converted into FO by reaction with O_3 ⁸³

$$k_{\{20\}} = 1.3 \times 10^{-11} \text{ cm}^3 \text{ molec}^{-1} \text{ s}^{-1}$$



Reaction of FO with ClO could proceed by two pathways to give the observed kinetics .,



$$\text{with a ratio } k_{\{21a\}} / k_{\{21b\}} = 4$$

Evidence for the intermediacy of F atoms is ;

- (a) , No OClo formation and no ClO decay was observed in the presence of C_2H_6 , which is a good scavenger of F atoms⁸⁴ .
- (b) No OClo formation and no rapid ClO decay was observed in the presence of Cl_2 (60 N m^{-2}) which reacts rapidly with F atoms $k_{\{22\}} = 1.6 \times 10^{-10} \text{ cm}^3 \text{ molec}^{-1} \text{ s}^{-1}$.⁸⁵
- $$\text{F} + \text{Cl}_2 \rightarrow \text{FCl} + \text{Cl} \quad \{22\}$$
- This experiment was not , unfortunately, quantitative as Cl_2 photolysis occurred .
- (c) Addition of O_2 (1.1 kN m^{-2}) to partially scavenge CF_3 radicals , reduced by more than half the OClo yield and the amount of ClO removed .
- (d) FO has been detected mass spectrometrically in the $\text{CF}_3\text{Br} / \text{O}_3$ system⁸⁶ . In the $\text{CF}_3\text{Cl} / \text{O}_3$ system it was not possible to distinguish between the FO and the Cl m/e peaks , but it seems reasonable to assume that FO was present .

Cross halogen oxide reactions between ClO and BrO have been reported by Clyne and Watson⁸⁷ , and by Basco and Dogra⁸⁸ . Clyne⁸⁷ showed that two pathways were of equal importance.



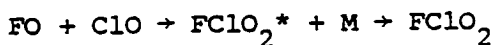
$$k_{\{23a\}} = k_{\{23b\}} = 6.7 \times 10^{-12} \text{ cm}^3 \text{ molec}^{-1} \text{ s}^{-1}$$

3.7 cont'd

Reactions {21a} and {21b} are thus reasonable. Reaction {21a} may yield $\text{FCl} + \text{O}_2$ ($\Delta H_{298}^\circ = -260 \text{ kJ mole}^{-1}$) or FCLO_2 ($\Delta H_{298}^\circ = -240 \text{ kJ mole}^{-1}$). FCLO_2 has a distorted pyramidal structure with the Cl atom at the apex⁸⁹.

It was first prepared by the reaction of F_2 with OCLO ⁹⁰.

Reaction {21b} may be an independent pathway, exactly analogous to {23b}, or it may arise from the disintegration of vibrationally excited FCLO_2



+



The decay of FCLO_2 has been shown to yield OCLO ⁸⁹.

The decay of ClO and the formation of OCLO were simulated, and the best fit is shown in figure 3.9.

Again it was assumed here that, as in the case of $\text{CF}_2\text{Cl}_2/\text{O}_3$ and CFCI_3/O_3 systems, reaction {5} and {19} could be written as one step, that is the intermediate CF_3O^* species disintegrates immediately on a μs time scale. The best fit equations are listed in table 3.4.

The decay of ClO after about 1 ms could be well simulated by a second order decay, corresponding to either reaction {18a} or {18b}, these reactions being indistinguishable in our system. The rate of decay, about $2 \times 10^{-14} \text{ cm}^3 \text{ molec}^{-1} \text{ s}^{-1}$, corresponds to a third order decay of about $3 \times 10^{-32} \text{ cm}^6 \text{ molec}^{-2} \text{ s}^{-1}$ which agrees well with the rate data for {18a} presented in table 3.5.

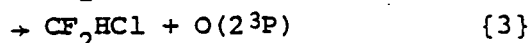
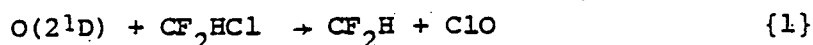
CHAPTER FOUR

REACTION OF O(2^1 D) WITH CF_2HCl

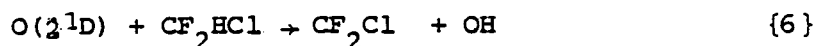


4.1 Introduction.

By analogy with the reactions of $O(2^1D)$ with CF_3Cl , CF_2Cl_2 and $CFCl_3$, the following reactions of $O(2^1D)$ with CF_2HCl bear consideration.

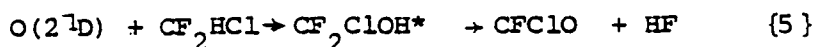


and by analogy with the reactions of $O(2^1D)$ with CH_4



Donovan et al ⁵², have reported a lower limit into {1}.

Lin ⁶⁰ observed HF, but not HCl, chemical laser emission following the reaction of $O(2^1D)$ with CF_2HCl , which he proposed proceeded by an insertion-elimination process.



In this chapter the reaction of $O(2^1D)$ with CF_2HCl is considered in some detail and branching ratios into channels {1} to {6} are presented. Some novel chemistry of CF_2 oxidation by ClO_x will also be discussed.

4.2 Experimental.

The apparatus for flash photolysis with time resolved kinetic spectroscopy has been described (Chapter 2).

The lower O_3 concentrations used in these experiments allowed the ClO concentrations to be measured at the (8,0) or (11,0) bands of the ($A^2\Pi_{3/2} + X^2\Pi_{3/2}$) system. Extinction coefficients of $\epsilon(11,0) = 3.0 \pm 0.2 \times 10^{-18.2} \text{ cm}^2 \text{ molec}^{-1}$ and $\epsilon(8,0) = 2.5 \pm 0.2 \times 10^{-18} \text{ cm}^2 \text{ molec}^{-1}$ were used. $\epsilon(8,0)$ was determined in the manner described in chapter 3, and is in good agreement with recent reports in the literature ^{69 70}.

The ($A^1B_1 + X^1A_1$) system of CF_2 consists of a series of regularly spaced bands in the region of 230 to 260 nm⁹². The concentration of CF_2 was monitored at the ($v_2^1 = 6$) band at 248.8 nm.

4.2 cont'd

An extinction coefficient for this band of $1.27 \times 10^{-18} \text{ cm}^2 \text{ molec}^{-1}$ was taken from the work of Tyerman⁹³. Absorbance of a band was found by Tyerman to be independent of slit width over 25 to 200 microns, the plate factor of Tyerman's spectrograph (2.5 \AA mm^{-1}) being similar to that of the Hilger Watts medium quartz spectrograph used in this work (1.5 \AA mm^{-1}). No significant variation in optical density was observed with pressures of added N_2 between 2.8 and 28 kN m^{-2} .

4.3 Results and discussion.

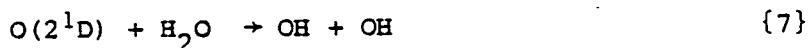
When O_3 (13 N m^{-2}) was photolysed in the presence of CF_2HCl (2.7 kN m^{-2}) strong spectra of CF_2 and ClO were observed, figures 4.1, 4.2. The formation of both CF_2 and ClO followed the integrated flash profile.

Branching ratio into ClO formation, {1} and Cl formation {2}.

The branching ratio into {1} + {2} is easily measured from figure 4.2. To determine the relative importance of {1} and {2}, C_2H_6 (66 N m^{-2}) was added. The result of this experiment is shown in figure 4.2, and indicates that the predominant source (> 80%) of ClO is {1}. The rapid decay of ClO to an undetectable concentration by 150 μs indicates that it is likely that there is a large branching ratio into $\text{O}(2^3\text{P})$ production. This will be discussed later. Branching ratios into {1} and {2} are listed in table 4.1

Branching ratio into OH formation, {6}.

The lack of secondary growth of ClO in the $\text{O}_3/\text{CF}_2\text{HCl}$ system suggests that there was little CF_2Cl formation and no OH was detectable by plate photometry. The much more sensitive technique of flash photolysis with OH resonance absorption detection was used to look for OH formation. The yield of OH following the photolysis of O_3 in an excess of H_2O was used as a standard.



This reaction was assumed to give 2 OH radicals⁹⁴.

Figure 4.f.

Temporal development of CF_2 in the O_3/CF_2 HCl system.

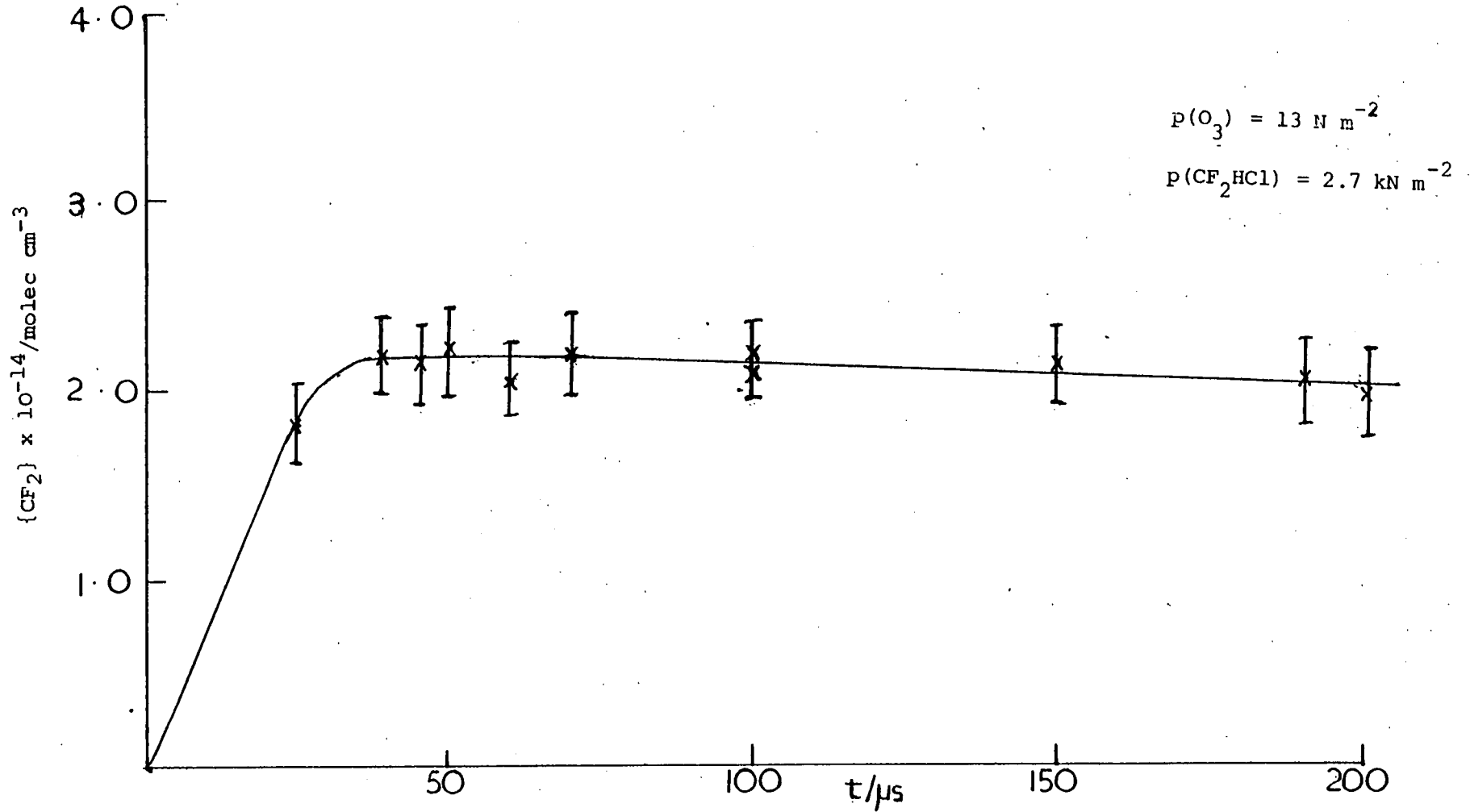


Figure 4.2

Temporal development of ClO in the O₃/CF₂HCl and the O₃/CF₂HCl/C₂H₆ systems.

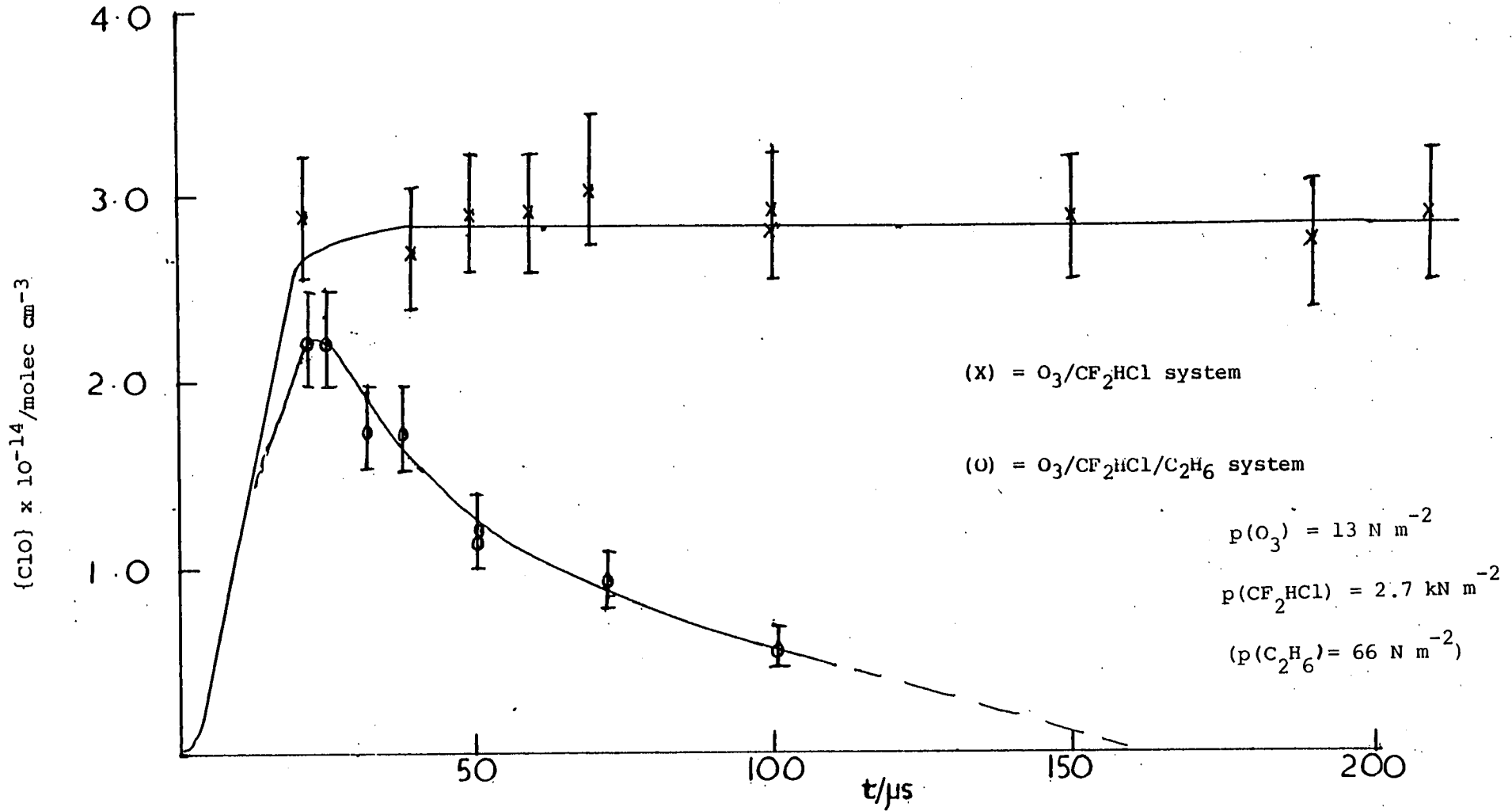


Table 4.1

Product branching ratios for the reaction of $O(^1D)$ with CF_2HCl

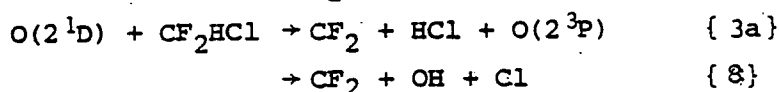
Reaction No.	1	2	4 + 5	6	3	3 (Addison)
Product	CF_2H + ClO	CF_2HO + $Cl.$	$CF_2O + HCl$ $CFCIO + HF$	CF_2Cl + OH	$O(^3P)$	$O(^3P)$
Branching ratio	0.55 ± 0.05	< 0.10	< 0.10	0.055 ± 0.01	0.42 ± 0.05	$0.28 \pm \begin{matrix} 0.10 \\ 0.15 \end{matrix}$

4.3 cont'd.

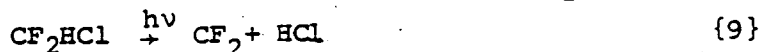
On this basis, the yield of OH from the reaction of $O(2^1D)$ with CH_4 was 0.75 ± 0.10 in excellent agreement with the results of Lin and De More³³. The branching ratio into {6} is shown on Table 4.1.

Branching ratio into CF_2 formation

Branching ratio into CF_2 production is 0.42 ± 0.05 . Two direct reactions leading to CF_2 production are possible, viz



{8} can be dismissed as a major pathway (< 0.05) as the yields of OH and Cl have been shown to be insignificant. Before considering {3a}, {9} to {14} will be discussed and shown not to contribute significantly to CF_2 production



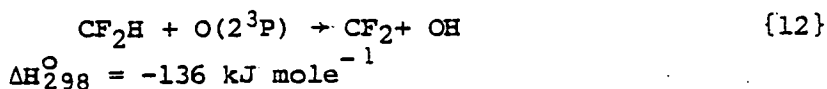
At the pressures of CF_2HCl used, no CF_2 was observed when CF_2HCl was flashed in the absence of O_3 .



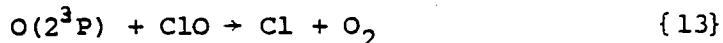
Disproportionation is a minor process competing with {11}, $k\{10\} / k\{11\} \sim 0.17$ ⁹⁵



Thus {10} can not account for all the CF_2 production but may contribute to an extent of < 0.10 .



A major contribution from this pathway may be ruled out, from the low branching ratio into OH formation. {12} would compete with {13}.



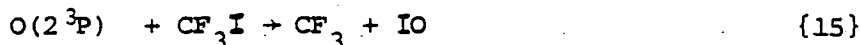
and any increase in ClO concentration would affect the CF_2 yield. No change in CF_2 yield was observed when the ClO concentration was varied from 3.0×10^{14} to 11.5×10^{14} molec cm^{-3} . This was achieved by the addition of Cl_2 ($< 95 \text{ N m}^{-2}$) to the O_3/CF_2HCl system, Cl atoms were produced by photolysis of Cl_2 and reacted with O_3 to give ClO



4.3 cont'd.

Finally, CF_3I was used to scavenge $\text{O}(2^3\text{P})$

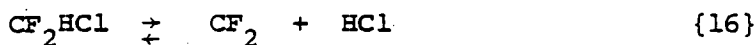
$$k = 1.1 \pm 0.2 \times 10^{-11} \text{ cm}^3 \text{ molec}^{-1} \text{ s}^{-1} \quad 55$$



and again no change in CF_2 yield was observed when small pressures of CF_3I (60 N m^{-2}) were added to the $\text{O}_3/\text{CF}_2\text{HCl}$ and $\text{N}_2\text{O}/\text{CF}_2\text{HCl}$ systems. These results all argue strongly against any significant occurrence (< 0.05) of {12}.

CF_2 was observed when N_2O was used as a source of $\text{O}(2^1\text{D})$, indicating that CF_2 is not formed by the reaction of some CF_2 containing molecule with O_3 . It was thus concluded that {3a} was the predominant CF_2 producing pathway.

{3a} is essentially similar to the quenching process observed in the reaction of $\text{O}(2^1\text{D})$ with CF_3Cl , CF_2Cl_2 and CFCl_3 , the only difference being that CF_2HCl can gain enough energy from the quenching of $\text{O}(2^1\text{D})$ to $\text{O}(2^3\text{P})$ to fragment to CF_2 and HCl . This process has been shown to occur readily on photolysis⁹⁶ and pyrolysis⁹⁷ of CF_2HCl , and, indeed, in pyrolysis an equilibrium is set up between CF_2HCl , CF_2 and HCl .



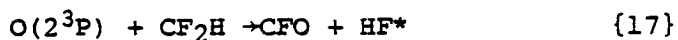
Similar disintegration reactions for CF_3Cl , CF_2Cl_2 and CFCl_3 are endothermic.

It is perhaps surprising that $\text{O}(2^3\text{P})$ escapes from the force field of CF_2 , as CF_2O is a very strongly bound molecule. This can be understood when it is realised that $\text{CF}_2(X^1\text{A}_1)$ and $\text{O}(2^3\text{P})$ do not correlate with the ground state of CF_2O , but with an excited triplet state which may not allow efficient combination. A similar explanation has been applied to the low reactivity of CF_2 to recombination⁹⁸.

The yield of CF_2 is taken as an upper limit into $\text{O}(2^3\text{P})$ formation (other processes may contribute to about 30% of the CF_2 yield). There is satisfactory agreement between the $\text{O}(2^3\text{P})$ yield based on the CF_2 yield, and that measured by Addison. The branching ratios for {1} to {6} are shown in Table 4.1.

4.3 cont'd.

Lin observed only HF laser emission, although formation of HCl is more exothermic following the flash photolysis of O_3/CF_2HCl mixtures⁶⁰. He postulated that reaction occurred by an insertion-elimination mechanism. The present results show that HF elimination cannot account for more than 10-20% of the total reaction cross section, (this is based on the error bounds for the products which are observed) and that elimination of ground state HCl is a major process. It seems unlikely that chemical laser emission would occur from a minor reaction channel. In a separate series of studies Lin has suggested that the reaction



can give rise to HF laser emission. The above results show that both $O(2^3P)$ and CF_2H are major products of the reaction of $O(2^1D)$ with CF_2HCl , and it is suggested here that reaction {17} could account for Lin's observations in the O_3/CF_2HCl photochemical laser system.

4.4 Effect of translational energy of $O(2^1D)$ on the CF_2 yield

The thermochemistry of {3a} ($\Delta H_{298}^{\circ} = +17 \pm 18.5 \text{ kJ mole}^{-1}$) would seem to disfavour the reaction, in that it would require essentially all the electronic energy of $O(2^1D)$ to be channelled into vibrational energy of CF_2HCl , and none to go into translational energy of $O(2^3P)$ or CF_2HCl . However this restraint may be relaxed somewhat if it is considered that $O(2^1D)$ reacts with CF_2HCl on every collision and has no time to lose its excess translational energy which is therefore available to the reaction. Transfer of electronic and translational energy into vibrational excitation of the products has been observed for the reaction of $O(2^1D)$ with O_2 . To determine whether the excess translational energy of $O(2^1D)$ affects the reaction, $O(2^1D)$ was thermolysed by the addition of He (7.2 kN m^{-2}), (pressure of CF_2HCl was 760 N m^{-2} in this experiment). No reduction in CF_2 yield was observed. It was thus concluded that {3a} is exothermic and that the excess translational energy of $O(2^1D)$ is not required for reaction to occur.

4.5 Decay of CF₂

CF₂ in the singlet ground state is surprisingly inert towards a wide range of molecules including O₂(³Σ) and alkenes¹⁰⁰. The major removal process under the conditions previously studied is dimerisation, $k_{\{18\}} = 3.7 \times 10^{-14} \text{ cm}^3 \text{ molec}^{-1} \text{ s}^{-1}$ ⁹³.

$$\text{CF}_2 + \text{CF}_2 + \text{M} \rightarrow \text{C}_2\text{F}_4 + \text{M} \quad \{18\}$$

CF₂, formed by the reaction of O(2¹D) with CF₂HCl, decayed at a rate considerably in excess of {18}. Species which could react with CF₂ under the experimental conditions were O₃, O₂(¹Δ) and ClO. The ClO concentration was varied as described above, and the results (figure 4.3) indicate a clear relationship between the rate of CF₂ removal and the ClO concentration. In the case when no ClO was present (obtained by the addition of C₂H₆, 130 N m⁻²) the rate of CF₂ decay was in excellent agreement with Tyerman's value for {18}⁹³. For most experiments the decay of ClO was about that due to the disproportionation reactions of ClO⁷⁹⁻⁸². At the highest ClO concentrations however, when sufficient Cl₂ was photolysed to remove all the O₃, the rate of ClO decay was greatly enhanced, and was similar to that of CF₂. These results suggest that Cl atoms are a product of the reaction of CF₂ with ClO,



$$\Delta H_{298}^{\circ} \{19\} = -428 \text{ kJ mole}^{-1}$$

This reaction is analogous to that proposed by Lin¹⁰¹



Rate of reaction of CF₂ with ClO

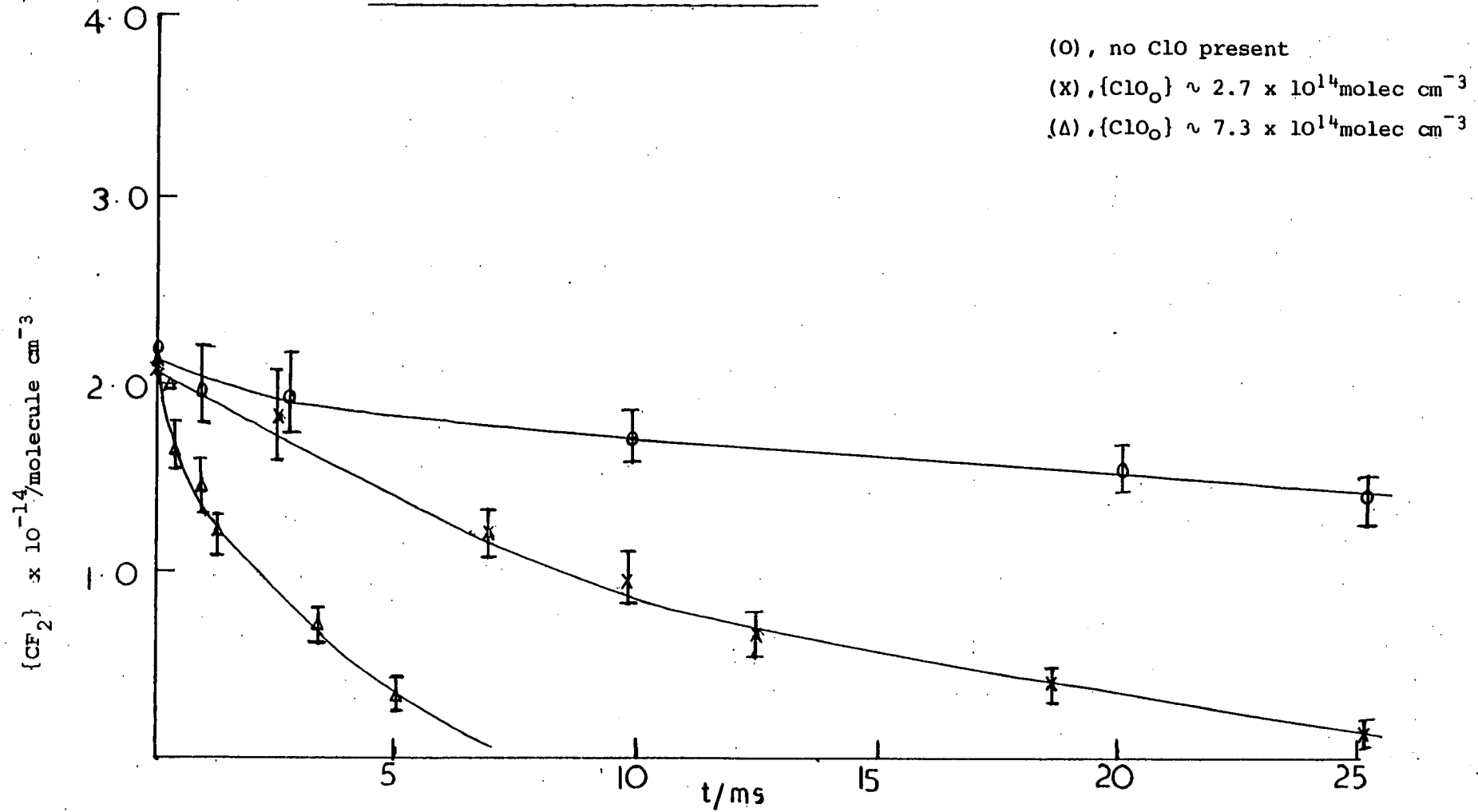
The rate of CF₂ decay is given by the expression,

$$-\frac{d\{\text{CF}_2\}}{dt} = k\{\text{CF}_2\}\{\text{ClO}\}$$

However, as ClO was being regenerated by {14}, and removal of ClO by disproportionation was slow, the concentration of ClO was approximately constant over a considerable portion of the CF₂ decay. It was thus possible to treat the CF₂ decay as pseudo first order. First order plots of the CF₂ decay were linear over several milliseconds.

Figure 4.3.

Decay of CF_2 in the presence of ClO .



4.5 cont'd

Table 4.2 lists the first order rate constants and the average ClO concentration over the time of the decay .

Least mean squares analysis gives $k_{\{19\}} = 6.3 \pm 0.6 \times 10^{-13} \text{ cm}^3 \text{ molec}^{-1} \text{ s}^{-1}$.

4.6 Decay of CF₂ in the presence of O₂

In the presence of O₂ (460 N m⁻²) , CF₂ decayed rapidly over the first millisecond , and then more slowly with a rate comparable to that of {19} over the remainder of the decay (figure 4.4) . If C₂H₆ (130 N m⁻²) was added , the decay of CF₂ was very slow over the entire decay and had a rate in excellent agreement with Tyerman's value for {18}⁹³ . This indicates that a Cl containing species is responsible for the rapid initial decay of CF₂ , the most likely species being ClO . In the presence of O₂ , ClO is formed by {20} in competition with {14} .



ClO is unstable and is removed by {21} to {23} .



and ClO will only be present in significant concentrations when there is a significant source of Cl atoms , *i.e.* during and just after the flash . Production of ClO by {24} is not likely to be significant due to the slow rate of {24}⁸².



There was no rapid removal of ClO during the time of the CF₂ decay

Due to the uncertainty in the rate of {20}^{102, 87} , it is difficult to estimate the ClO concentration accurately , however from the value of Clyne, the ClO concentration should be less than 1% of the ClO concentration and it is therefore difficult to explain such a large removal of CF₂ .

Table 4.2

First order rate constants of CF₂ decay and ClO concentration

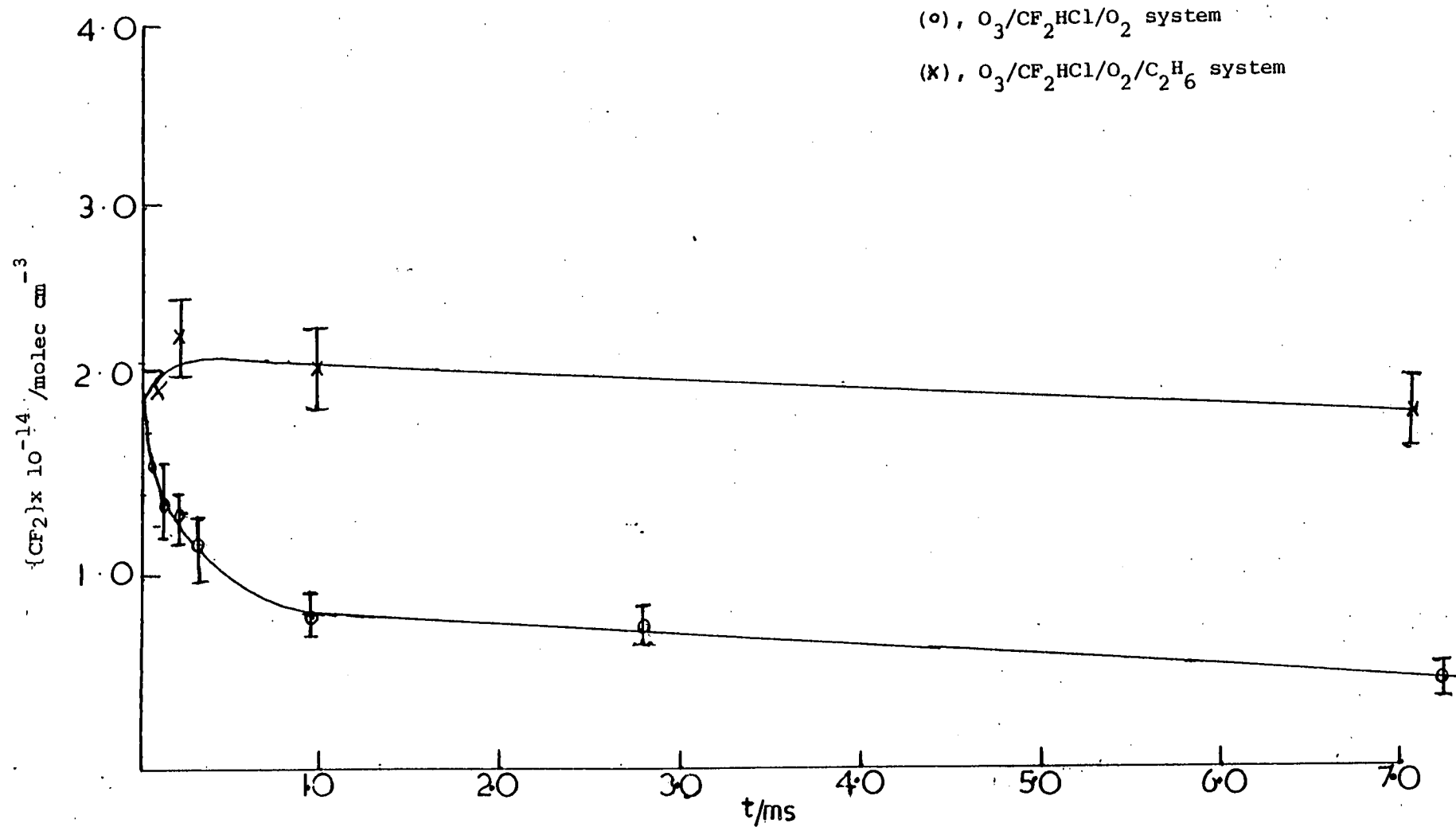
Exp. No.	ClO x 10 ⁻¹⁴ /molec cm ⁻³	k/ s ⁻¹
10	2.1	75
10	2.7	120
19	5.4	270
18	5.1	360
18	7.3	435
16	7.5	463
16	10.5	590



$$k_{\{19\}} = 6.3 \pm 0.6 \times 10^{-13} \text{ cm}^3 \text{ molec}^{-1} \text{ s}^{-1}$$

Figure 4.4

Decay of CF_2 in the presence of O_2

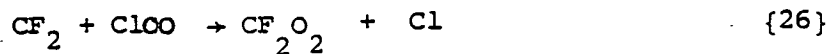


4.6 cont'd

Reaction of CF_2 with ClOO could proceed either by {25} analogous to {19} ,



or , since the Cl-O_2 bond is much weaker than the ClO-O bond , by {26} ,

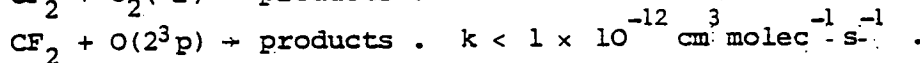
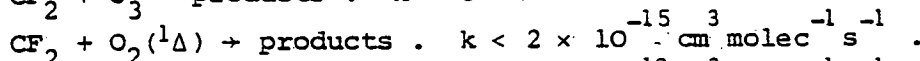
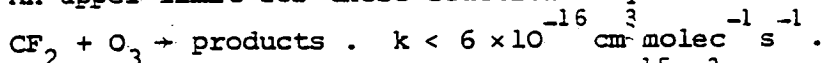


More work is required to determine whether ClOO or some other Cl containing species is responsible for the observed CF_2 kinetics .

4.7 Reaction of CF_2 with O_3 , $\text{O}_2(^1\Delta)$ and $\text{O}(2^3\text{P})$

In the absence of ClO the decay of CF_2 was second order with a rate constant of $4 \times 10^{-14} \text{ cm}^3 \text{ molec}^{-1} \text{ s}^{-1}$ in excellent agreement with Tyerman's value for {18}⁹³. There was no evidence for removal of CF_2 by reaction with O_3 , $\text{O}_2(^1\Delta)$ or $\text{O}(2^3\text{P})$.

An upper limit for these reactions may be estimated .



CHAPTER FIVE

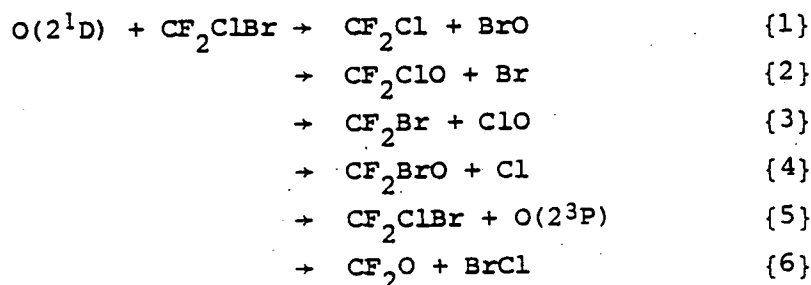
REACTION OF O(2¹D) WITH CF₂ClBr AND DISCUSSION

OF THE REACTION OF O(2¹D) WITH HALOMETHANES

5.1 Reaction of O(2¹D) with CF₂ClBr and CF₃Br

Photolysis of O₃ (27 N m⁻²) in the presence of CF₂ClBr (530 N m⁻²) and SF₆ (4.2 kN m⁻²) led to strong spectra of BrO and OClO (figure 5.1) . The BrO concentration was measured at the (4,0) band of the (A²Π ← X²Π) absorption at 338 nm . In this work an extinction coefficient for this band , $\epsilon = 4.8 \pm 1.2 \times 10^{-18} \text{ cm}^2 \text{ molec}^{-1}$, was taken from the work of Clyne¹⁰³ . This value is in good agreement with an earlier determination of Basco and Dogra's⁸⁸ , but is in poor agreement with an earlier value of Clyne's¹⁰⁴ .

The following pathways in the reaction of O(2¹D) with CF₂ClBr bear consideration .



No ClO was detected (limit of detectability $0.5 - 0.75 \times 10^{14} \text{ molec cm}^{-3}$) . However addition of C₂H₆ (60 N m⁻²) completely suppressed the formation of OClO . This may be understood if OClO is formed by {7}



and that ClO is formed by the reaction of Cl atoms with O₃ , {8} .

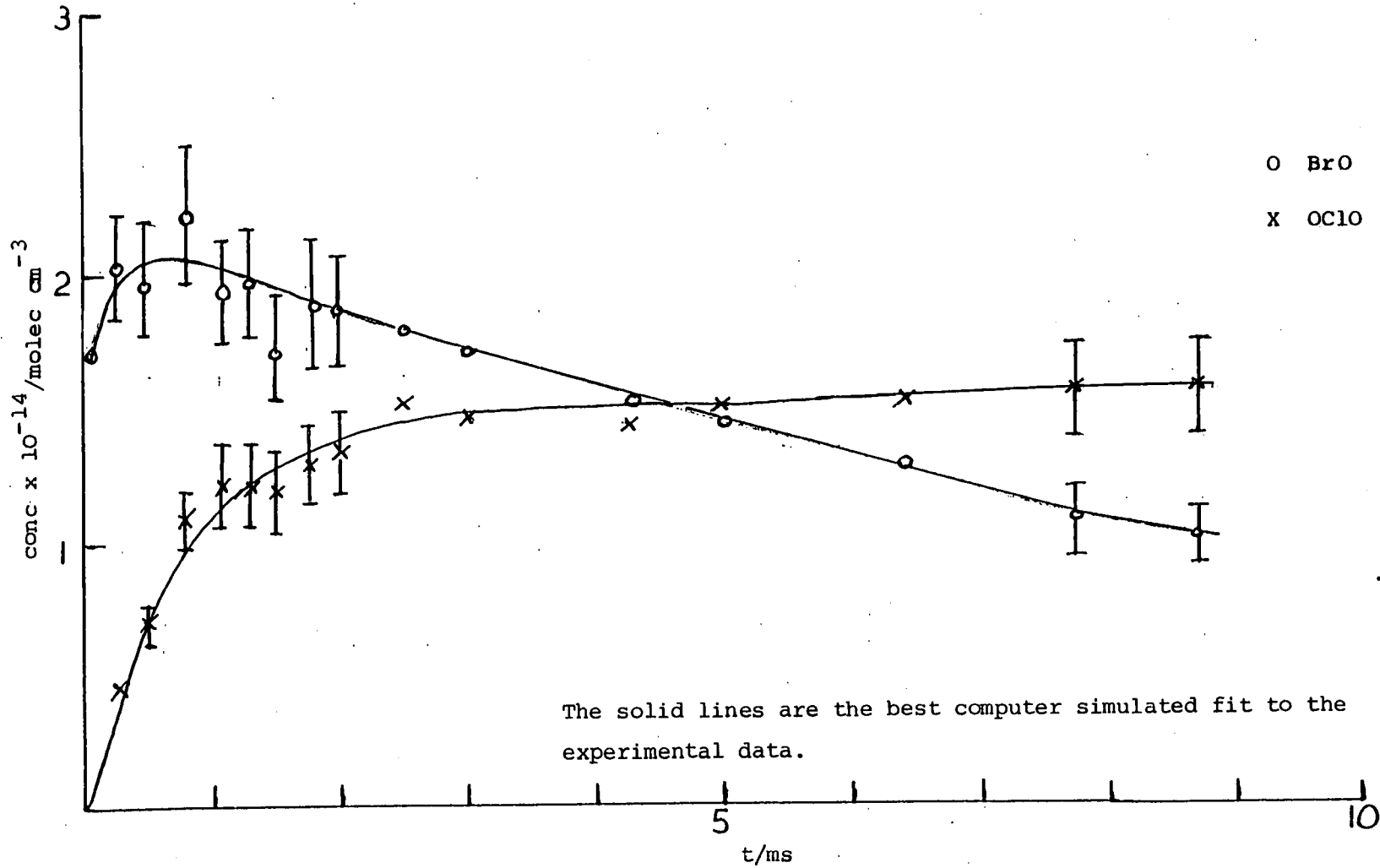


Cl atoms being formed by {4}

or by the reaction of CF₂Cl with O₃ (chapter 3) .

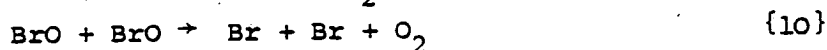
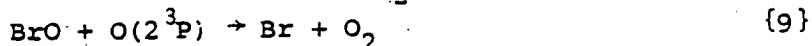
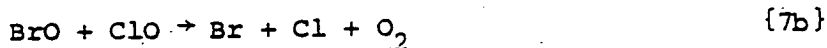
Figure 5.1.

Temporal development of BrO and OClO in the O_3/CF_2Cl Br system



5.1 cont'd

It was not possible to determine branching ratios into reactions ({1} + {2}) directly, because removal of BrO by {7b} , {9} and {10} is fast ,



while reformation by {11} is slow.



And thus a significant proportion of BrO_x is present as Br atoms. Nor was it possible to distinguish between {1} and {2} as Br atoms are not removed to any significant extent by reaction with C₂H₆ .

However approximate branching ratios were obtained by computer simulation of the BrO and OClO concentration profiles . Initial values were taken from the work on the reaction of O(2¹D) with CF₂Cl₂ , and assuming that Br atoms were abstracted in preference to Cl atoms . It proved possible to simulate accurately the BrO and OClO concentration profiles after a few attempts . The simulated profiles are shown in figure 5.1 and the best fit equations are listed in table 5.1 .

The slow decay of BrO is presumably due to {12}



in competition

with {10} . The decay was second order with a rate of $k_{\{12\}} \approx 3 \times 10^{-13} \text{ cm}^3 \text{ molec}^{-1} \text{ s}^{-1}$, and accounts for about 5% of the total reaction cross section.

The temporal development of BrO following the flash photolysis of O₃ (27 N m⁻²) in the presence of CF₃Br (2.7 kN m⁻²) is shown in figure 5.2

Table 5.1

Best fit computer simulation of the reaction of $O(^1D)$ with CF_2ClBr

No.	Equation	$k/cm^3 \text{ molec}^{-1} s^{-1}$	Ref.
	$O_3 \rightarrow O_2(^1\Delta) + O(^1D)$		61-65
1	$O(^1D) + CF_2ClBr \rightarrow CF_2Cl + BrO$	$2.6 \text{ E } -11$	calc.
2	$O(^1D) + CF_2ClBr \rightarrow CF_2O + Br + Cl$	$1.0 \text{ E } -11$	calc.
5	$O(^1D) + CF_2ClBr \rightarrow CF_2ClBr + O(^3P)$	$2.5 \text{ E } -11$	calc.
6	$O(^1D) + CF_2ClBr \rightarrow CF_2O + BrCl$	$3.9 \text{ E } -11$	calc.
8	$Cl + O_3 \rightarrow ClO + O_2$	$1.2 \text{ E } -11$	74
11	$Br + O_3 \rightarrow BrO + O_2$	$1.2 \text{ E } -12$	103
	$O(^3P) + ClO \rightarrow Cl + O_2$	$5.3 \text{ E } -11$	75
9	$O(^3P) + BrO \rightarrow Br + O_2$	$2.5 \text{ E } -11$	151
10	$BrO + BrO \rightarrow Br + Br + O_2$	$6.4 \text{ E } -12$	103
	$BrO + BrO \rightarrow Br_2 + O_2$	$3.3 \text{ E } -12$	calc.
	$Cl + BrCl \rightarrow Cl_2 + Br$	$1.5 \text{ E } -11$	170
	$Cl + OClO \rightarrow ClO + ClO$	$5.9 \text{ E } -11$	171
	$CF_2Cl + CF_2Cl \rightarrow C_2F_4Cl$	$2.0 \text{ E } -11$	78
	$CF_2Cl + O_3 \rightarrow CF_2O + O_2 + Cl$	$2.0 \text{ E } -13$	calc.
	$O(^3P) + BrCl \rightarrow BrO + Cl$	$2.1 \text{ E } -11$	151
7a	$BrO + ClO \rightarrow Br + OClO$	$6.7 \text{ E } -12$	87
7b	$BrO + ClO \rightarrow Br + Cl + O_2$	$6.7 \text{ E } -12$	87
	$O_2(^1\Delta) + O_3 \rightarrow O_2 + O_2 + O(^3P)$	$4.0 \text{ E } -15$	169

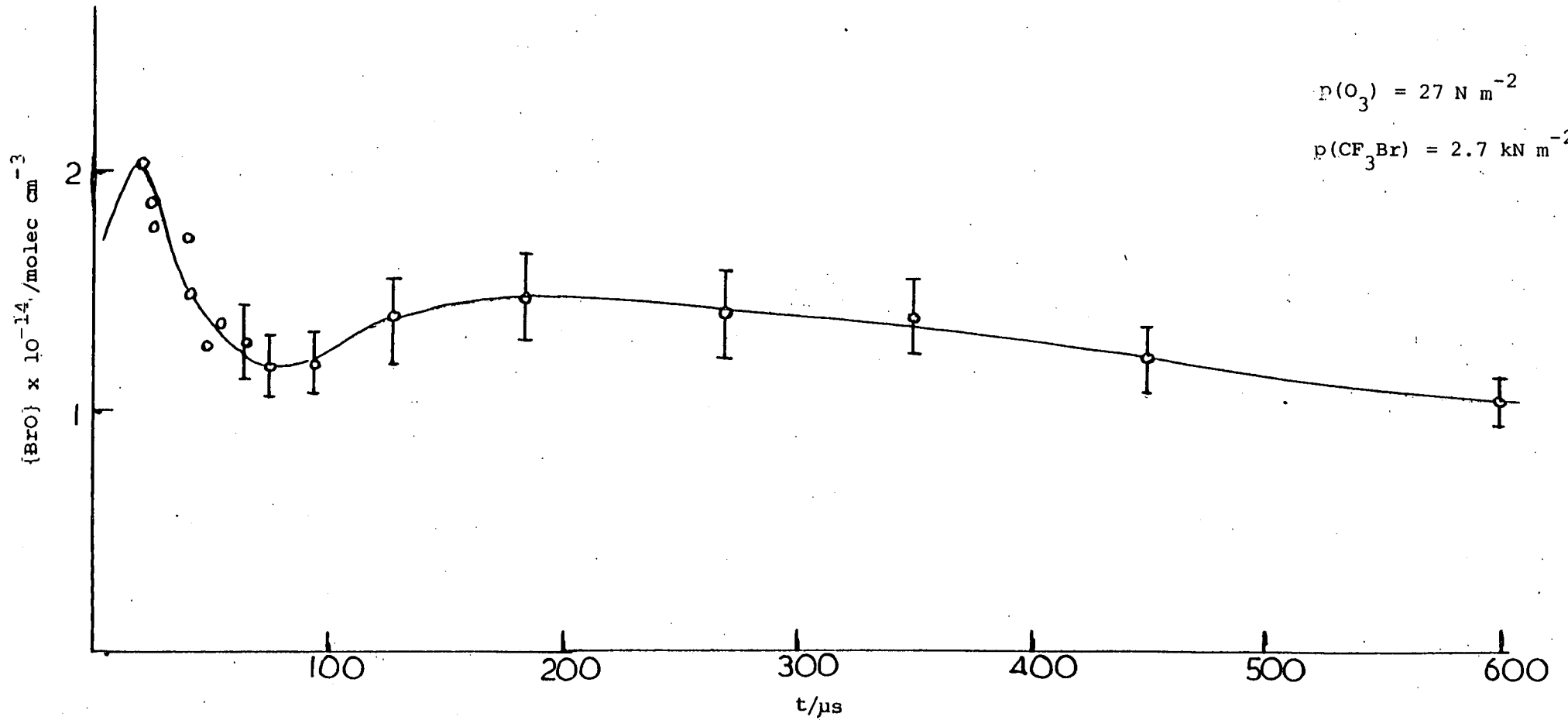
The simulated branching ratios are thus :-

Reaction

1	26 %
2	10 %
5	25 %
6	39 %

Figure 5.2.

Temporal development of BrO in the O₃/CF₃ Br system



5.1 cont'd

The decay of BrO after $\sim 30 \mu\text{s}$ is too fast to be due to {9}, and may be due to the involvement of F atoms or FO radicals, whose formation in this system has been observed by Kaufmann⁸⁶.

It did not prove possible to simulate the reaction kinetics. A lower limit into BrO formation of 0.25 may be estimated.

5.2 Discussion.

Table 5.2 lists the branching ratios for the reactions of $\text{O}(2^1\text{D})$ with CF_3Cl , CF_2Cl_2 , CFCl_3 , CF_2HCl , CH_3Cl and CCl_4 . (Values for the last two species were obtained by M.C. Addison using the apparatus described in Chapter 2). It can be seen that the branching ratio into any particular channel is approximately similar over the entire range of compounds. This mirrors the similarity in branching ratios found by Cvetanovic³² for the reaction of $\text{O}(2^1\text{D})$ with a series of alkanes. However, there is a considerable contrast between the products of the reaction of $\text{O}(2^1\text{D})$ with CFCs and hydrogen containing CFCs (collectively halomethanes) and with alkanes. For the former direct abstraction of a halogen atom, and quenching of $\text{O}(2^1\text{D})$ to $\text{O}(2^3\text{P})$ are the major pathways, while for alkanes insertion into a C-H bond is the major channel and quenching is insignificant, $\leq 3\%$.

It is interesting to compare the branching ratios for the reactions of $\text{O}(2^1\text{D})$ with halomethanes with the bond additivity relationship of Davidson⁶ et al which relates the total rate constant to the number of F, H and Cl atoms in a particular molecule, viz,

$$k(\text{C}_n \text{H}_a \text{F}_b \text{Cl}_c) = ak_{\text{H}} + bk_{\text{F}} + ck_{\text{Cl}}$$

where

$$k_{\text{H}} = 0.32 \pm 0.02 \times 10^{-10} \text{ cm}^3 \text{ molec}^{-1} \text{ s}^{-1}$$

$$k_{\text{F}} = 0.030 \pm 0.003 \times 10^{-10} \text{ cm}^3 \text{ molec}^{-1} \text{ s}^{-1}$$

$$k_{\text{Cl}} = 0.74 \pm 0.03 \times 10^{-10} \text{ cm}^3 \text{ molec}^{-1} \text{ s}^{-1}$$

Table 5.2

Branching ratios for the reaction of $O(^1D)$ with some CFCs and H containing CFCs

Compound	Halogen oxide (XO)	Halogen atom X	Halogen molecule X_2	$O(^3P)$	OH
CF_3Cl	0.55 ± 0.10	0.23 ± 0.10	< 0.10	0.27 ± 0.10 0.30 ± 0.10 0.15	-
CF_2Cl_2	0.50 ± 0.10	0.05 ± 0.10 0.05	< 0.25	0.20 ± 0.10	-
$CFC1_3$	0.45 ± 0.10	0.10 ± 0.10	< 0.25	0.20 ± 0.10	-
CF_2HCl	0.55 ± 0.05	< 0.10	< 0.10	$< 0.42 \pm 0.05$ 0.28 ± 0.10 0.15	0.055 ± 0.01
CCl_4	0.28 ± 0.18	< 0.33	< 0.20	0.22 ± 0.10	
CH_3Cl	< 0.36	> 0.29	< 0.20	not measured	0.35 ± 0.06

5.2 cont'd.

It would appear reasonable to assume that these figures reflect the preference of $O(2^1D)$ towards attack at a particular atom. For attack at Hydrogen the major reactions are likely to be insertion into the C-H bond or H atom abstraction, both leading to OH formation in the presence of O_3 , and thus the branching ratio into OH formation following the reaction of $O(2^1D)$ with hydrogen containing species should be close to the value of the fractional reactivity at the H atom. For CF_2HCl the expected yield is then $0.32/1.06 = 0.30$, against an experimental value of 0.05 ± 0.01 , and for CH_3Cl $0.96/1.70 = 0.56$ against 0.35 ± 0.06 observed experimentally. It thus appears that the trends in reactivity observed by Davidson *et al* are not directly related to $O(2^1D)$ attack at individual sites on a molecule.

This preference for abstraction of halogen atoms by $O(2^1D)$ is similar to the behaviour of the isoelectronic species CH_2 (1A_1). Singlet CH_2 reacts with alkanes by insertion into the C-H bond, but with chloroalkanes predominantly by Cl atom abstraction¹⁰⁵.

This behaviour can be understood if the interaction which occurs between the vacant p orbital of $O(2^1D)$ (or CH_2 (1A_1)) and the lone pairs on the halogen atom is considered. The potential surface contains an attractive basin surrounding the chlorine atom which facilitates attack at this point on the molecule. There will be a further attractive region in the potential surface, corresponding to $O(2^1D)$ insertion to form a hypochlorite, however, this region is apparently less accessible, possibly due to inertial effects. Both Cl and CF_3 are relatively heavy species and need to move a considerable distance for insertion to occur (in contrast to the situation for C-H insertion, where the much lighter H atom can move rapidly to accommodate the insertion process). And possibly because $O(2^1D)$ will feel the outer attractive basin surrounding the chlorine atom and will react there, before it can experience the inner attractive well.

5.2 cont'd.

An argument similar to that used to explain the products of the reaction of $O(2^1D)$ with CH_4 , may thus be applied.

The large rate constants for overall removal of $O(2^1D)$ by halomethanes, indicate that reaction occurs at large impact parameter collisions where the $O(2^1D)$ atom will only experience to any significant extent the attractive well surrounding the Cl atom and will react by abstraction. At closer impact parameter collisions, in addition to Cl atom abstraction, insertion into C-Cl bonds and C-H bonds will occur and at small impact parameters a concerted insertion-elimination process leading to molecular elimination may occur.

By this explanation the total rate of $O(2^1D)$ removal would be expected to increase as the number of Cl atoms was increased or as Cl was replaced by Br or I. The first trend is well established⁶. And in this laboratory the total rates of $O(2^1D)$ removal by CF_3Br and CF_3I were found to be 1.4, and 5.3 relative to CF_3Cl ¹⁰⁶, in support of the second prediction.

However, in addition to the above reactions, quenching of $O(2^1D)$ to $O(2^3P)$ is an important process, indicating that the singlet surface must be crossed by one or more triplet surfaces correlating with $O(2^3P)$ and halomethane, and that non adiabatic transitions at these crossings must be favourable, as evidenced by the relatively high branching ratios into $O(2^3P)$ formation. A possible potential energy diagram is shown in figure 5.3. The species $RCIO$, postulated as a reaction complex, is not known but the CF_3I analogue CF_3IO ¹⁰⁷ has been prepared in solution at low temperature, and is a singlet molecule. It is suggested that the $RCIO$ (or RIO) species is sufficiently long lived to pass through the singlet-triplet crossing region several times leading to quenching. It may also break up to yield $R + ClO$ (or IO).

Figure 5.3
Potential energy diagram of the reaction of $O(2^1D) + RCl$

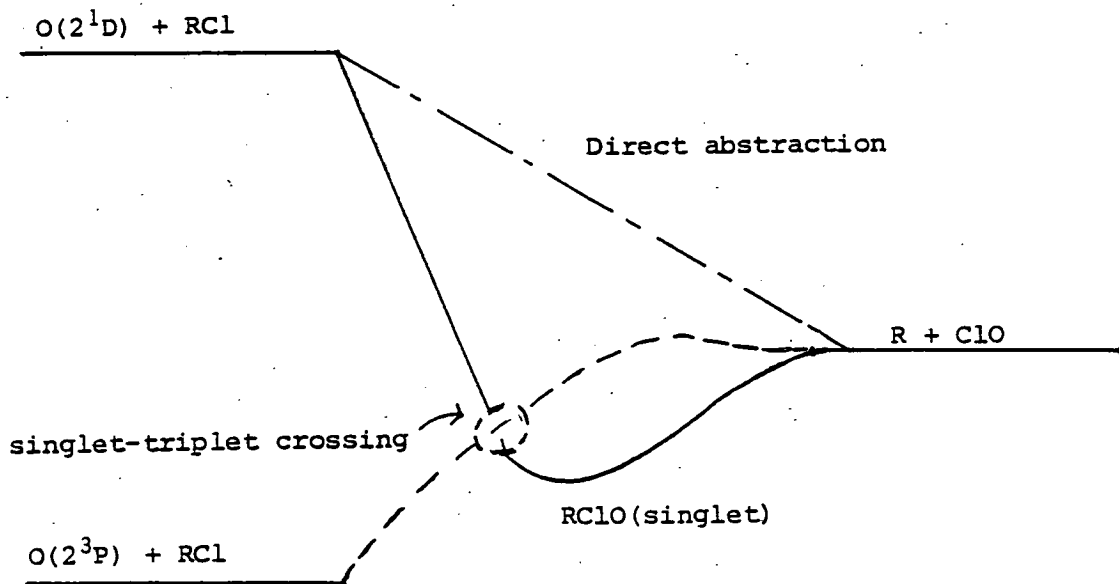
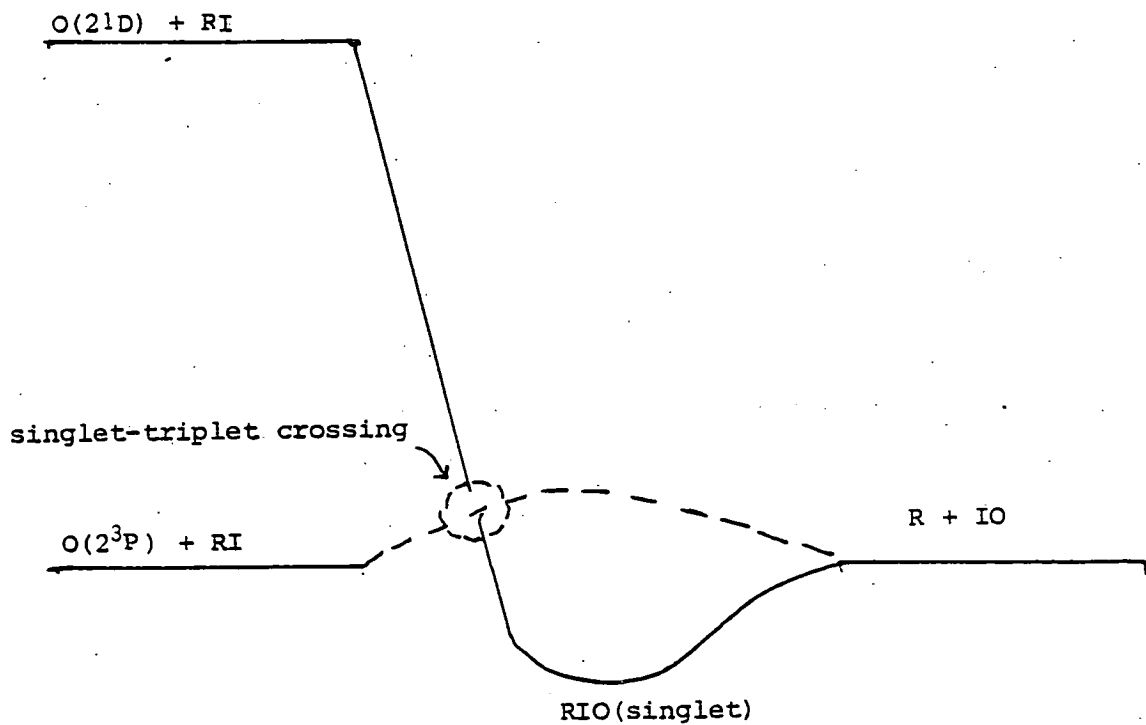


Figure 5.4
Potential energy diagram for the reaction of
 $O(2^1D)$ and $O(2^3P) + RI$



5.2 cont'd.

The reactions of $O(2^3P)$ with CF_3I ¹⁰⁸ and with halogens¹⁰⁹⁻¹¹¹ have been shown to proceed via a long lived complex, CF_3IO or OXY . For reaction of $O(2^3P)$ with the interhalogens the least electronegative atom is observed to be in the central position, in accord with the predictions of Walsh's rules. And species such as $FCIO$ ¹¹² and $ClClO$ ¹¹³ have been observed in matrix isolation experiments, these species have a normal Cl-O bond, but a weaker and longer F-Cl or Cl-Cl bond. Insertion of $O(2^3P)$ into the halogen molecule to give the most stable configuration XOY is not observed. There is predicted to be a considerable barrier to this process¹¹⁰.

The reaction of $O(2^3P)$ with CF_3Br is endothermic ($\Delta H^\circ_{298} = +65 \pm 5 \text{ kJ mole}^{-1}$) and is negligibly slow at 300 K. However, the reaction has been studied at elevated temperatures¹¹⁴ (800 - 1200 K) and Arrhenius parameters determined as $A = 1.5 \pm 0.5 \times 10^{-11} \text{ cm}^3 \text{ molec}^{-1} \text{ s}^{-1}$ and $E = 57 \pm 4 \text{ kJ mole}^{-1}$. The activation energy is thus close to the endothermicity. The Arrhenius pre-exponential factor for the reaction of $O(2^3P)$ with CF_3I is likely to be similar to that of $O(2^3P)$ with CF_3Br . Donovan⁵⁵ *et al* have shown that the activation energy for the former reaction is $<6 \text{ kJ mole}^{-1}$, and the fact that the rate constant for $O(2^3P)$ reacting with CF_3I ⁵⁵ is close to the pre-exponential factor for the reaction of $O(2^3P)$ with CF_3Br , suggests that the assumption of similar pre-exponential factors is valid. Thus it would seem that the reactions of $O(2^3P)$ with halomethanes and halogens proceed with negligible activation energies but with low pre-exponential factors relative to $O(2^1D)$. This is surprising as the kinematic features are similar for $O(2^1D)$ and $O(2^3P)$.

This has been explained by the suggestion that the reaction complex OXY ¹⁰⁹ is only stable in a near linear configuration, and hence that only colinear or near colinear approach leads to successful reaction.

5.2 cont'd.

Herschbach¹¹⁰ has suggested that the OXY species will be a triplet in a near linear configuration if the $3\sigma^*$ molecular orbital falls below the $3\pi^*$ molecular orbital.

However, Andrews *et al*^{112, 113} estimate the bond angle in FClO and ClClO to be about 120° , and CF_3IO has been shown to be a singlet molecule¹⁰⁷.

It is, therefore, suggested here that the reaction of $O(2^3P)$ with CF_3I and CF_3Br proceeds by a singlet surface, and that the low pre-exponential factor is the result of a low triplet-singlet transition probability (figure 5.4). An exactly similar explanation may be applied to the reaction of $O(2^3P)$ with halogens.

5.3 Conclusion:

In conclusion, the branching ratios for the reaction of $O(2^1D)$ with various CFCs are approximately constant, with abstraction of a Cl atom to form ClO, or quenching to $O(2^3P)$ being the major process.

The reaction is considered to proceed predominantly by a RC1O complex. This complex is likely to be a singlet, but crossing to a triplet surface corresponding to RCl and $O(2^3P)$ is favourable. Fragmentation of RC1O to R and ClO is also a likely process.

OH formation occurs in the reaction of $O(2^1D)$ with hydrogen containing CFCs, but the relatively low yields of OH indicate that attack at the H atoms is disfavoured relative to attack at Cl atom(s).

Minor pathways in the reaction of $O(2^1D)$ with CFCs and hydrogen containing CFCs are insertion into a C-Cl bond, leading to RO and Cl atom formation, and a concerted insertion elimination mechanism leading to molecular elimination.

Chapter Six

Reaction of OH with CHCl_3 , CDCl_3 , CH_2Cl_2 , CD_2Cl_2 and NH_3

6.1 Introduction

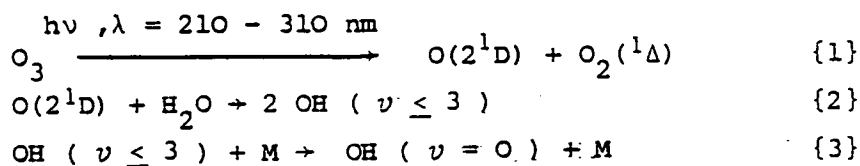
In this chapter the rates of abstraction of H atoms from NH_3 , CHCl_3 and CH_2Cl_2 by OH will be presented. These rates are well established in the literature and will serve as a comparison to the rates obtained here. The rate of abstraction of D atoms from CDCl_3 and CD_2Cl_2 will also be presented and the kinetic isotope effect, $k_{\text{H}}/k_{\text{D}}$, will be discussed.

Howard¹⁶ observed a good correlation between the rate of reaction of OH with halomethanes and the C-H bond strength. As the pre-exponential factors for all these compounds are similar this suggests a relationship between activation energy and bond strength. In this chapter the correlation between rate of reaction and dipole moment of the H donor will be discussed in terms of nascent product repulsion.

Finally, the yield of OH from the reaction of $\text{O}(2^1\text{D})$ with NH_3 will be presented.

6.2 Experimental

The apparatus to monitor OH has been described in chapter 2. OH was produced by the reaction of $\text{O}(2^1\text{D})$ with H_2O following the flash photolysis of O_3 in the Hartley continuum

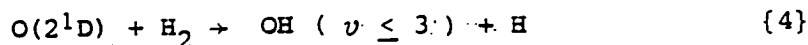


Simoniatis and Heicklen have shown that {2} accounts for > 96 % of the reaction cross section of $\text{O}(2^1\text{D})$ with H_2O^{94} .

OH^* is efficiently quenched by H_2O^{115} , and no problems with vibrationally excited OH were observed in the above system.

6.2 cont'd

However, when H_2 was used as a source of OH, the observed yield of OH ($v = 0$) was greatly reduced. The reaction scheme was then,

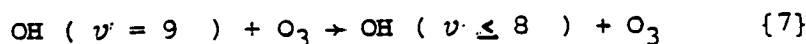


OH ($v \leq 9$) is also formed by the reaction of OH with H_2 ,

$$k\{6\} = 8.0 \times 10^{-15.3} \text{ cm}^3 \text{ molec}^{-1} \text{ s}^{-1} \quad 116$$



followed by {5}. Reaction of OH ($v = 9$) with O_3 is approximately 100 times faster than that of OH ($v = 0$) and leads to quenching and reaction.¹⁷⁶



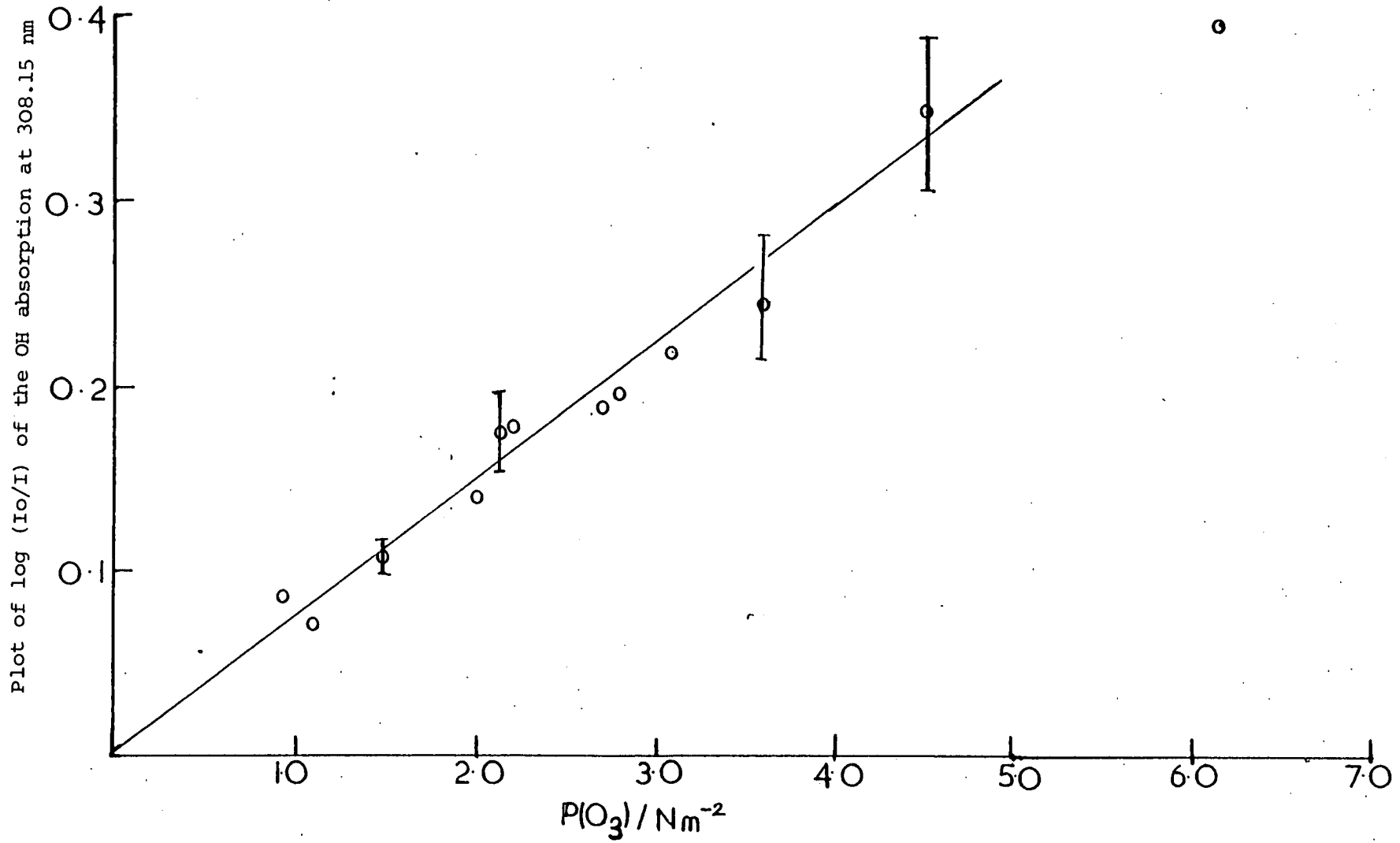
and hence vibrationally excited OH is likely to react chemically with O_3 , thus leading to removal of OH from the system, before it can be quenched all the way down to OH ($v = 0$). A low yield of OH ($v = 0$) would then be expected. Addition of small pressures of H_2O greatly increased the OH ($v = 0$) concentrations.

Experiments with varying O_3 concentrations and constant flash energy showed the expected logarithmic dependence of the maximum OH absorption on the O_3 concentration, that is $\log(I_0/I) = k\{O_3\}$, for absorbances up to ≈ 0.30 (figure 6.1). A plot of $\log(\log(I_0/I))$ versus $\log\{O_3\}$ was linear with a slope of 1.01 ± 0.06 , as expected from a non self-reversed emission line. Thus the Beer Lambert law was used in its normal form.

Experiments were done in a standard fashion. The pressure of O_3 was normally about 4 N m^{-2} , H_2O , 2.0 kN m^{-2} , varying pressures of added reactant, and diluted to about 5.3 kN m^{-2} with He or SF_6 .

Figure 6.1

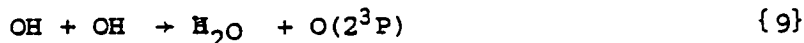
plot of $\log (I_0/I)$ of the OH absorption at 308.15 nm against O_3 pressure.



6.3 Results and discussion

Figure 6.2 shows a typical OH decay trace (from the reaction of OH with NH_3) . Figure 6.3 shows the first order plots of the decay shown in figure 6.2 , and of decays at other NH_3 pressures. The plots were linear over about two halflives , after which the absorption was generally too small to measure accurately . Figures 6.4 , 6.5 and 6.6 show plots of first order rate constants against reactant for the reaction of OH with NH_3 , CHCl_3 , CDCl_3 , CH_2Cl_2 , and CD_2Cl_2 . Second order rate constants for these reactions (least mean squares) are listed in table 6.1 .

These values required to be corrected for the effects of {9} and {10} on the kinetics of the OH decay .



As the pressure of added reactant is increased two opposing effects occur

- (a) the rate of removal of OH by reaction with added reactant increases .
- (b) the rate of removal of OH by {9} and {10} decreases .

Effect (b) may be understood if it is considered that at any given time during the OH decay , the OH concentration will be less in experiments with higher pressures of added reactant relative to experiments with lower pressures .

This is due to effect (a) . Thus removal of OH by {9} and {10} , which is dependent on the OH concentrations , becomes progressively less important as the pressure of added reactant increases . In consequence the observed increase in rate of OH removal with increase in pressure of added reactant is less than the true increase due to this reaction , and the experimentally measured second order rate constant will be low .

To determine the quantitative effects of {9} and {10} , the decay of OH , due to the former reactions and due to reaction with varying pressures of added reactant , was simulated using the CHEK program .

Figure 6.2

Decay of the OH absorption at 308.15 nm in the presence of NH₃

$$P(\text{NH}_3) = 48 \text{ N m}^{-2}$$

full time sweep = 2 ms

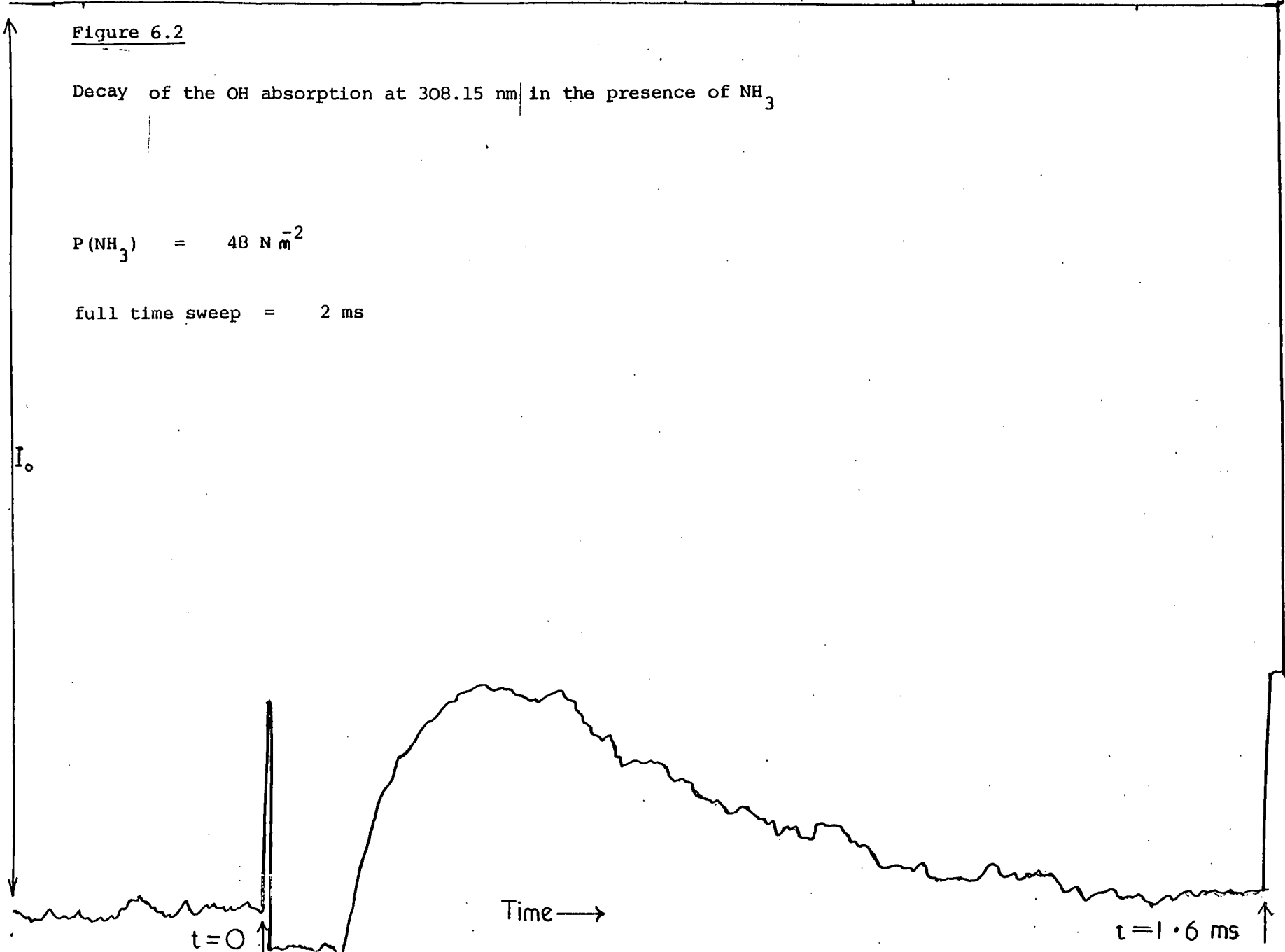


Figure 6.3.

First order plots of the decay of OH in the presence of NH_3

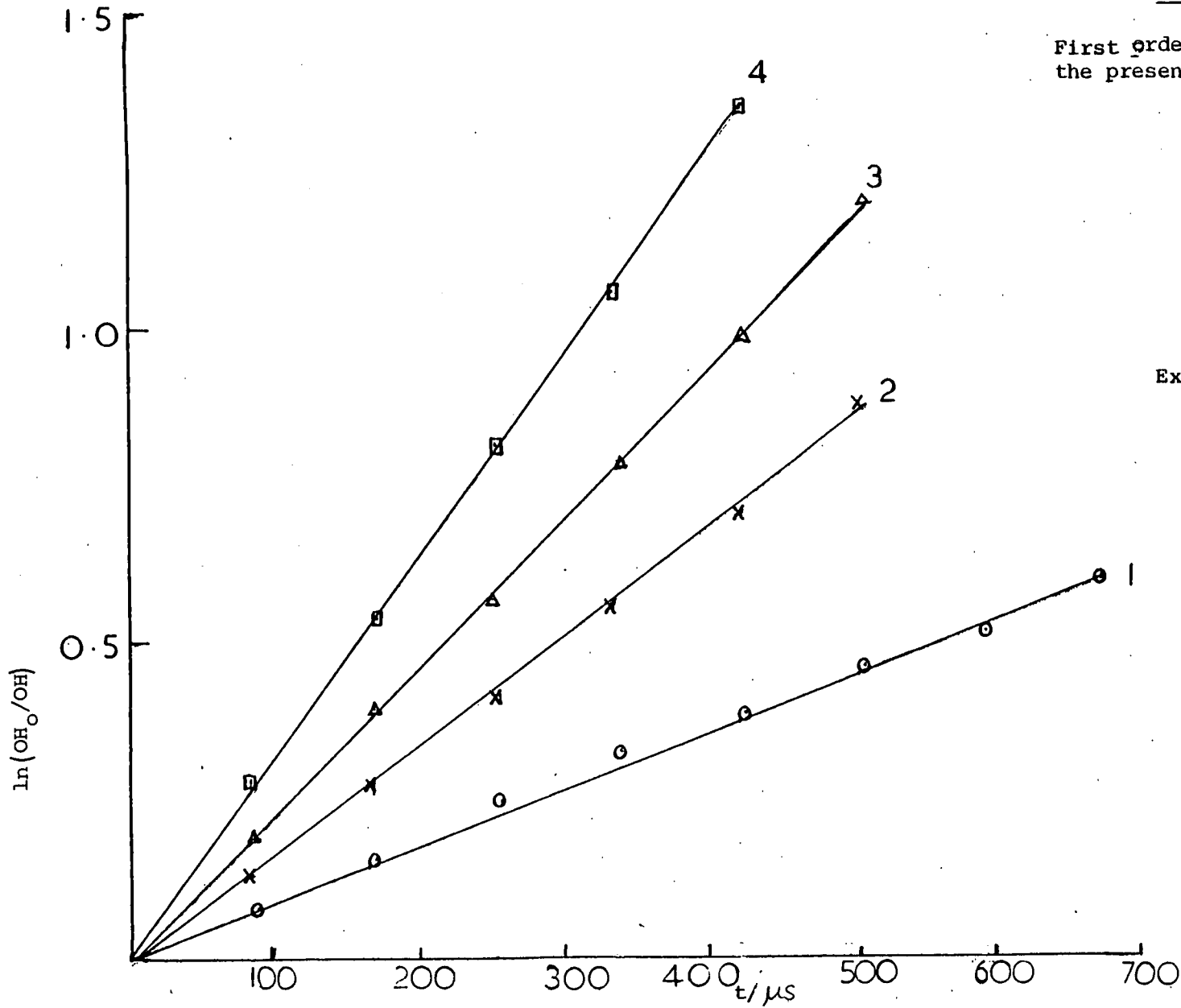


Figure 6.4

Plot of first order decay constants of OH against NH_3 pressure

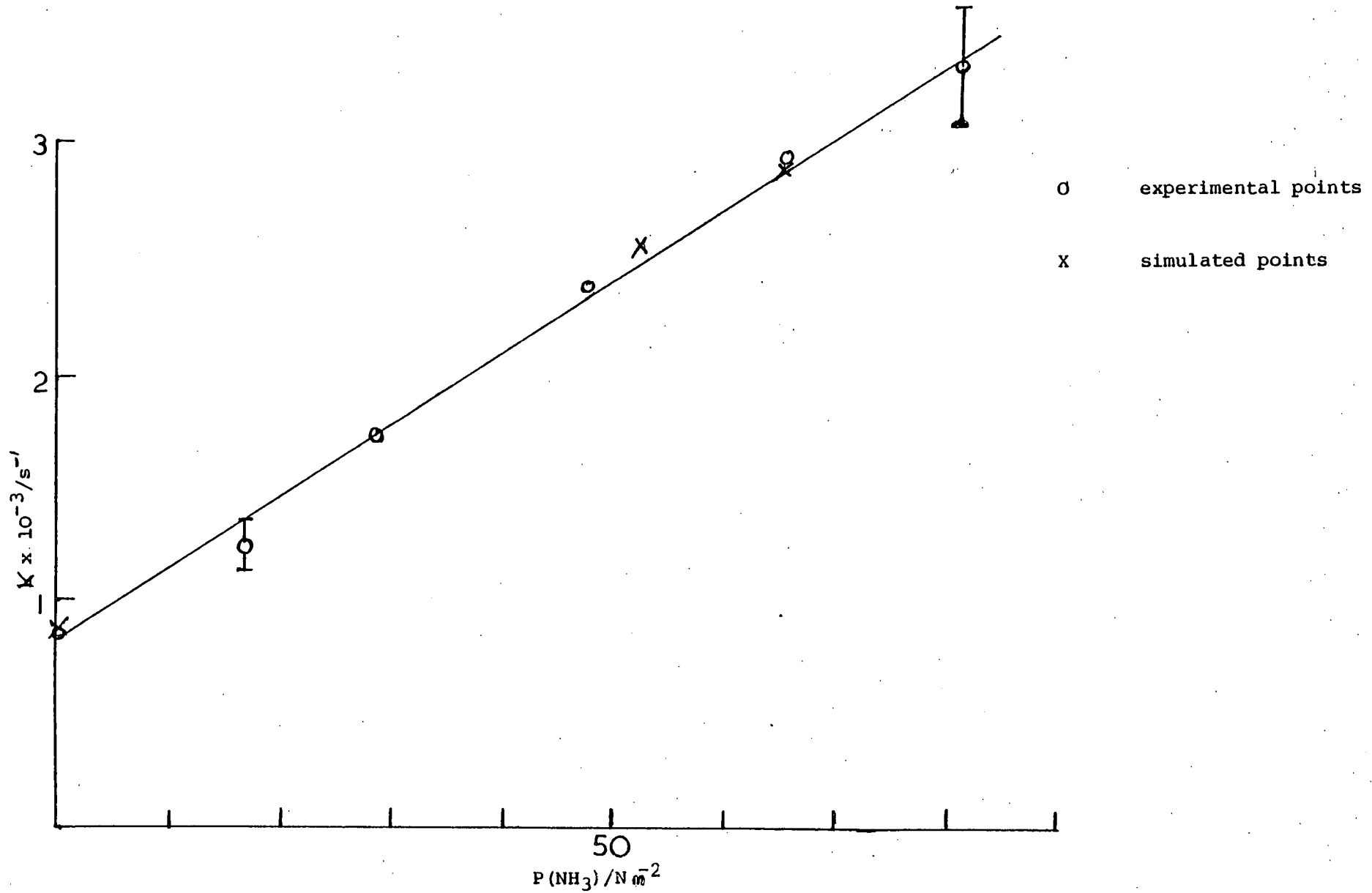


Figure 6.5

Plot of first order OH decay rates against CCl_3X pressure

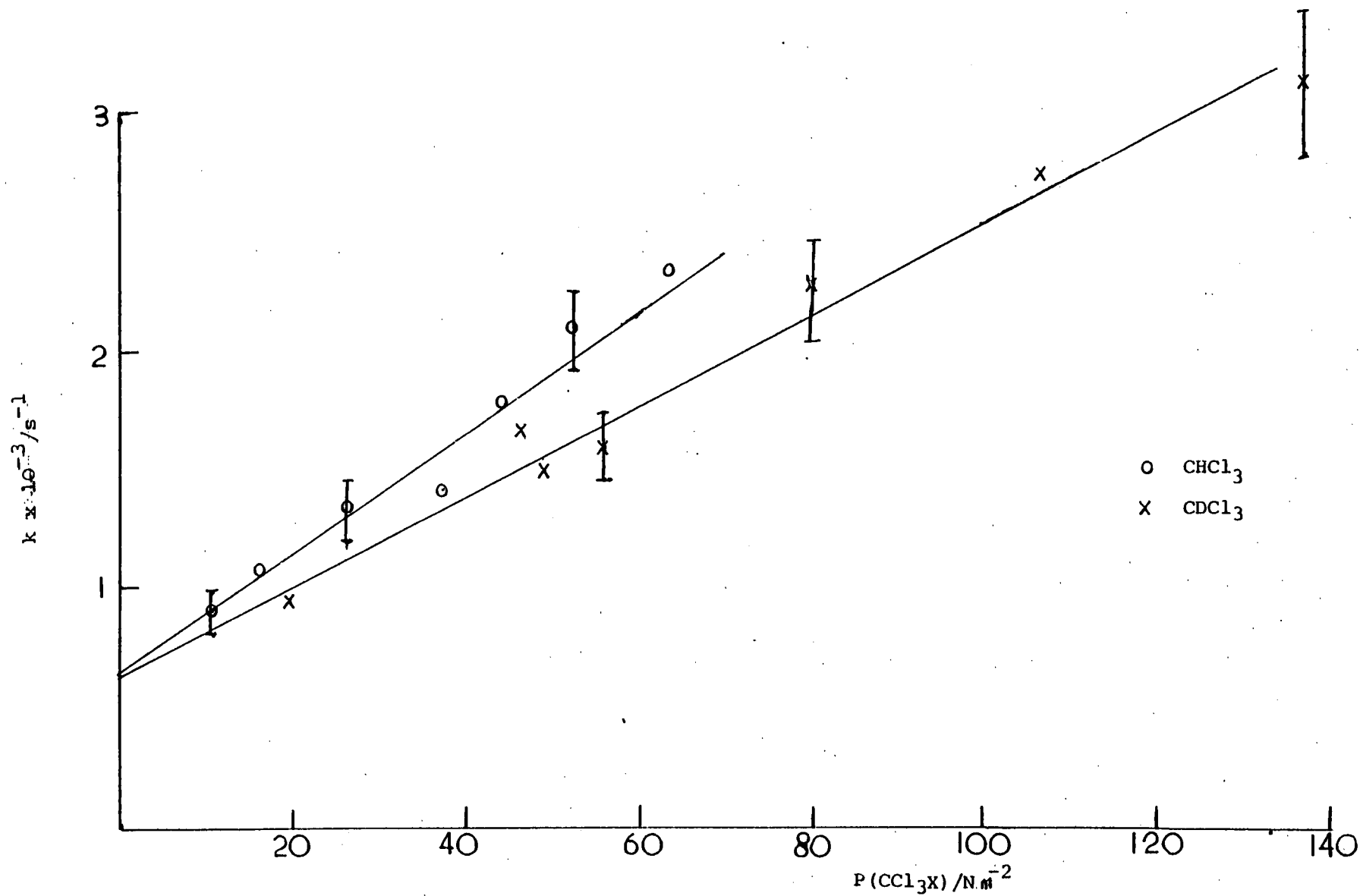


FIGURE 6.6.

Plot of first order OH decay rates against CCl_2X_2 pressure

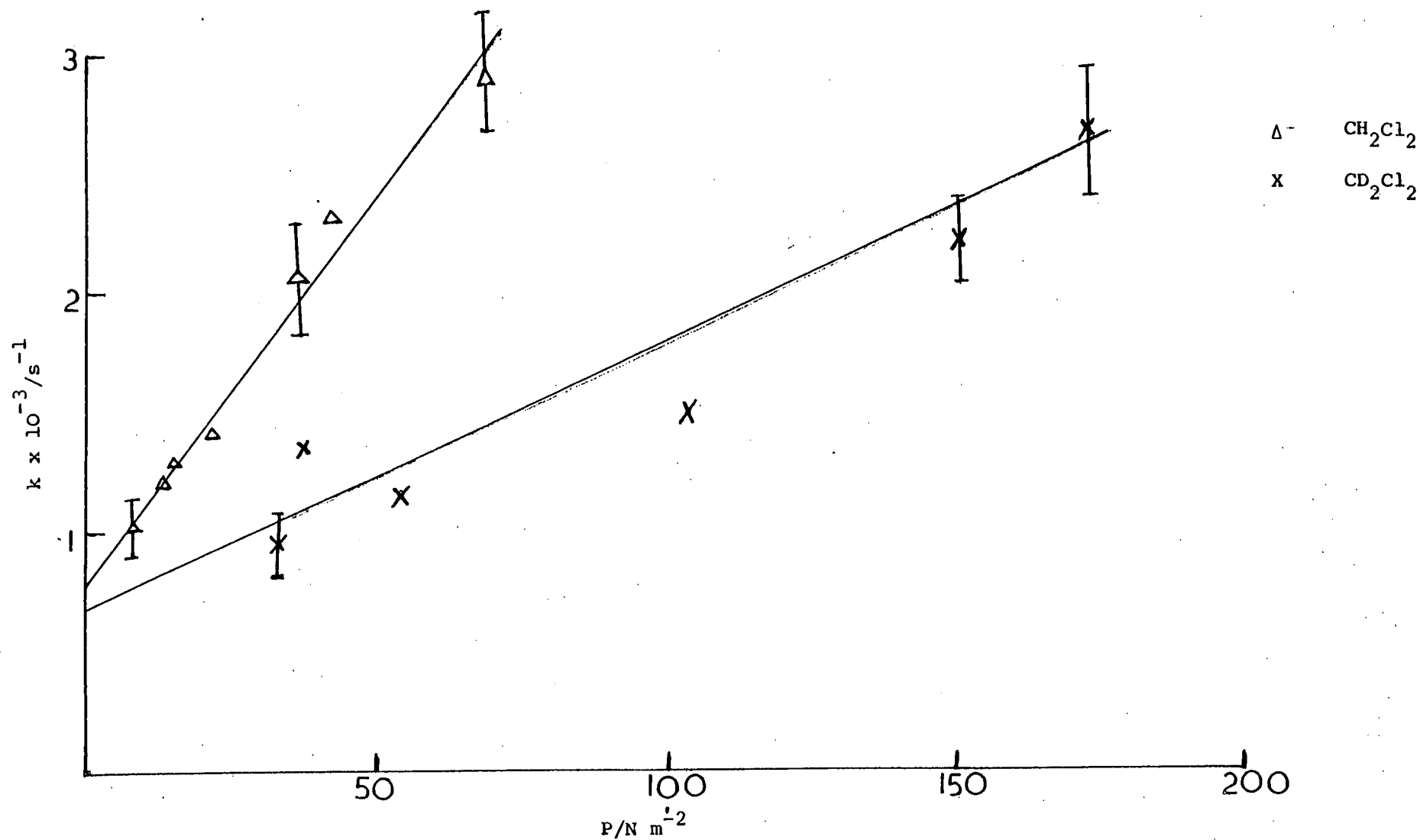


Table 6.1

Rate of reaction of OH with NH_3 , CHCl_3 , CDCl_3 , CH_2Cl_2 and CD_2Cl_2

Reaction	experimental rate / $\text{cm}^3 \text{ molec}^{-1} \text{ s}^{-1}$	corrected rate / $\text{cm}^3 \text{ molec}^{-1} \text{ s}^{-1}$	literature value $\text{cm}^3 \text{ molec}^{-1} \text{ s}^{-1}$	Ref .
$\text{OH} + \text{NH}_3 \rightarrow \text{H}_2\text{O} + \text{NH}_2$	$1.2 \pm 0.1 \times 10^{-13}$	$1.4 \pm 0.1 \times 10^{-13}$	$1.5 \pm 0.1 \times 10^{-13}$ $1.5_6 \pm 0.1 \times 10^{-13}$ $1.4 \pm 0.1 \times 10^{-13}$	117 118 119
$\text{OH} + \text{CHCl}_3 \rightarrow$ $\text{H}_2\text{O} + \text{CCl}_3$	$1.0 \pm 0.1 \times 10^{-13}$	$1.15 \pm 0.1 \times 10^{-13}$	$1.01 \pm 0.15 \times 10^{-13}$ $1.04 \pm 0.20 \times 10^{-13}$	16 121
$\text{OH} + \text{CDCl}_3 \rightarrow$ $\text{DHO} + \text{CCl}_3$	$7.6 \pm 0.5 \times 10^{-14}$	$8.7 \pm 0.6 \times 10^{-14}$		
$\text{OH} + \text{CH}_2\text{Cl}_2 \rightarrow$ $\text{H}_2\text{O} + \text{CHCl}_2$	$1.3 \pm 0.1 \times 10^{-13}$	$1.5 \pm 0.1 \times 10^{-13}$	$1.45 \pm 0.2 \times 10^{-13}$ $1.55 \pm 0.14 \times 10^{-13}$ $1.09 \pm 0.2 \times 10^{-13}$	122 16 121
$\text{OH} + \text{CD}_2\text{Cl}_2 \rightarrow$ $\text{HDO} + \text{CDCl}_2$	$4.4 \pm 0.4 \times 10^{-14}$	$5.1 \pm 0.5 \times 10^{-14}$		

6.3 cont'd

First order rate constants were measured on the simulated decays and second order rate constants for the reaction of OH with the added reactant obtained in the normal way. The simulated second order rate constants refer to the net increase in rate of OH removal (*i.e.* the net result of effects (a) and (b)) as the pressure of added reactant increases. Comparison of this value with the nominal value of the second order rate constant (*i.e.* the value used in the computer simulation) gives a measure of the underestimation caused by {9} and {10}.

This procedure is illustrated in figure 6.4 for the reaction of OH with NH₃. The equations used in these simulations are shown in table 6.2. It can be seen that whereas least mean squares analysis of the experimental points gives $k_{\{11\}} = 1.2 \pm 0.1 \times 10^{-13} \text{ cm}^3 \text{ molec}^{-1} \text{ s}^{-1}$, $k_{\{11\}} = 1.4 \pm 0.2 \times 10^{-13} \text{ cm}^3 \text{ molec}^{-1} \text{ s}^{-1}$ is required to give the correct simulated points. In general it was found that a 15% increase in the experimental second order rate constant was required, and the corrected values are shown in table 6.1.

It was necessary to know the absolute OH concentration in the simulations. To obtain this the yield of O(2¹D) on photolysis of O₃ was determined as described in chapter 3, except that the O₃ concentration was measured spectrophotometrically at 282 nm (a convenient emission line from the flow lamp).

The values for CHCl₃, CH₂Cl₂ and NH₃ are in satisfactory agreement with literature values. The simulated result for the reaction of OH with NH₃ was not affected by inclusion of {16} and / or {17}.

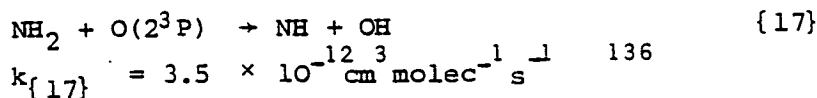
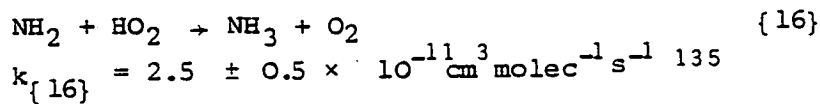


Table 6.2

Equations used in the simulation of the OH + NH₃ reaction

No.	Equation	k/cm ³ molec ⁻¹ s ⁻¹	Ref.
1	O ₃ → O ₂ (¹ Δ) + O(¹ D)		61-65
2	O(¹ D) + H ₂ O → OH + OH	2.3 E -10	130
	OH + O ₃ → HO ₂ + O ₂	5.6 E -14	131
	OH + HO ₂ → H ₂ O + O ₂	3.0 E -11	132
9	OH + OH → H ₂ O + O(³ P)	2.1 E -12	133
10	OH + OH + M → H ₂ O ₂ + M	6.8 E -13 *	133
			134
11	OH + NH ₃ → H ₂ O + NH ₂	1.4 E -13	calc.

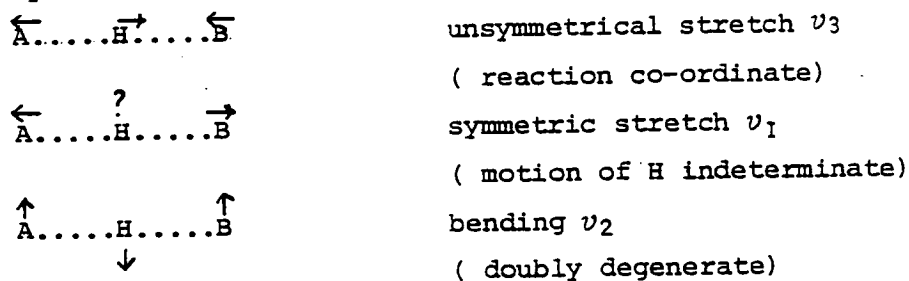
* To obtain k₁₀ for M = H₂O (2.0 kN m⁻²), the value of k₁₀, M = N₂¹³³ was combined with the relative data of Caldwell and Black¹³⁴.

6.4 Isotope effects in the reactions of OH with $\text{CHCl}_3 / \text{CDCl}_3$
and $\text{CH}_2\text{Cl}_2 / \text{CD}_2\text{Cl}_2$

There is observed to be an isotope effect of $k_{\text{H}}/k_{\text{D}} = 1.3 \pm 0.2$ and $k_{\text{H}}/k_{\text{D}} = 2.9 \pm 0.4$ for the reactions of OH with $\text{CHCl}_3 / \text{CDCl}_3$ and $\text{CH}_2\text{Cl}_2 / \text{CD}_2\text{Cl}_2$ respectively .

The simplest explanation of isotope effects ascribes the cause to the difference in zero point energies between the isotopic substrates . For C-H and C-D species this difference is about $4.75 \text{ kJ mole}^{-1}$, and the predicted isotope effect is thus at 298 K about seven . While some reactions do show isotope effects of this size , many show a much smaller effect . This indicates that isotopic substitution affects not only the initial substrate but also the transition state. The isotope effect on this basis is related to the change in zero point energy in the isotopic substrates minus the change in zero point energy in the isotopic transition states .

If the transition state is regarded as a linear triatomic species , its normal modes of vibration can be represented as



Westheimer¹²⁰ writes for motion along the line of centres of



$$2\Delta V = k_1 \Delta r_1^2 + k_2 \Delta r_2^2 + k_{12} \Delta r_1 \Delta r_2$$

where the distance A.....H is r_1 , and H.....B is r_2 .

V is the potential energy and k is the force constant .

With the assumption that $k_{12} = (k_1 k_2)^{\frac{1}{2}}$, (k_{12} is not known)

Westheimer derives a simple expression for the isotope effect.

For $\text{CHCl}_3 / \text{CDCl}_3$ and $\text{CH}_2\text{Cl}_2 / \text{CD}_2\text{Cl}_2$ this is calculated to be about 4 .

6.4 cont'd

The large value is due to the fact that the C-H and O-H force constants are similar (5×10^5 and 7.5×10^5 dynes cm^{-1} respectively). Had the force constants been equal, ν_1 would have been totally symmetric (corresponding to no movement of H) and an isotope effect of 7 would have been predicted.

The assumption that $k_{12} = (k_1 k_2)^{1/2}$ has been criticised by Bell¹²⁴ who claimed that k_{12} was at least $2(k_1 k_2)^{1/2}$ and showed that increasing k_{12} reduced the isotope effect. Albery¹²⁵ has calculated the effects of varying k_{12} .

However, Bell considers that the above approach is not a satisfactory explanation of low isotope effects and suggests that five centred transition states should be considered.

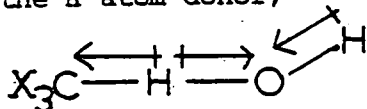
The above discussion has only considered the effect on the rate of reaction of isotopic substitution of an atom which is transferred in the reaction. However the rate of reaction may also be affected by isotopic substitution near to the reaction centre of an atom which is not directly involved in the reaction. This is the secondary kinetic isotope effect, which likely contributes to the isotope effect measured for $\text{CH}_2\text{Cl}_2 / \text{CD}_2\text{Cl}_2$.

The low isotope effect for $\text{CHCl}_3 / \text{CDCl}_3$ may reflect a transition state in which the C-H or C-D bond is not greatly perturbed, and thus there being little net change in zero point energy between the substrate and transition state. The situation may be analogous for $\text{CH}_2\text{Cl}_2 / \text{CD}_2\text{Cl}_2$ but is complicated by the secondary kinetic isotope effect.

6.5 Correlation of H donor dipole moment with rate of reaction with OH

Nascent reaction product repulsion has been suggested as a significant factor in determining the magnitudes of activation energies of reactions with similar C-H bonds¹²⁶.

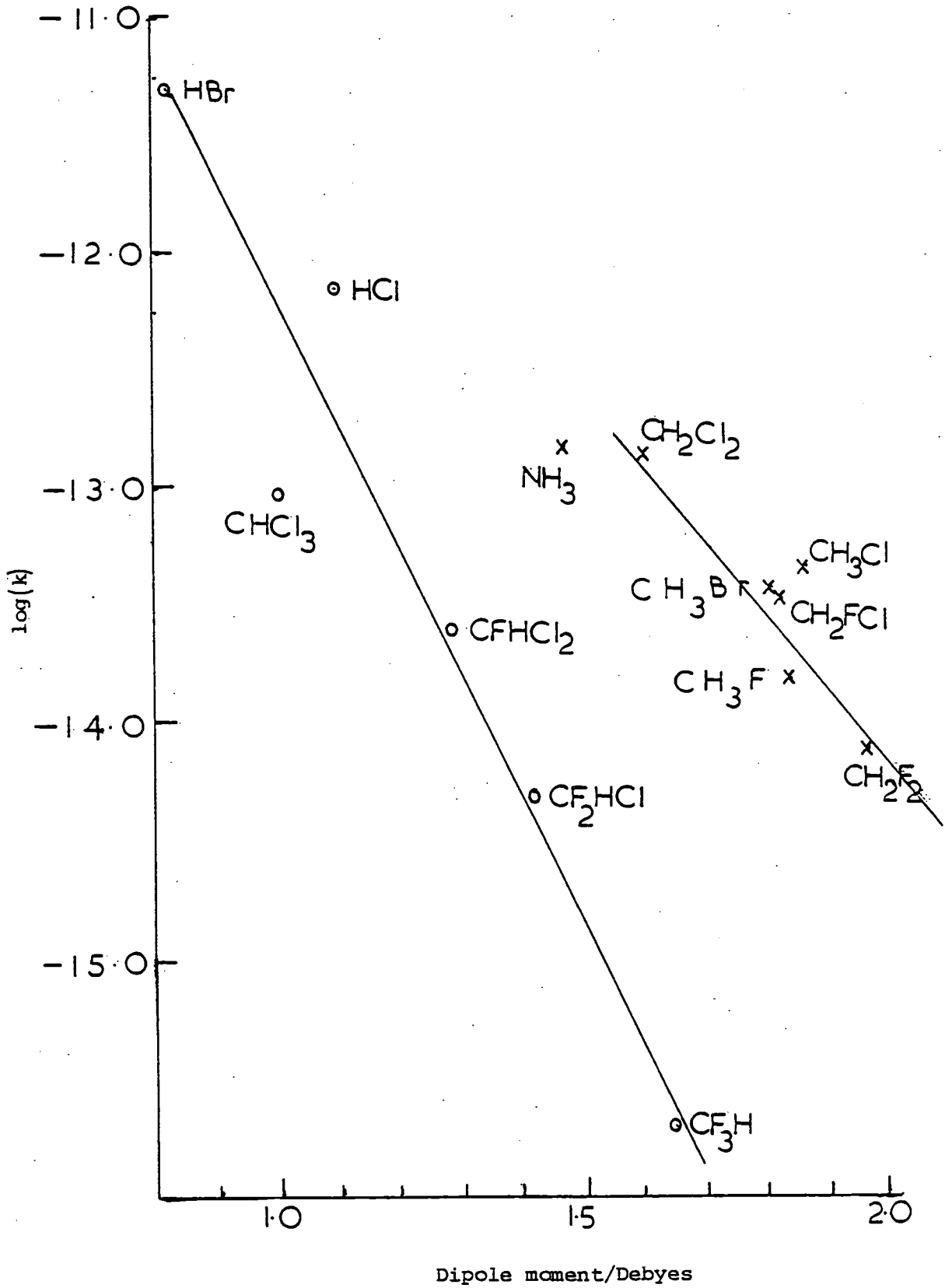
On this basis the activation energy should depend on the dipole moment of the H atom donor,



The dipole moments of the CX_3H and the nascent HOH oppose each other, and may be considered to give rise to a repulsive term, opposing the formation of the new O-H bond, and hence affecting the rate of reaction. Such a relationship between rate of reaction of F atoms and the dipole moment of CX_3H has been demonstrated by Clyne¹²⁷. Figure 6.7 shows a plot of rate of reaction of OH with halomethanes, HCl, HBr and NH_3 against dipole moment. The pre-exponential factors of all the compounds shown in figure 6.7 are similar ($\approx 10^{-12} \text{ cm}^3 \text{ molec}^{-1} \text{ s}^{-1}$) and thus it may be valid to correlate activation energy with dipole moment.

It can be seen that there are two distinct correlations in figure 6.7. Sensibly the CX_3H and HX molecules in which the dipole moment lies along the C-H or H-X axis show a more sensitive dependence on the dipole moment than do CX_2H_2 , CXH_3 and NH_3 molecules in which the dipole moment is directed off the C-H or N-H bond axis. Both correlations show an increase in rate constant with decrease in dipole moment. These results strongly indicate a dependence of activation energy on the dipole moment of the H atom donor and suggest that this activation energy arises, in part at least, from opposing dipole repulsion of the nascent products in the transition state.

Figure 6.7

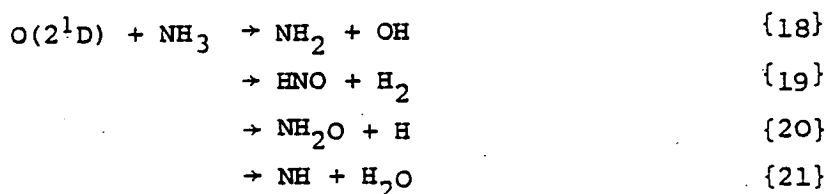
Plot of \log (rate of reaction of OH with X) against dipole moment of X

6.6 Yield of OH from the reaction of O(2¹D) with NH₃

The method of production of OH used in this work, the reaction of O(2¹D) with H₂O, can readily be adapted to give quantitative information on the yield of OH following the reaction of O(2¹D) with hydrogen containing molecules.

The technique has been described in chapter 4 for the reaction of O(2¹D) with CF₂HCl.

Norrish and Wayne¹²⁸ observed OH and NH formation following the flash photolysis of O₃ in the presence of NH₃. The following reactions bear consideration.



The yield of OH was measured following the flash photolysis of O₃ / NH₃ / He mixtures, (there is a slow reaction between O₃ and NH₃¹²⁹, however removal of O₃ and NH₃ was observed to be insignificant in the time required to mix and flash the system).

Figure 6.8 shows the OH yields from the O₃ / NH₃ / He and O₃ / H₂O / He systems. Unfortunately OH removal by {9}



is fast¹¹⁷⁻¹²⁰, and the pressure of NH₃ was kept at < 60 N m⁻²

to permit accurate extrapolation of the OH concentration to zero time. There was consequently some loss of O(2¹D) by

reaction with O₃. The yield of OH, after correction for this loss (≈ 18%) was found to be close to 100%.

Reaction {18} is likely to be the dominant pathway leading to OH formation, and hence the dominant pathway in the reaction of O(2¹D) with NH₃. Although {20} followed by {5} would lead to OH formation, the vibrationally excited OH so formed, would be likely to react with O₃ or NH₃ before it was quenched to the ground state, and hence {20} is not likely to contribute significantly to OH (ν = 0) formation.

174

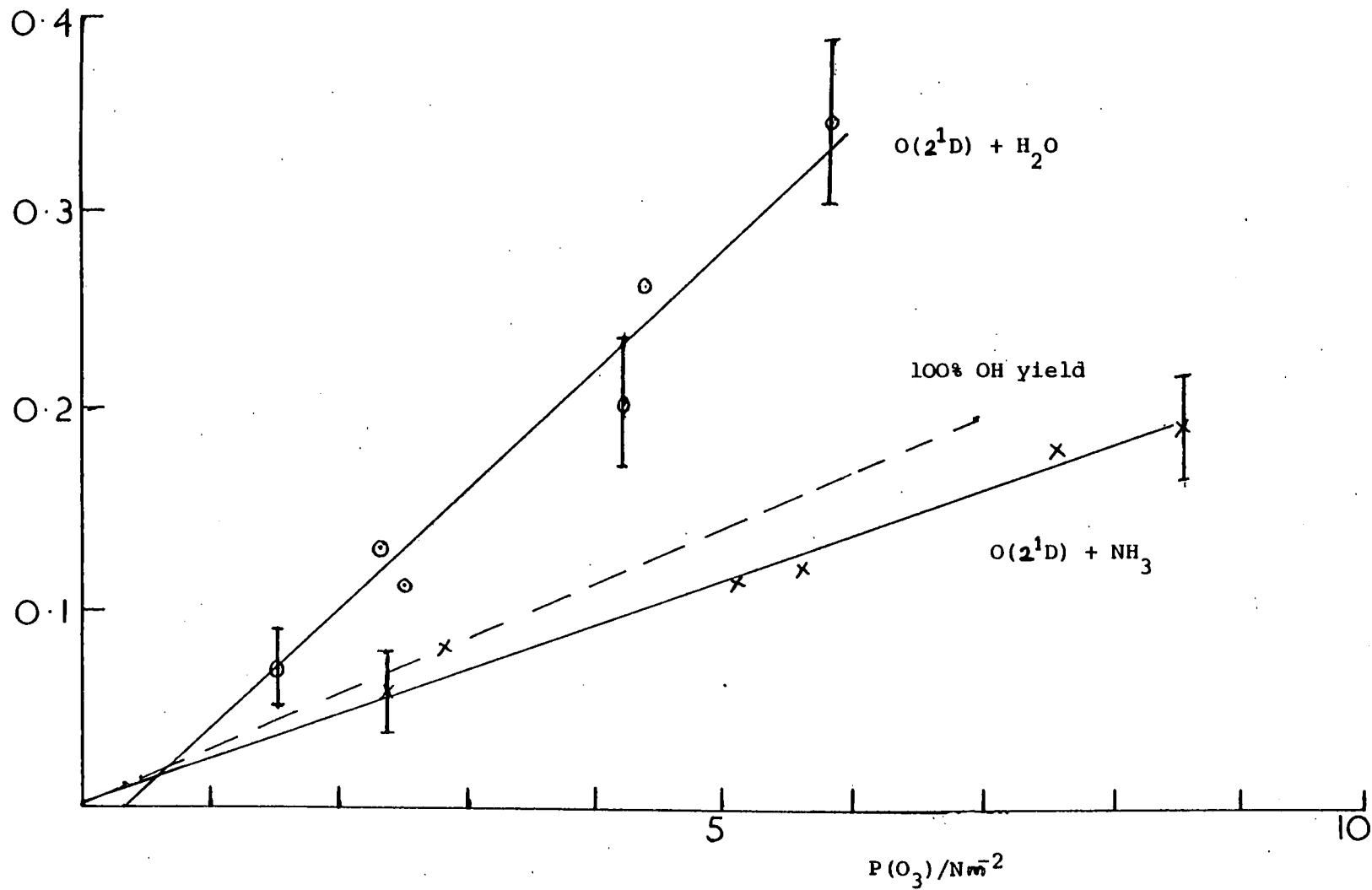
Reaction {18} has been investigated by Kinsey et al

to determine how the excess energy is distributed. They observed that the reaction yielded both ground state NH₂ and electronically excited NH₂.

log(I₀/I) of the OH absorption at 308.15 nm

Figure 6.8

Yield of OH from O(2¹D) + H₂O, and O(2¹D) + NH₃



6.7 Conclusion

Rate constants for the reaction of OH with CHCl_3 , CH_2Cl_2 and NH_3 have been measured and are in satisfactory agreement with literature values. New data are reported for the reactions of OH with CDCl_3 and CD_2Cl_2 .

The major pathway in the reaction of $\text{O}(2^1\text{D})$ with NH_3 has been shown to be OH formation.

There is a good correlation between the rate of reactivity of OH with halomethanes, hydrogen halides and NH_3 and the dipole moment of the H atom donor. This may be interpreted as indicating that the activation energy of these reactions arises, in part at least, from nascent product repulsion.

CHAPTER SEVEN

REACTION OF OH WITH ALKYL IODIDES AND MOLECULAR

CHLORINE

7.1 Introduction

A large number of H atom abstraction reactions of OH have been reported, however, there has been no report of halogen atom abstraction reactions. This is somewhat surprising as halogen atom abstraction from RI, RBr and molecular halogens has been reported for O(2³P)^{108, 114}, F^{137, 138}, Br¹³⁹, I¹⁴⁰, CF₃¹⁴¹, and CH₃¹⁴¹. The reaction of O(2³P) with CF₃I has previously been discussed in chapter 5, and proceeds via a complex. A similar reaction mechanism obtains for the reaction of F atoms with RI.

Kaufman and Bozzelli¹³⁷ showed that the major reaction was I atom abstraction {1}, although I displacement {2}, was more exothermic, and that reaction proceeds via complex formation..



Farrar and Lee¹³⁸ obtained similar results for the reaction of F atoms with CH₃I and were able in other experiments to detect CH₃IF¹⁴².

The reaction of O(2³P) with molecular halogens has been discussed in chapter 5. Again this reaction proceeds via complex formation, with the most electropositive atom in the centre.

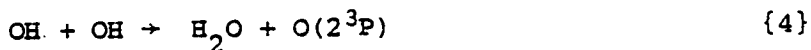


OXY species have been observed in matrix isolation experiments^{112, 113}. Similar results have been obtained for the reactions of D atoms¹⁴³, halogen atoms^{144, 145}, and CH₃¹⁴⁶ with halogen molecules.

In this chapter evidence and rate data for the reaction of OH with CH₃I, CF₃I, C₂F₅I, C₃F₇I and Cl₂ will be presented. It is considered likely that these reactions proceed by halogen atom abstraction.

7.2 Reaction of OH with CH₃I , CF₃I , C₂F₅I and C₃F₇I

The experimental apparatus has been described in chapter 2 and the technique in chapter 6 . A rapid decay of OH (figure 7.1) was observed when small pressures of RI (< 75 N m⁻²) were added to the O₃ / H₂O / SF₆ system . Figures 7.2 and 7.3 show plots of the first order rate constant against RI concentration . The second order rate constants are shown in table 7.1 . These values were corrected as described in chapter 6 for {4} and {5} .



The corrected values are shown in table 7.1 .

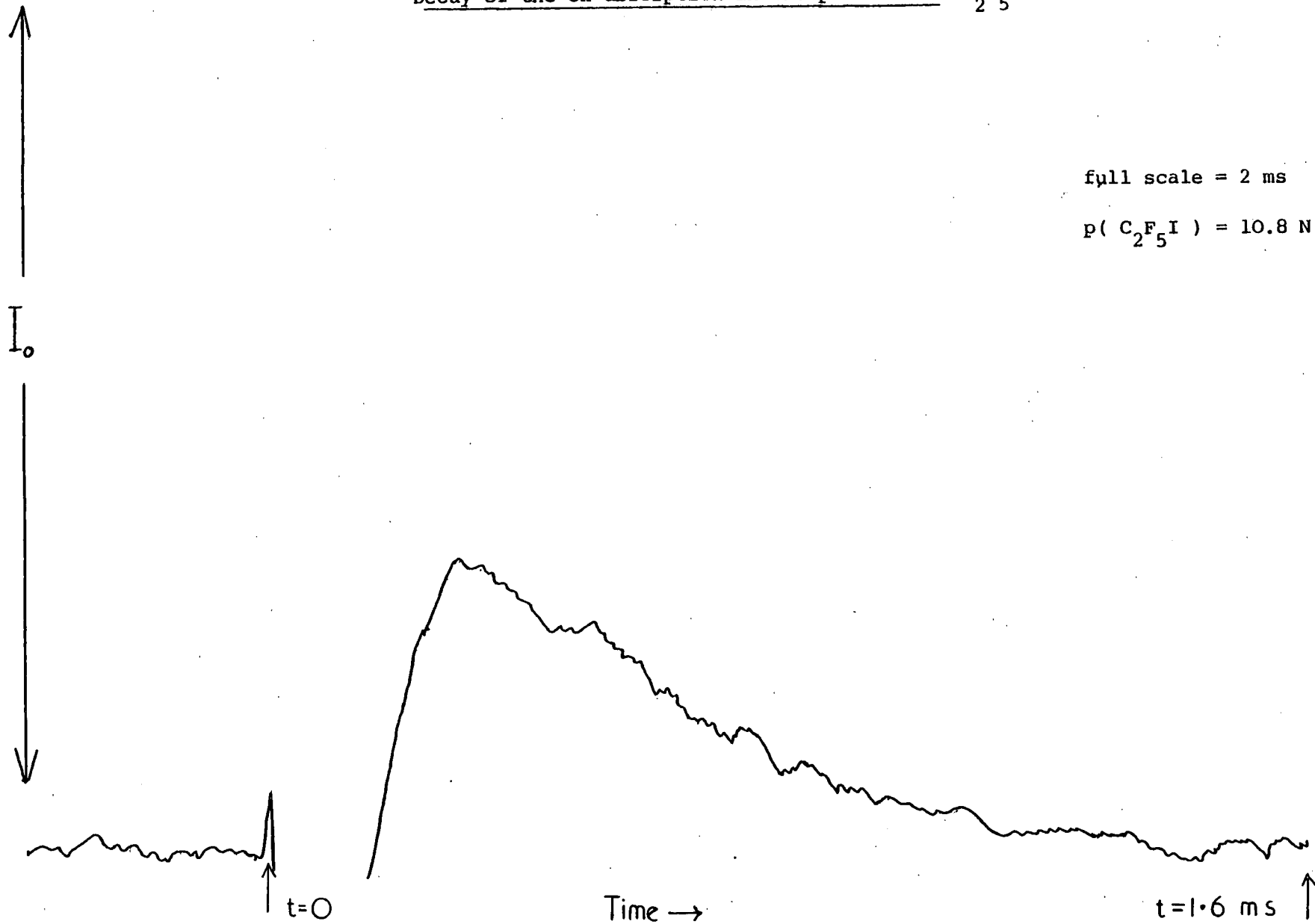
RI absorbs in a broad continuum from about 230 to 310 nm . To determine whether photolysis of RI affected the kinetics of the OH decay , experiments were done at differing flash energies . The results for the reaction of OH with CF₃I and CH₃I at 100 and 50 J flash energies are shown in figure 7.2 .

It can be seen that varying the flash energy has no effect on the reaction kinetics . It was thus concluded that secondary reactions of photolysis products of RI with OH were insignificant . It was considered reasonable to extend this conclusion to cover C₂F₅I and C₃F₇I , as these compounds were present in lower pressures , but absorb to about the same extent as CF₃I and CH₃I .

It should be noted that in the experiments at low flash energy the concentration of O₃ was increased , so that the yield of OH was similar to that in experiments at high flash energy . Thus the effect of {4} and {5} was similar in both sets of experiments .

Figure 7.1

Decay of the OH absorption in the presence of C_2F_5I



full scale = 2 ms

$p(C_2F_5I) = 10.8 \text{ N m}^{-2}$

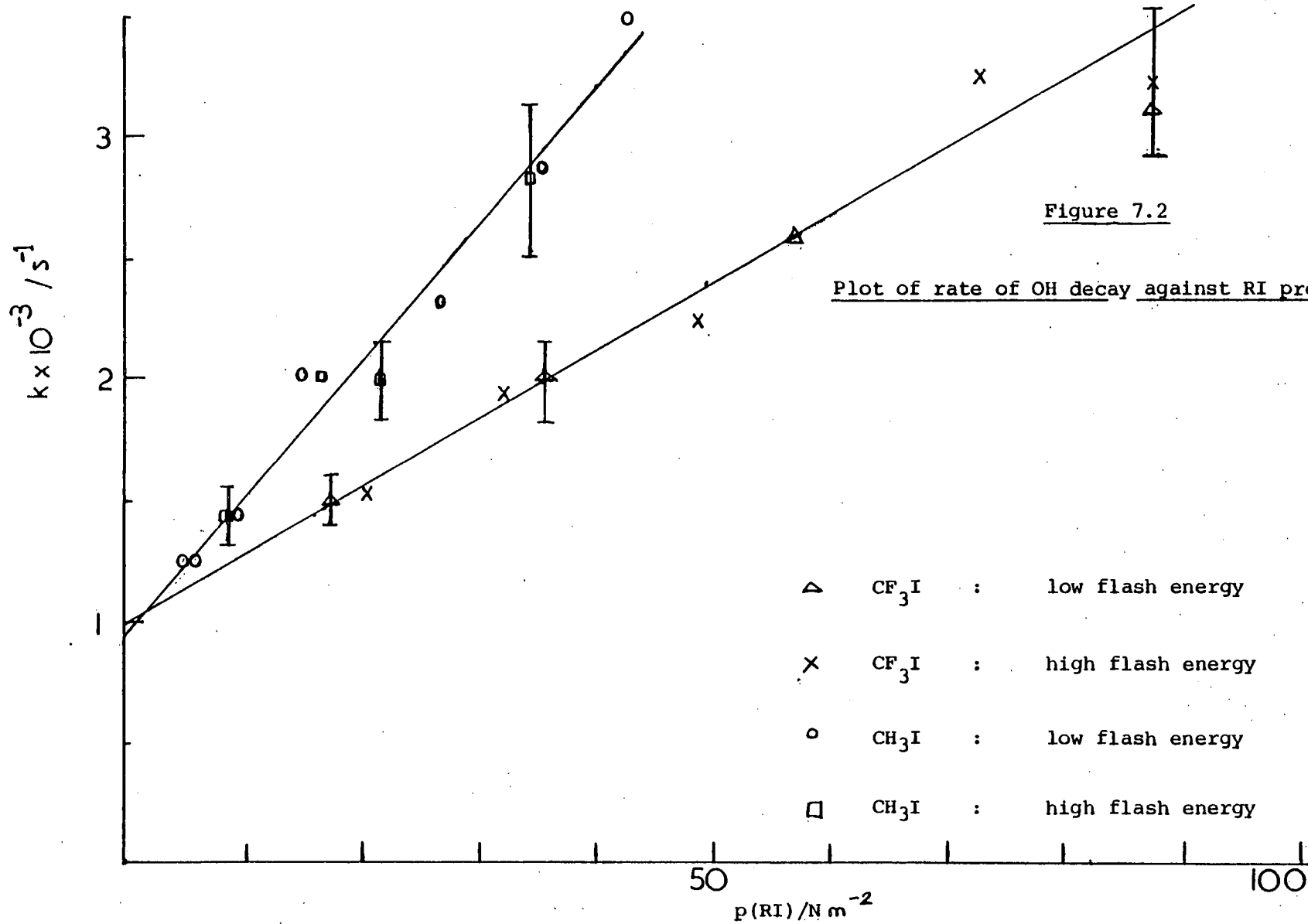


Figure 7.3

Plot of first order decay rates of OH against RI pressure

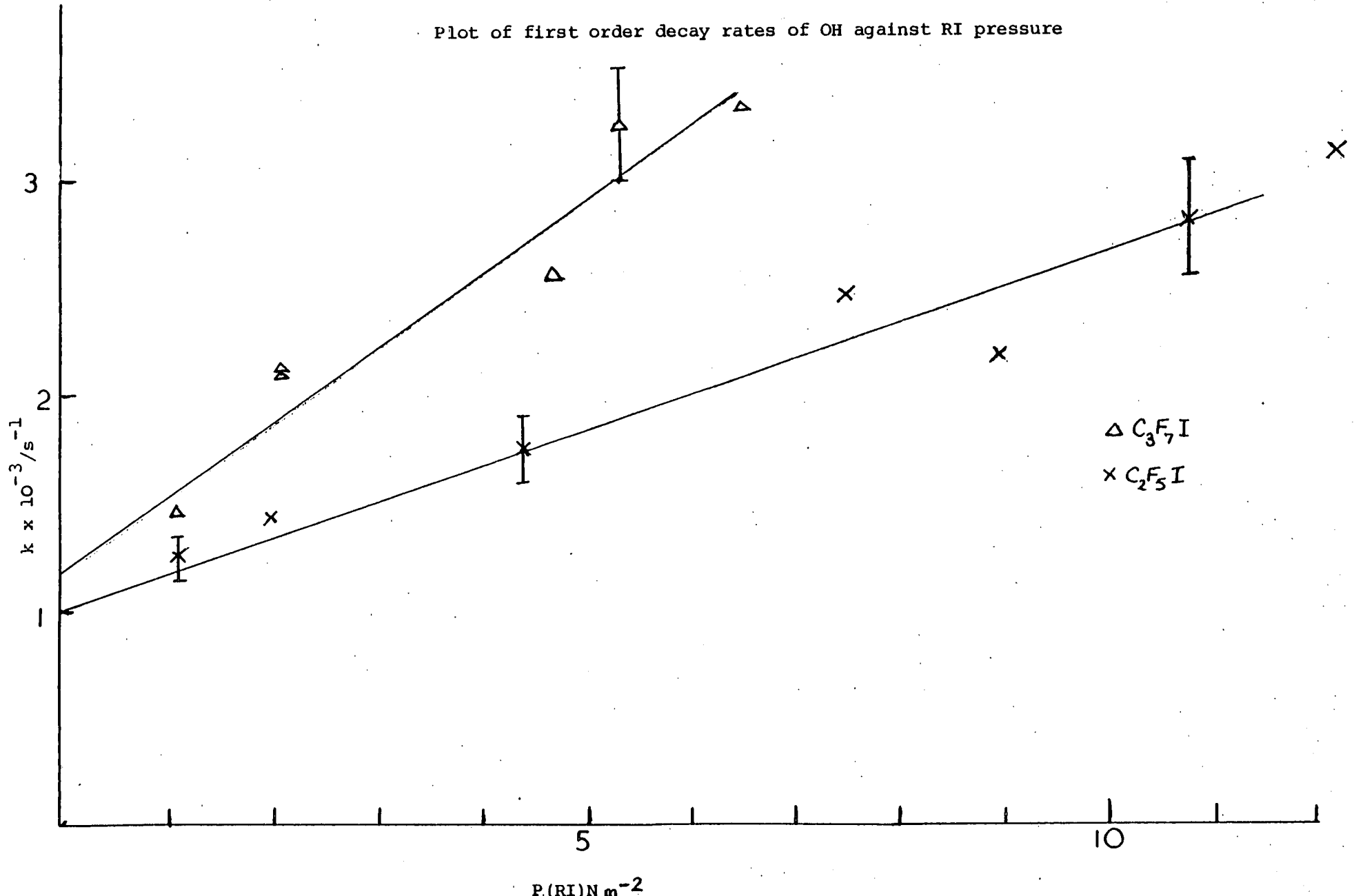


Table 7.1

Experimental and corrected rate constants for OH + RI and OH + Cl₂

Compound	Experimental rate / cm ³ molec ⁻¹ s ⁻¹	Corrected rate / cm ³ molec ⁻¹ s ⁻¹
CH ₃ I	2.3 ± 0.1 × 10 ⁻¹³	2.7 ± 0.2 × 10 ⁻¹³
CF ₃ I	1.0 ₅ ± 0.1 × 10 ⁻¹³	1.2 ± 0.1 × 10 ⁻¹³
C ₂ F ₅ I	6.3 ± 0.7 × 10 ⁻¹³	7.5 ± 0.8 × 10 ⁻¹³
C ₃ F ₇ I	1.4 ± 0.1 ₅ × 10 ⁻¹²	1.6 ± 0.2 × 10 ⁻¹²
Cl ₂	1.6 ± 0.1 × 10 ⁻¹³	1.9 ± 0.1 × 10 ⁻¹³

The reaction between OH and CH₂I₂ was investigated and found to be very fast ~ 5 × 10⁻¹² cm³ molec⁻¹ s⁻¹. Accurate rate data could not be obtained because the low vapour pressure of this compound could not be accurately measured on the glass spiral guage.

7.3 Nature of the reaction

Reaction of OH with CF_3I , $\text{C}_2\text{F}_5\text{I}$ and $\text{C}_3\text{F}_7\text{I}$ could proceed by two pathways {6} and {7},



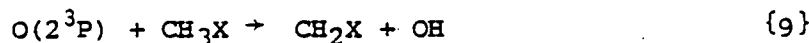
and for CH_3I additionally {8}.



Walden inversion {7} is rare in the gas phase and thus {7}

is unlikely. It is interesting to compare the rates of reactions of OH and $\text{O}(2^3\text{P})$ with RX , these are shown (where known) in table 7.2. The large increase in rate of reaction of $\text{O}(2^3\text{P})$ with RX , on going from the F, Cl, or Br species to the I species reflects a change in reaction mechanism.

With CH_3X , where $\text{X} = \text{Cl}, \text{Br}$; $\text{O}(2^3\text{P})$ reacts by H atom abstraction.



and with CF_3X where $\text{X} = \text{F}, \text{Cl}, \text{or Br}$, the rate of reaction is insignificant at room temperature. For CF_3I however

$\text{O}(2^3\text{P})$ reacts rapidly via complex formation to abstract I atoms, $k_{\{10\}} = 1.1 \pm 0.3 \times 10^{-11} \text{ cm}^3 \text{ molec}^{-1} \text{ s}^{-1}$ 55



A similar reaction has been suggested between $\text{O}(2^3\text{P})$ and CH_3I ¹⁴⁹.

In view of the similar pattern in the rates of reactions of OH with CH_3X and CF_3X to $\text{O}(2^3\text{P})$ and the general propensity of diverse species to react with CH_3I and CF_3I by I atom abstraction (although more exothermic channels may be available) it is reasonable to suggest that OH reacts with RI by I atom abstraction. For {6} to be exothermic requires $\Delta H_{298}^{\circ} \{\text{HOI}\} < -29 \text{ kJ mole}^{-1}$ which may be compared to a literature value of $-86 \pm 40 \text{ kJ mole}^{-1}$ 150. In support of the contention that OH reacts via I atom abstraction, there is observed a good correlation between the rate of reaction with OH, and the R-I bond strength for CF_3I , $\text{C}_2\text{F}_5\text{I}$ and $\text{C}_3\text{F}_7\text{I}$ (figure 7.4)

Table 7.2 Rates of reaction of $O(2^3P)$ and OH with CH_3X and CF_3X

$$k_{O(3P)} / \text{cm}^3 \text{molec}^{-1} \text{s}^{-1}$$

$$k_{OH} / \text{cm}^3 \text{molec}^{-1} \text{s}^{-1}$$

	CH_3X	Ref.	CF_3X	Ref.	CH_3X	Ref.	CF_3X	Ref.
F	-	-	reaction endothermic	-	$1.6 \pm 0.2 \times 10^{-15}$ *	16	4×10^{-16}	16
Cl	4.5×10^{-17}	172	reaction endothermic	-	$3.6 \pm 0.8 \times 10^{-14}$ *	16	7×10^{-16}	16
Br	$\sim 4.5 \times 10^{-17}$	172	reaction endothermic		$3.6 \pm 0.8 \times 10^{-14}$ *	16	-	
I	no data but fast	149	$1.1 \pm 0.3 \times 10^{-11}$	55	$2.7 \pm 0.2 \times 10^{-13}$		$1.2 \pm 0.1 \times 10^{-13}$	

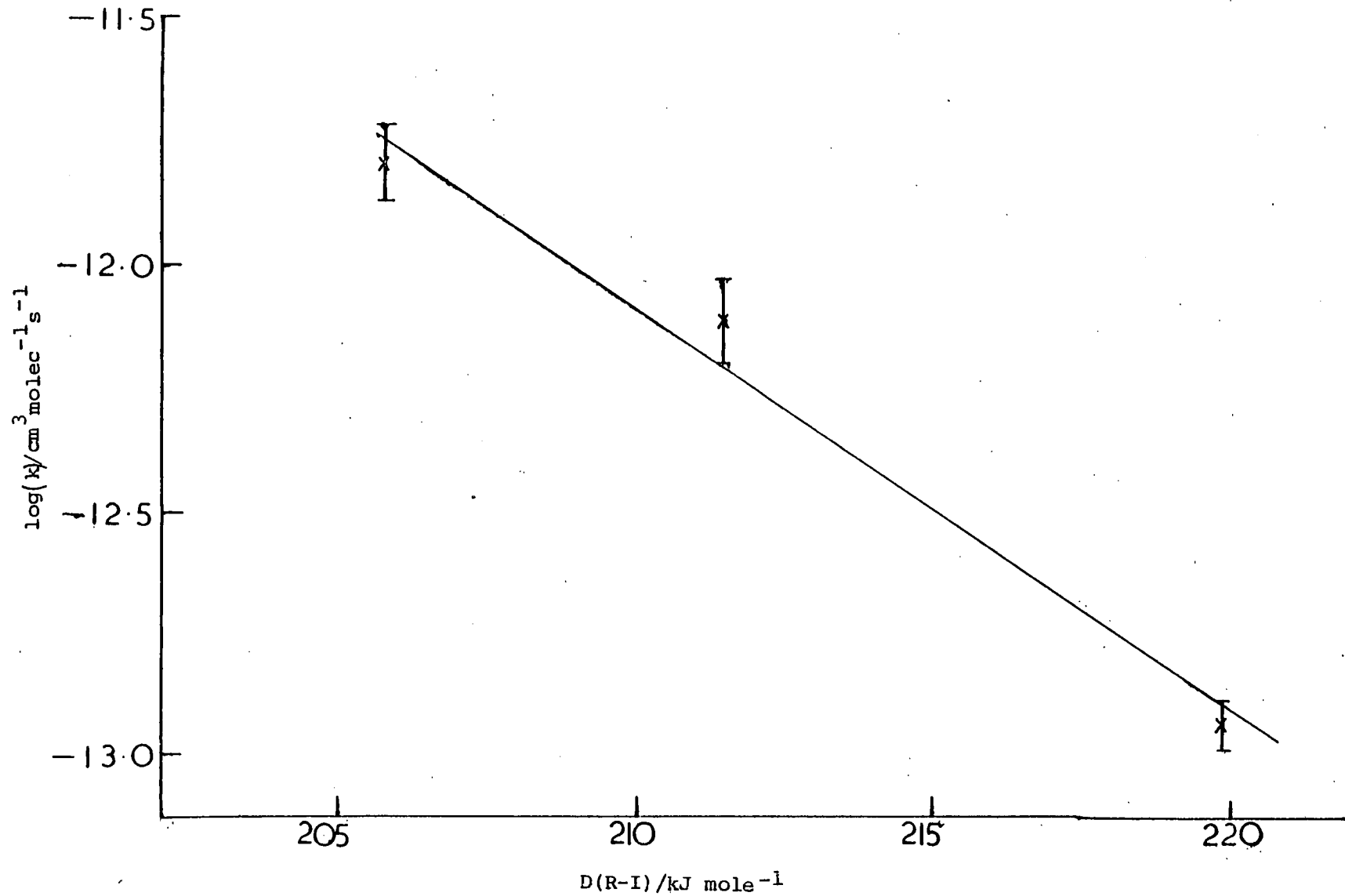
* denotes H abstraction

Table 7.3 Calculated activation energies for OH + RI

	CH_3I	CF_3I	C_2F_5I	C_3F_7I
$E / \text{kJ mole}^{-1}$ $p = 1.0$	16.1	17.7	13.6	11.5
$E / \text{kJ mole}^{-1}$ $p = 0.01$	4.6	6.6	2.1	0.3

Figure 7.4

Plot of log of rate of reaction of OH with RI against D(R-I)



7.3 cont'd

Reaction of OH may proceed by either I atom , or H atom abstraction with CH_3I . However in view of the large increase in rate of reaction between CH_3I and $\text{CH}_3\text{Cl} / \text{CH}_3\text{Br}$, it is reasonable to suppose that the major reaction is I atom abstraction . Activation energies for I atom abstraction by OH from RI may be calculated from the expression ,

$$k = p \cdot Z_{ab} \cdot \exp(-E/RT)$$

where p is the possibility of a collision leading to reaction and Z_{ab} is the collision frequency . Activation energies , assuming $p = 1.0$, are listed in table 7.3 . The actual activation energies are , however , likely to be considerably smaller than these values , as the pre-exponential values ($\equiv p \cdot Z_{ab}$) of OH reactions with halomethanes are commonly about $10^{-12} \text{ cm}^3 \text{ molec}^{-1} \text{ s}^{-1}$. This corresponds to a p equal to about 0.01 . Activation energies assuming $p = 0.01$ are also shown in table 7.3

A molecular beam study of these reactions would be of interest to determine conclusively the reaction products , and to determine the reaction mechanism , *i.e.* whether reaction is direct abstraction or occurs via complex formation .

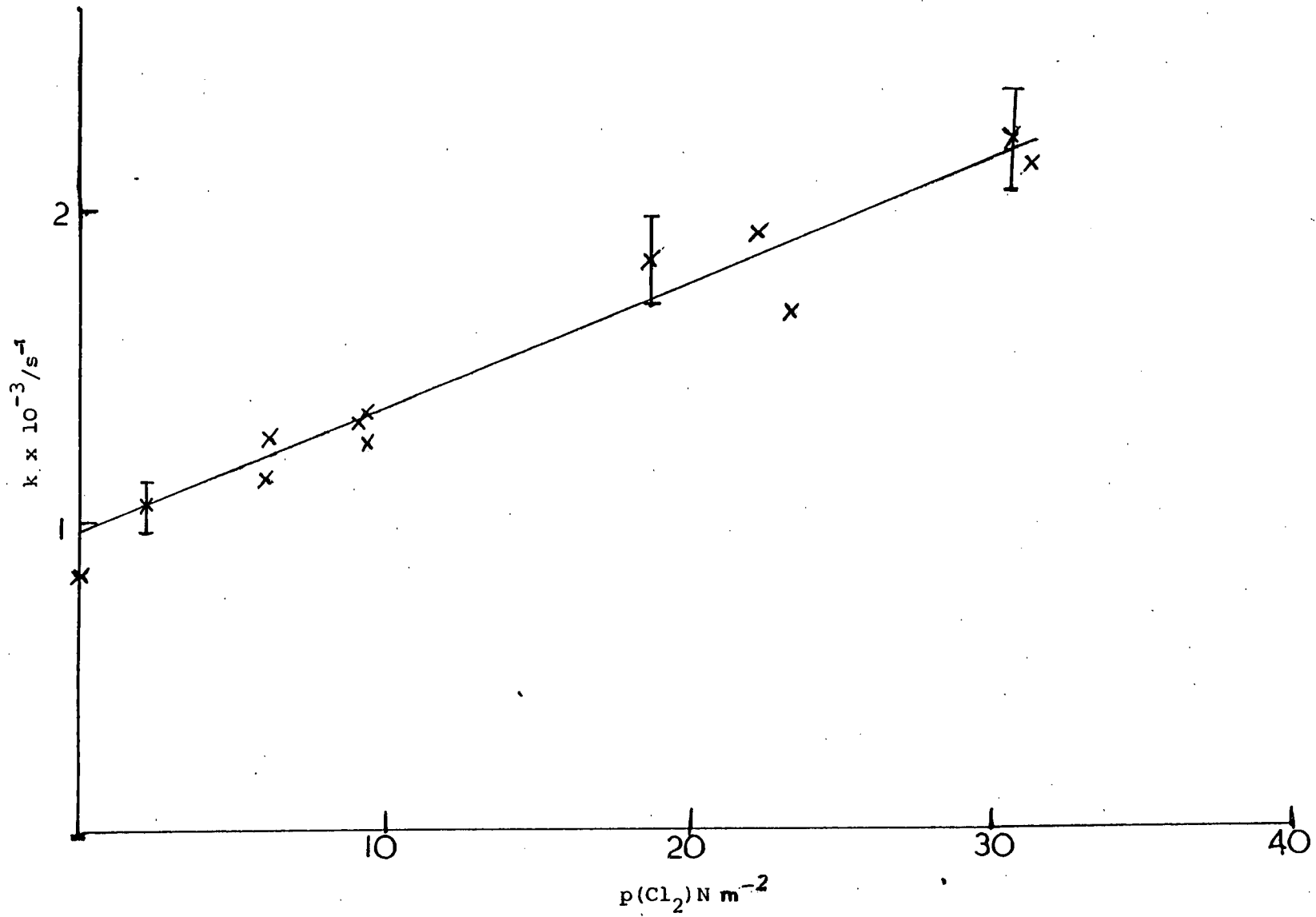
7.4 Reaction of OH with Cl_2

Addition of small pressures of Cl_2 ($\leq 30 \text{ N m}^{-2}$) to the $\text{O}_3 / \text{H}_2\text{O} / \text{SF}_6$ system led to a rapid decay of OH . The pressure of Cl_2 was kept at $\leq 30 \text{ N m}^{-2}$, as at higher pressures appreciable absorption of the OH emission line by Cl_2 occurred . Photolysis of Cl_2 was prevented by the Cl_2 filter surrounding the reaction vessel .

Figure 7.5 shows a plot of first order rate constants of OH decay against Cl_2 pressure . The experimental second order rate constant , and the rate constant corrected for {4} and {5} . are shown in table 7.1

Figure 7.5.

Plot of first order decay rates of OH versus Cl_2 pressure



7.4 cont'd

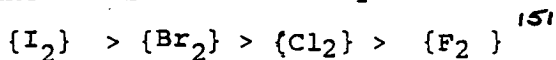
The Cl_2 contained a small amount of HCl impurity, which it was not found possible to remove completely by fractional distillation due to the closeness of the melting points (Cl_2 172 K, HCl 158 K). The percentage impurity was estimated at < 2% from the intensity of the I.R. spectrum of HCl near 3000 cm^{-1} . This leads to an error in the rate of reaction of OH with Cl_2 of < 10%.¹⁵⁴

It would seem reasonable to suggest that the reaction of OH with Cl_2 is similar to that of $\text{O}(2^3\text{P})$ with Cl_2

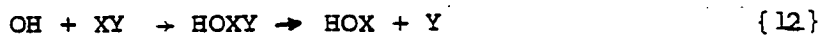


For {11} to be exothermic requires $\Delta H_{298}^{\circ} \{\text{HOCl}\} < -80 \text{ kJ mole}^{-1}$ which may be compared to a literature value of $-87 \pm 41 \text{ kJ mole}^{-1}$

Unfortunately it was not possible to extend this work to cover the other halogens. This was because Br_2 , IBr , ICl and I_2 all react spontaneously and rapidly with O_3 , and hence the experimental apparatus could not be used in its present design. Further work on the other halogens would be interesting in order to determine whether the trend of reactivity of OH with the halogens mirrors that of $\text{O}(2^3\text{P})$ and $\text{S}(3^3\text{P})$, i.e., whether the order of reactivity is -



And secondly the reaction of OH with halogens might, by analogy with the reactions of $\text{O}(2^3\text{P})$, proceed via a complex, and lead to formation of HOX, where X is the more electropositive halogen atom



Molecular beam studies would be of interest to determine whether reaction occurs by direct abstraction or by complex formation.

7.5 Conclusion

OH radicals react rapidly with RI and Cl_2 , the most plausible mechanism is halogen atom abstraction.

CHAPTER EIGHT

REACTION OF OH WITH ClO

8.1 Introduction:

Reaction between OH and ClO was first indicated by unexpected results from the $O_3/CF_3Cl/H_2$ system. As discussed in Chapter 3, there is considerable evidence of production of F atoms following the reaction of $O(2^1D)$ atoms with CF_3Cl .

H_2 (130 N m^{-2}) was added to remove F atoms by {1}¹⁵²



The formation of ClO was totally suppressed, but the rapid decay of ClO over the first millisecond only partially so (note, > 95 % of the F atoms were removed by {1}). This may be understood when it is considered that {1} leads to OH formation in the presence of O_3 by {2}.

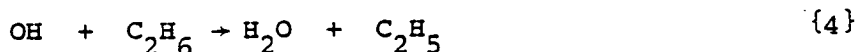


and that OH may then react with ClO.



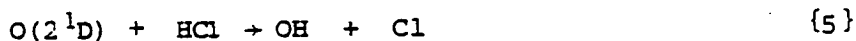
It should be noted that while OH was formed in the $O_3/CFC/C_2H_6$ experiments by the reaction of $O(2^1D)$ with C_2H_6 , OH would have been rapidly removed by {4}.

$$k_{\{4\}} = 2.64 \pm 0.17 \times 10^{-13} \text{ cm}^3 \text{ molec}^{-1} \text{ s}^{-1}$$



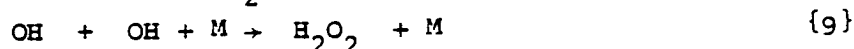
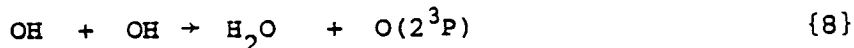
and reaction of OH with ClO would have been insignificant.

Further indication of a reaction between OH and ClO was obtained from measuring the ClO yield following the flash photolysis of O_3 in the presence of HCl. At high HCl pressures (1.3 KN m^{-2}), {5}¹⁵³ {6}¹⁵⁴ and {7} completely describe the reaction kinetics.



and thus the ClO yield is twice the $O(2^1D)$ yield.

This was observed experimentally. At lower HCl pressures, the yield of ClO decreases because {6} now competes with {8} to {11}.



However, the drop in ClO yield was greater than that due to reactions {8} to {11}, indicating the possible occurrence of other reaction (s).

8.1 cont'd.

Although these experiments provide only tenuous evidence of a reaction between OH and ClO, it was decided that in view of the potential stratospheric importance of such a reaction a full investigation was merited. The results are presented below.

Subsequent to the completion of this work, there has been a report at a Gordon Conference of a reaction between OH and ClO. Leu and Lin¹⁵⁵ used a discharge flow system with resonance fluorescence detection of OH, in an excess of ClO, to determine $k_{\{3\}} = 9.1 \pm 1.3 \times 10^{-12} \text{ cm}^3 \text{ molec}^{-1} \text{ s}^{-1}$. They considered that {3} might proceed by two pathways, viz:



and estimated a lower limit into $\{3a\} / (\{3a\} + \{3b\})$ of 0.65 by measuring $\{\text{HO}_2\}$ produced/ $\{\text{OH}\}$ removed. As HO_2 could be removed by secondary kinetic processes the authors conclude that $\{3a\} / (\{3a\} + \{3b\})$ could approach unity.

8.2 Results:

The rate of reaction of OH with ClO was measured by following the decay of OH by resonance absorption in the presence of an excess of ClO. OH and ClO were produced, in situ, by the reaction of $\text{O}(2^1\text{D})$ with H_2O (160 N m^{-2}) and CF_2Cl_2 (1.04 kN m^{-2}), following the flash photolysis of O_3 . The concentration of ClO was varied by varying the pressure of O_3 . Figure 8.1 shows a typical OH decay trace, and figure 8.2 shows a plot of first order rate constants of OH decay against O_3 pressure. The ClO concentration is related to the O_3 pressure by expression (A).

$$(A), \quad \{\text{ClO}\} = \{\text{O}_3\} \cdot y \cdot (k_1\{\text{CF}_2\text{Cl}_2\} / (k_1\{\text{CF}_2\text{Cl}_2\} + k_2\{\text{H}_2\text{O}\})) \cdot f$$

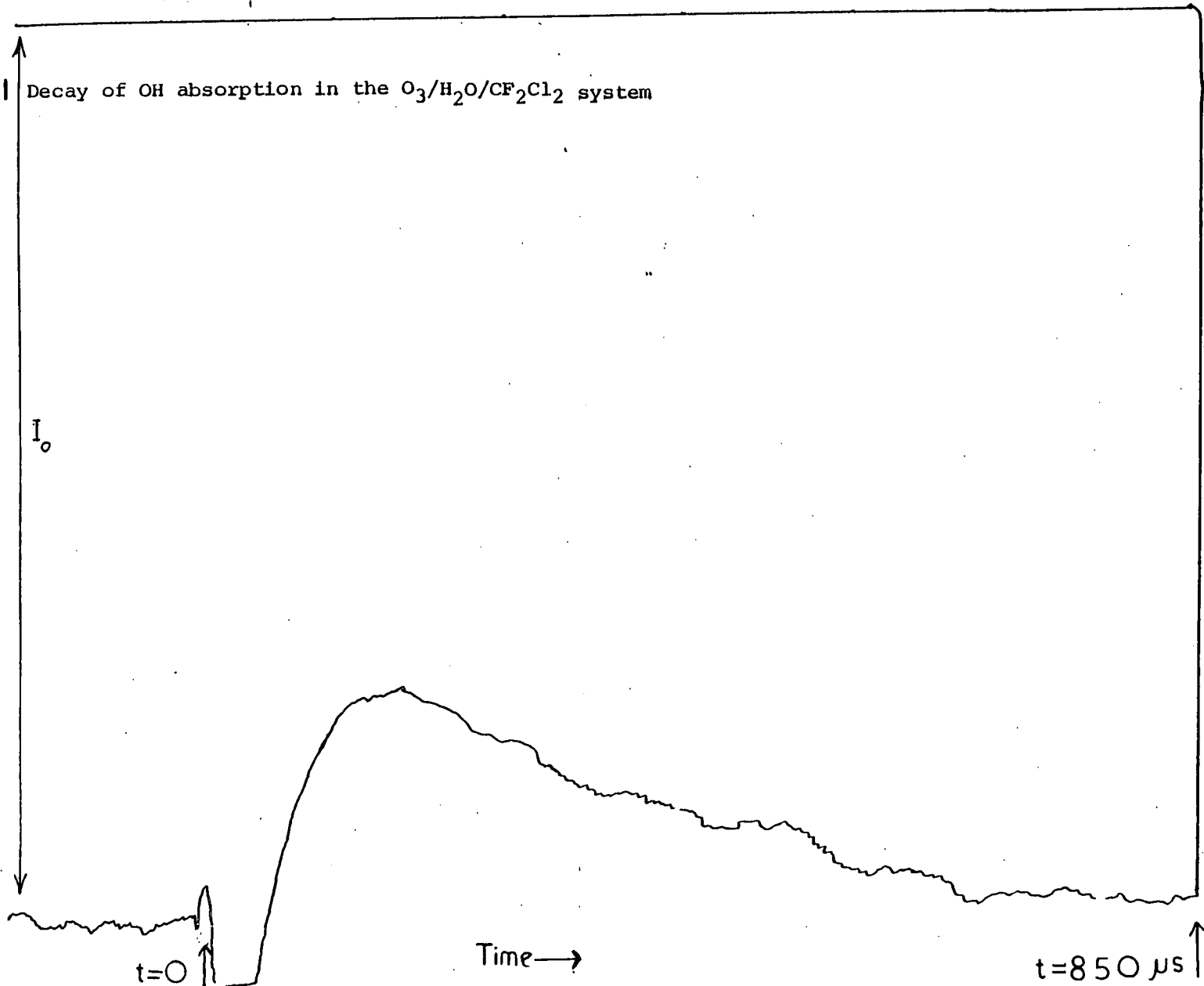
where,

y = the yield of $\text{O}(2^1\text{D})$ following the photolysis of O_3 .

f = the yield of ClO following the reaction of $\text{O}(2^1\text{D})$

with CF_2Cl_2 , and is equal to 0.9

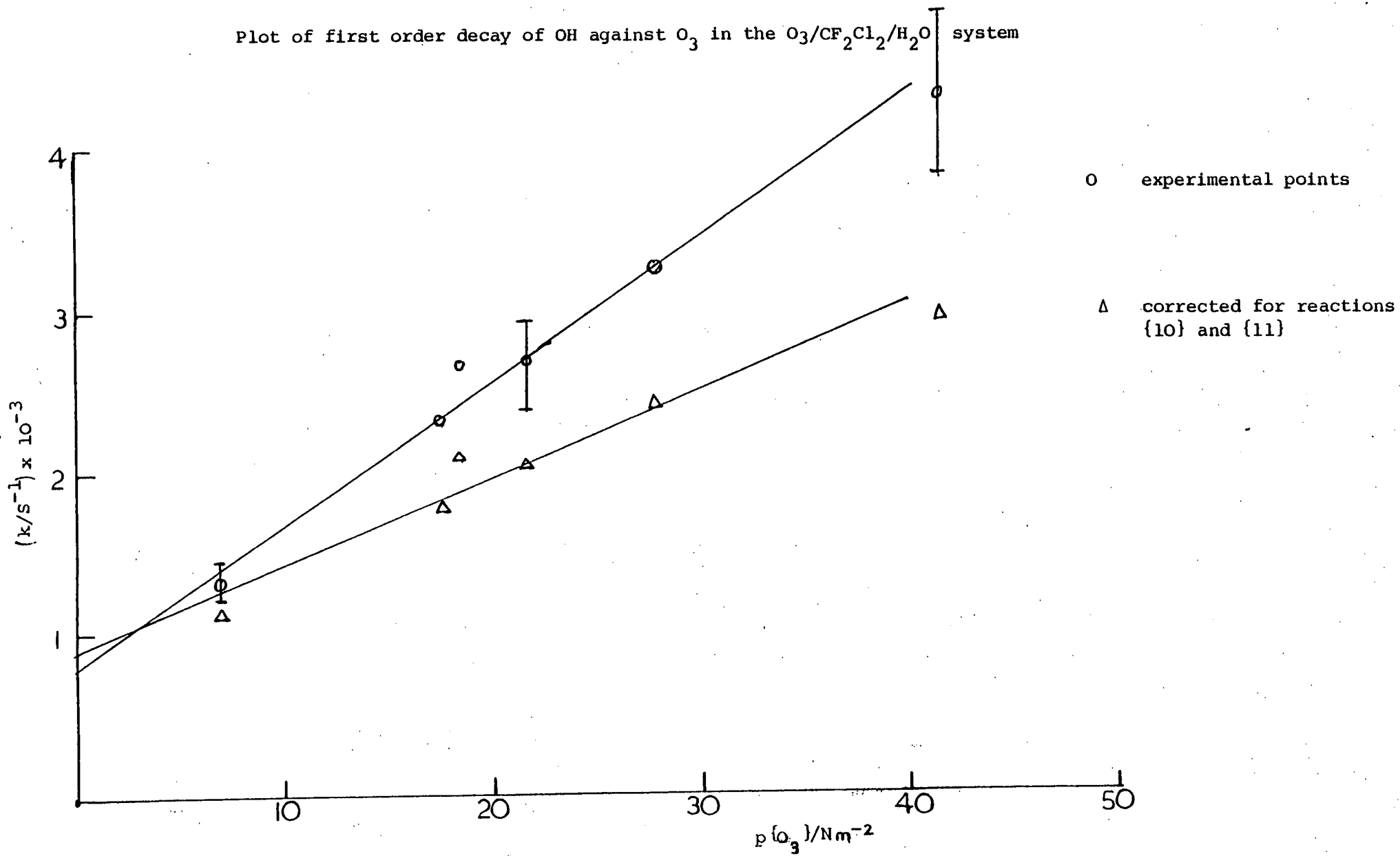
8.1 Decay of OH absorption in the $O_3/H_2O/CF_2Cl_2$ system



full scale = 1 ms
 $\rho\{O_3\} = 38.8 \text{ N m}^{-2}$

Figure 8.2.

Plot of first order decay of OH against O_3 in the $O_3/CF_2Cl_2/H_2O$ system



8.2 cont'd.

k_1 and k_2 are the rate constants for the reaction of $O(2^1D)$ with CF_2Cl_2 and H_2O respectively. k_1 and k_2 have been measured by Davidson et al.¹³⁰ and Husain et al.⁸⁻¹⁰ and are shown in table 8.1.

It should be noted that the values quoted from Husain's work, assume $\beta = 1.0$ and not $\beta = 0.41$ as preferred by Husain. This question of which β value to adopt has been discussed above (chapter 3) where it was shown that $\beta = 1.0$ is the preferred value. In this context of course no uncertainty in the ClO yield arises from the uncertainty in β as the same value for the fraction of $O(2^1D)$ reacting with CF_2Cl_2 is obtained whether k_1 and k_2 is calculated assuming $\beta = 0.41$ or 1.0

The yield of ClO, expressed as a fraction of the O_3 pressure, is shown in column 4 of table 8.1. For O_3 ($p = 40 \text{ N m}^{-2}$), the ClO concentration is calculated to be in the range $5.3 - 5.9 \times 10^{14} \text{ molec cm}^{-3}$ (photolysis of $O_3 = 7.3 \%$).

However, the increase in OH decay in figure 8.2 with increase of O_3 pressure is due to increase in OH removal by both {3} and {10}.

The contribution from {10} was measured in separate experiments wherein the O_3 pressure in an $O_3/H_2O/SF_6$ system was varied.

To minimise the effects of {8} and {9} on the decay kinetics the decay of OH was measured from a standard initial OH concentration, although the total OH yield increased with the O_3 pressure. Figure 8.3 shows a plot of first order rate constants of OH decay against O_3 pressure. The second order rate constant is $\approx 1.2 \times 10^{-13} \text{ cm}^2 \text{ molec}^{-1} \text{ s}^{-1}$.

This is approximately twice the literature value for reaction {10}^{131,156-158} and is because {10} is rapidly followed by {11} ($k_{\{11\}} = 3.0 \times 10^{-11} \text{ cm}^3 \text{ molec}^{-1} \text{ s}^{-1}$)¹³². Thus two OH molecules are removed for each one reacting by {10}. Computer simulation of the OH decay in the $O_3/H_2O/SF_6$ system showed that this interpretation was correct, and gave a value of $k_{\{10\}} = 7.5 \times 10^{-14} \text{ cm}^3 \text{ molec}^{-1} \text{ s}^{-1}$ (assuming $k_{\{11\}} = 3.0 \times 10^{-11} \text{ cm}^3 \text{ molec}^{-1} \text{ s}^{-1}$).

Table 8.1

Rate constants for the reactions of $O(2^1D)$ with H_2O and CF_2Cl_2 and yields of ClO

$k\{O(2^1D) + H_2O\}$	$k^1\{O(2^1D) + CF_2Cl_2\}$	$y, O(2^1D)$ reacting * with CF_2Cl_2	yield of ClO + relative to $\{O_3\}$	ref.
$1.3 \pm 0.1 \times 10^{-10}$ $cm^3 molec^{-1} s^{-1}$	$2.0 \pm 0.1 \times 10^{-10}$ $cm^3 molec^{-1} s^{-1}$	0.91 ± 0.09	0.060 ± 0.07 and 0.065 ± 0.07	8,10
$2.3 \pm 0.1 \times 10^{-10}$ $cm^3 molec^{-1} s^{-1}$	$1.45 \pm 0.5 \times 10^{-10}$ $cm^3 molec^{-1} s^{-1}$	0.80 ± 0.41	0.053 ± 0.027 and 0.057 ± 0.030	6,130

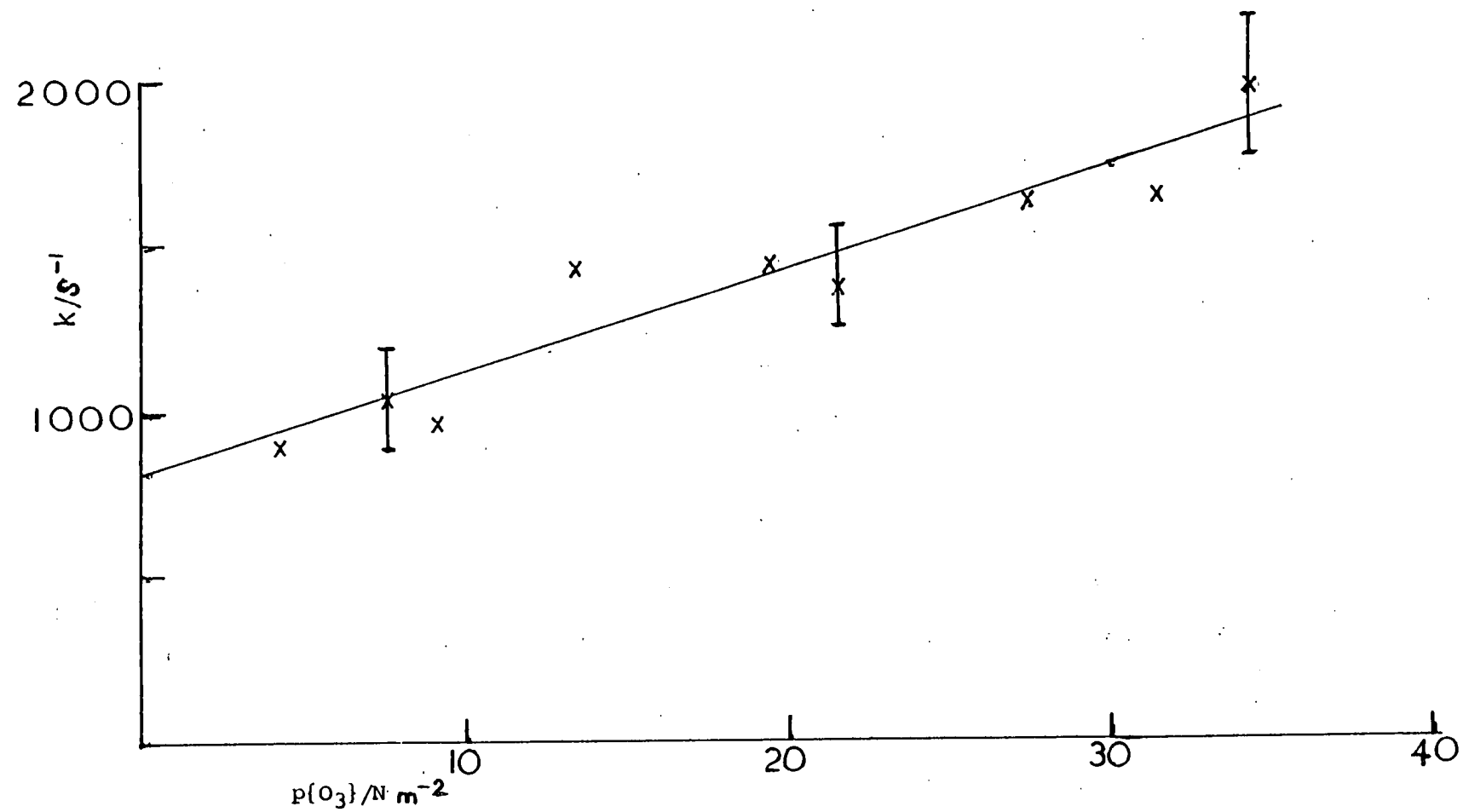
* Yield calculated from formula, $y = \frac{k^1\{CF_2Cl_2\}}{k^1\{CF_2Cl_2\} + k\{H_2O\}}$
 $p\{H_2O\} = 160 \text{ Nm}^{-2}$, $p\{CF_2Cl_2\} = 1.04 \text{ kN m}^{-2}$

+ Yield of ClO calculated from the formula, $= \frac{\{O(2^1D)\}}{\{O_3\}} \times y \times f$

where f = the yield of ClO from the reaction of $O(2^1D)$ with CF_2Cl_2 , (= 0.9)
 The photolysis lamp was refilled during the course of the experiments so that $\{O(2^1D)\}/\{O_3\}$, the % photolysis, has two values, 7.3 ± 0.4 , and 7.9 ± 0.9 %.

Figure 8.3.

Plot of first order decay of OH against O_3 pressure



8.2 cont'd.

The experimental decays obtained in the $O_3/CF_2Cl_2/H_2O$ system were corrected for the effects of {10} and {11}, and the revised values are shown in figure 8.2. These revised points are then a measure of the rate of reaction {3}.

In the following section, the kinetic analysis of this data will be discussed, as the rate constants calculated from the data depended on the nature of the reactions involved.

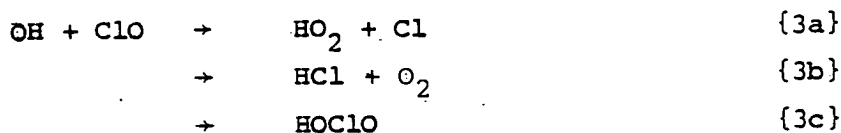
Addition of SF_6 ($p < 36 \text{ kN m}^{-2}$) lead to a definite increase in the rate of OH removal. A much smaller effect was observed with He ($p < 36 \text{ kN m}^{-2}$).

These effects will be discussed quantitatively in the following section.

8.3 Nature and rate of reaction of OH with ClO.

The value for the rate constant of {3} obtained from figure 8.2 is dependent on the reaction products. No direct evidence on the nature of the reaction was provided in this work, but the experiments discussed in Sections 1 and 2 do indicate that both ClO and OH are removed from the system.

Three reactions will be considered -

Reactions ({3b} and {3c}).

These will be considered together, since if it is assumed that HOClO is stable, then {3b} and {3c} are indistinguishable in the present experiments.

Reaction {3b} is exothermic, $\Delta H_{298}^{\circ} = - 229 \text{ kJ mole}^{-1}$, and there is evidence from molecular beam studies of the reaction of H atoms with OClO, that HOClO is thermodynamically stable 159.

8.3 cont'd.

The rate of {3bc} is obtained directly from figure 8.2 as $3.5 \times 10^{-12} \text{ cm}^3 \text{ molec}^{-1} \text{ s}^{-1}$ or $3.9 \times 10^{-12} \text{ cm}^3 \text{ molec}^{-1} \text{ s}^{-1}$ (based respectively on Husain's or Davidson's value for k_1 and k_2).

Figure 8.4 shows some simulated OH decay rate constants (based on Husain's rates for k_1 and k_2) superimposed on the experimental data. (The simulated OH decays gave good first order plots, supporting the validity of a first order analysis of the experimental data, although the ClO concentration is only about 5 times the OH concentration). The simulated points lie slightly below the experimental points (it should be noted that the uncorrected experimental data were used here, as the simulation included {10} and {11}).

The discrepancy is due partly to the small change in ClO concentration over the period of the OH decay (the simulated change in ClO concentration was 12 %), and probably to errors in the correction applied for the effects of {10} and {11}.

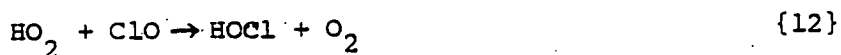
The corrected rate constant for {3bc} is shown in table 8.2.

Figure 8.5 shows the pressure dependency results evaluated on the above mechanism.

Reaction 3a

Reaction {3a} would lead to removal of OH. Removal of ClO, (in the above experiments ClO would be regenerated by the reaction of Cl with O_3 , reaction {7}) would be effected by {12}

$$k_{\{12\}} = 3.8 \times 10^{-12} \text{ cm}^3 \text{ molec}^{-1} \text{ s}^{-1}$$



Reaction {3a} is thermoneutral, $\Delta H_{298}^\circ = -1 \pm 8 \text{ kJ mole}^{-1}$

Computer simulation of this scheme, assuming $k_{\{3a\}} = 3.5 \times 10^{-12} \text{ cm}^3 \text{ molec}^{-1} \text{ s}^{-1}$ is shown in figure 8.4

This value leads to too high a value as OH is, in turn removed by the HO_2 produced in {3a}. The corrected values for {3a} are shown in table 8.2. Figure 8.6 shows the pressure dependency results evaluated on the above mechanism.

Figure 8.4 and table 8.2. also show the intermediate case, where {3a} and {3bc} each account for 50 % of the reaction cross section.

Figure 8.4.

Plot of experimental and simulated first order decay of OH against O_3 pressure.

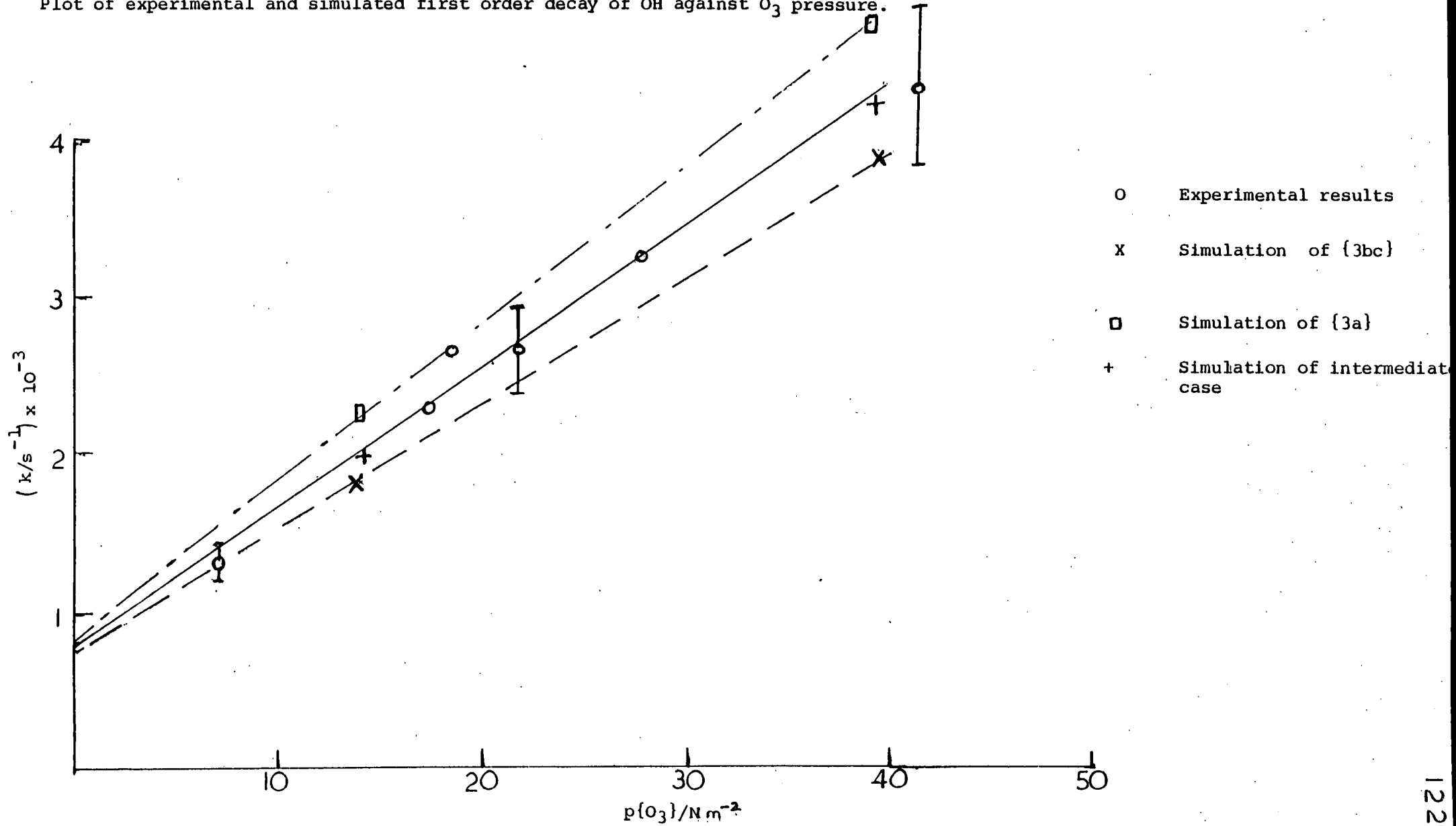


Table 8.2

Rate constants for reactions {3a} and {3bc}

No.	reaction	$k/\text{cm}^3 \text{molec}^{-1} \text{s}^{-1}$ * (Husain)	$k/\text{cm}^3 \text{molec}^{-1} \text{s}^{-1}$ * (Schiff)
{3bc}	OH + ClO → HOClO → HCl + O ₂	$\sim 4.0 \pm 0.8 \times 10^{-12}$	$\sim 4.5 \pm 2.2 \times 10^{-12}$
{3a}	OH + ClO → HO ₂ + Cl	$\sim 3.3 \pm 0.7 \times 10^{-12}$	$\sim 3.7 \pm 1.9 \times 10^{-12}$
{3a} + {3bc}	OH + ClO → HO ₂ + Cl ~ 50 % → HOClO) ~50 % HCl + O ₂)	$\sim 3.5 \pm 0.7 \times 10^{-12}$	$\sim 3.9 \pm 1.9 \times 10^{-12}$

Leu & Lin¹⁵³ measured $k\{3\} = 9.1 \pm 1.7 \times 10^{-12} \text{ cm}^3 \text{ molec}^{-1} \text{ s}^{-1}$

$$\text{with } \frac{k\{3a\}}{k\{3a\} + k\{3b\}} > 0.65$$

* % O₃ photolysis in fig.8.2. was 7.3 %

Figure 8.5

Plot of the second order rate constant for the reaction, $\text{OH} + \text{ClO} \rightarrow \text{HOClO}/\text{HCl} + \text{O}_2$ versus pressure of He or SF_6

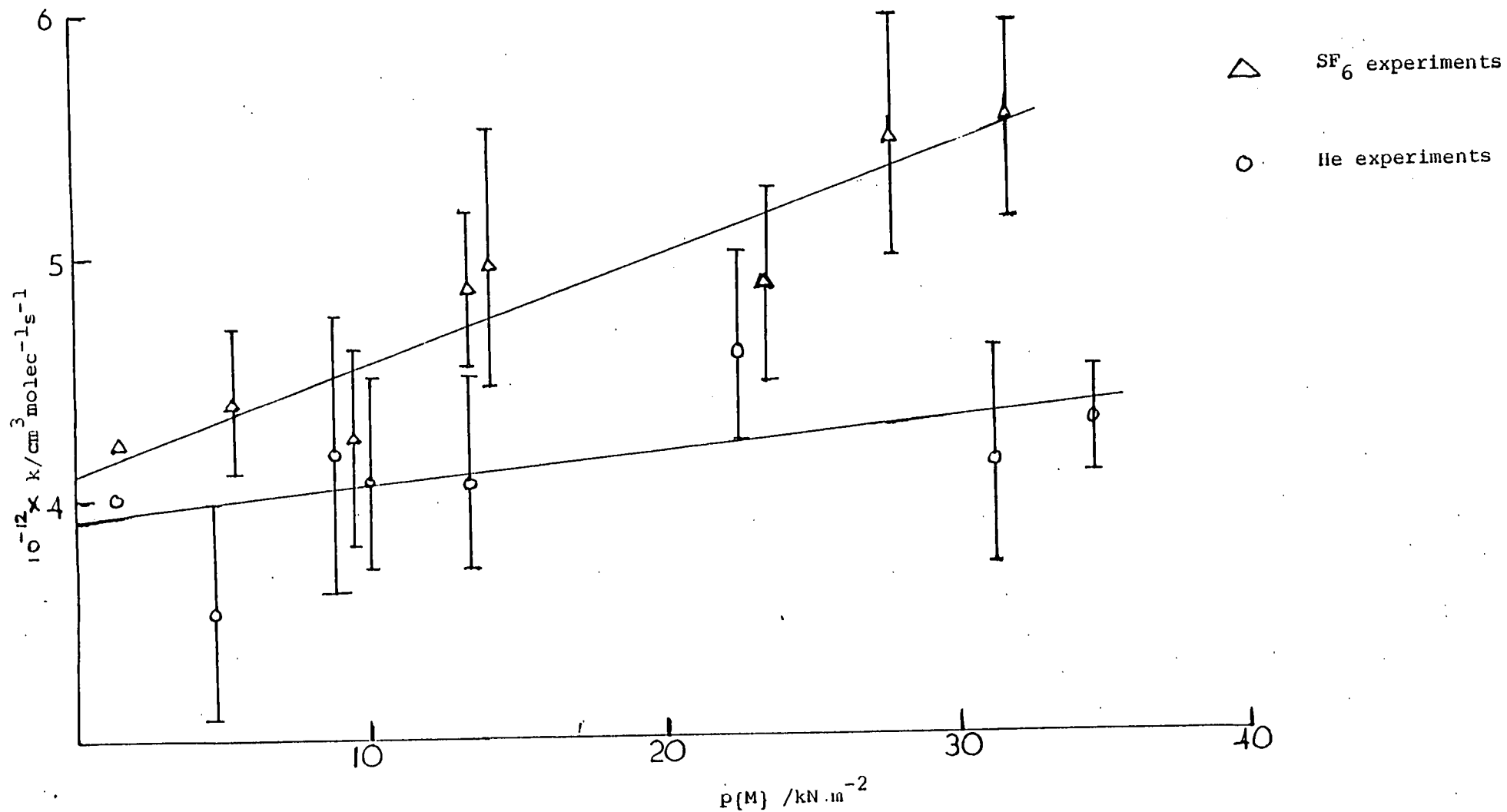
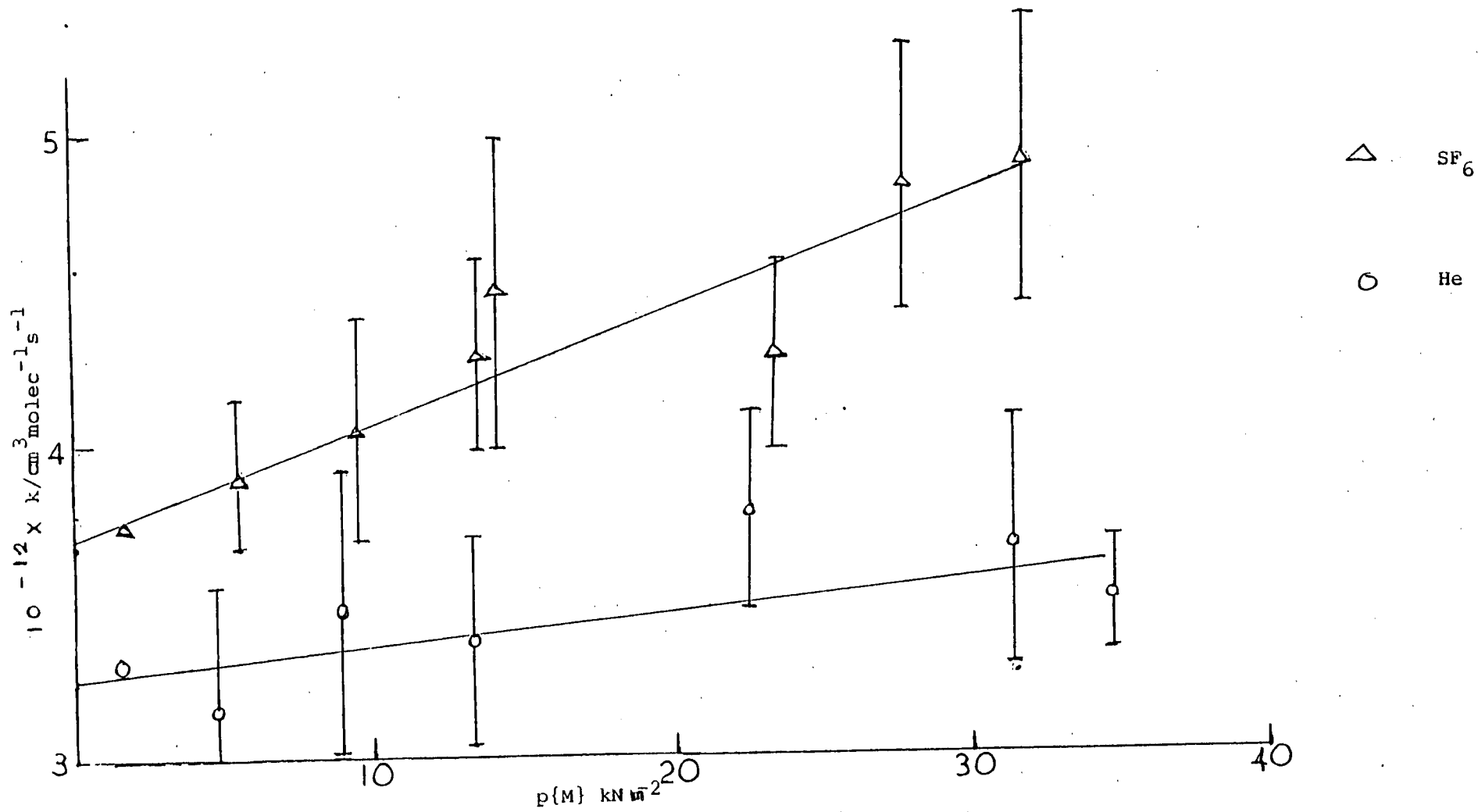


Figure 8.6

Plot of the second order rate constant for the reaction, $\text{OH} + \text{ClO} \rightarrow \text{HO}_2 + \text{Cl}$ versus pressure of He or SF_6



8.4 Discussion:

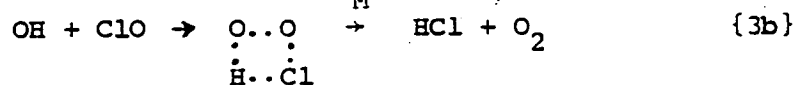
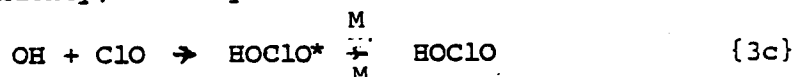
In the preceding section, several reactions between OH and ClO were postulated to enable rate data to be determined from the experimental data. As previously stated, there is no direct evidence for the nature of the reaction in this work, except that both OH and ClO are removed. Two reactions are postulated in this work.



and a third has been postulated by Beu and Lin

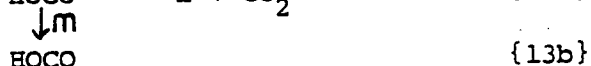
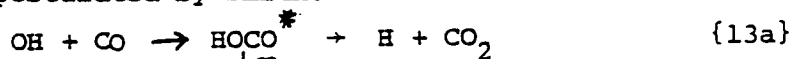


Reaction {3a} and {3c} would be expected to show a pressure dependency, and may be rewritten as:

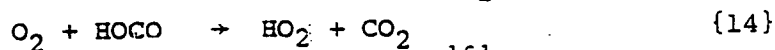


Of the two {3c} is the preferred reaction. {3b} would require considerable internal re-arrangement of the reaction intermediate for successful reaction, which may be considered to disfavour it.

It is interesting to compare the reaction of OH with ClO to the reaction of OH with CO. This reaction displays a pressure dependency^{161, 162} and the following mechanism has been postulated by Smith¹⁶³



an essentially similar mechanism has been proposed by Beremann et al.¹⁶². HOCO has been observed in matrix isolation experiments¹⁶⁴. Smith¹⁶³ has concluded that HOCO is stable to dissociation to OH + CO, and H + CO₂, and suggests that HOCO is removed by reaction with O₂



also, Overend and Paraskevopoulos¹⁶¹ suggested HOCO removal by -



8.4 cont'd.

As there is evidence for HOClO being thermodynamically stable¹⁵⁹, reaction {3c} (which is exactly analogous to {13b}) seems sensible.

However, it is unlikely that HOClO will re-arrange to give HO₂ + Cl. This channel, for which Leu and Lin claim evidence of direct observation, is likely to be a distinct pathway, arising from a HO...OCl collision geometry. Reactions ({3a} and {3c}) may thus be considered as reasonable possible reactions, although it is not possible to say to what extent either occurs. Reaction {3b} is considered unlikely.

Agreement between the rate data obtained in this work and that reported by Leu and Lin is not good. The discharge flow system with resonance fluorescence detection of OH, used by these authors, should be capable of giving more reliable and accurate results than the rather unsatisfactory technique used in this work. Sources of errors in this work are, the low excess of ClO (only 5 X) over the OH concentration, and the fact that the ClO concentration was not measured directly, but calculated.

It was assumed above that HOClO was a stable molecule, at least on the time scale of the experiment. However, HOClO, has not been isolated and is only known in solution (chlorous acid) where it rapidly decomposes, OClO being one of the products. Thus it may be that self reaction of HOClO (this is considered to be important for HOClO¹⁶⁵) or reaction with species such as O₂ or O₃ may be important, and could lead to the formation of OH or H atoms (which would form OH by reaction {2}). Any such reactions are more likely in the system used in this study due to the much higher concentrations of reactants compared to the flow system of Leu and Lin, and could lead to a low value for k_{3}.

Conversely, if HOClO is less efficiently removed by the reactions discussed above, then {17} may be important in flow system.



which would lead to a high value for k_{3}. These explanations for the discrepancy between the rate data reported in this work and in the work of Leu and Lin are purely speculative and more work is required to resolve the matter.

8.5 Conclusion.

Reaction between OH and ClO has been shown to occur.

The reaction exhibits a pressure dependency and two reaction pathways are considered likely, *viz*:



but it is not possible to estimate the relative importance of each.

Appendix 1Materials

- CF_3Cl : I.C.I. 'Arcton' liquified gas was thoroughly degassed by repeated freeze-pump-thaw cycles before use .
- CF_2Cl_2 : as CF_3Cl
- CFCl_3 : as CF_3Cl
- CF_2HCl : as CF_3Cl
- CF_2ClBr : as CF_3Cl
- CF_3Br : Mathieson , degassed as for CF_3Cl
- C_2H_6 : see Appendix 2
- Cl_2 : B.O.C. Degassed as for CF_3Cl , and purified by fractional distillation .
- CDCl_3 : B.O.C. 98 % D . Was degassed by repeated freeze-pump-thaw cycles .
- CD_2Cl_2 : as CDCl_3
- CHCl_3 : Fisons laboratory reagent . Was degassed by repeated freeze-pump-thaw cycles .
- CH_2Cl_2 : as CHCl_3
- CF_3I : Pierce chemical company . Was degassed by repeated freeze-pump-thaw cycles , and stored in a blackened bulb .
- $\text{C}_2\text{F}_5\text{I}$: as CF_3I
- $\text{C}_3\text{F}_7\text{I}$: as CF_3I
- CH_3I : as CHCl_3 and stored in a blackened flask .
- He : B.O.C cylinder grade . Used directly after passing through liquid N_2 traps to remove water .
- Kr : B.O.C 'grade X' . Used directly from breakseal flasks .
- NH_3 : B.O.C . Degassed by repeated pump-freeze-thaw cycles .
- N_2 : B.O.C. 'white spot' grade . Used directly after passing through liquid N_2 traps to remove water .
- SF_6 : Mathieson . Was thoroughly degassed by repeated freeze-pump-thaw cycles

Appendix 2Preparation of C₂H₆

Mixtures of O₃ and C₂H₆ (Mathieson research grade) were observed to react spontaneously and rapidly , too rapidly to allow the preparation of mixtures for experimental purposes . This reaction was much faster than that reported in the literature for the reaction between O₃ and C₂H₆¹⁶⁶ . Olefinic impurities were considered to be the likely reactive species and their presence in the C₂H₆ was shown by proton NMR .

To remove the alkenes (and any acetylenic impurities) the ethane was treated with Br₂ , thus converting the alkenes into relatively high molecular weight dibromo compounds . The ethane was recovered by successive fractionations from a solid CO₂/isopropanol bath through a pet-ether/ liq. N₂ bath to a trap held at liquid N₂ temperatures .

Reaction of ethane , so purified , with O₃ was slow (< 10 % removal per hour) allowing the preparation of O₃/C₂H₆ mixtures for experimental purposes .

Appendix 3Preparation of Ozone

Ozone was prepared by the method of Thrush and Clough¹⁶⁷. The trap, filled with 4-6 mesh silica gel, was cooled to 195 K using a solid CO₂/isopropanol slush, and attached to a Tower's ozone apparatus. After flushing out the apparatus with O₂ (dried over H₂SO₄) the ozoniser was turned on and O₃ allowed to absorb onto the gel. When sufficient O₃ was collected (about 30 minutes to an hour) the trap was closed and the ozoniser switched off. The ozoniser was flushed with O₂ (by-passing the trap) for a few moments.

The trap was attached to a greaseless vacuum line (using silicon grease), and slowly pumped down to remove O₂. Any O₃ coming off was destroyed by passage over a hot nickel catalyst, before reaching the rotary pump.

When the trap was pumped down the slush bath was removed, and the O₃ desorbing off the gel was collected in an aged blackened bulb. Pressures of O₃ in the bulb were kept at $\leq 3.5 \text{ kN m}^{-2}$. He was added as a dilutant gas. The decay of O₃ was very slow (1% per day).

At regular intervals the trap was baked for several hours in an oil bath to remove impurities. After this process several loads of O₃ were required to deactivate the gel with respect to O₃ destruction.

The safety aspects of this method of preparing and handling O₃ have been considered by Cook¹⁶⁸.

The following lecture courses were attended:-

Why Chemists use Neutrons

History of the Chemistry Department

N.M.R. Spectroscopy

Chemistry of the Atmosphere

Detergency

Computing

In addition, regular departmental colloquia and group meetings were attended.

REFERENCES

1. D.Husain and R.J. Donovan,
Chem.Rev., 70, 489 (1970)
2. R.J.Donovan and H.Gillespie,
Specialist Periodical Reports, (Chemical Society)
Gas kinetics, vol. 1, 56 (1975)
3. R.J. Cvetanovic,
Can.J.Chem., 52, 1453 (1974)
4. M.R.Levy,
Progress in Reaction Kinetics, 10, 140 (1979)
5. R.J.Donovan,
Progress in Reaction Kinetics, 10, 286 (1979)
6. J.A. Davidson, C.M. Sadowski, H.I.Schiff,
G.E. Streit, C.J.Howard, D.A.Jennings and A.L.Schmeltekopf
J.Chem.Phys., 64, 57 (1976)
7. G.E. Streit, C.J.Howard, A.L.Schmeltekopf,
J.A. Davidson and H.I.Schiff,
J.Chem.Phys., 65, 4761 (1976)
8. J.A. Davidson, M.I.Schiff, J.J.Brown and C.J.Howard,
J.Chem.Phys., 69, 4277 (1978)
9. R.F.Heidner, D.Husain and J.R.Wiesenfeld
a) Chem.Phys. Lett., 16, 530 (1972)
b) J.C.S. Faraday Trans. 2, 69, 927 (1973)
10. I.S. Fletcher and D.Husain,
Can.J.Chem., 54, 1765 (1976)
11. I.S. Fletcher and D.Husain,
J.Phys. Chem., 80, 1837 (1976)
12. M.Yamazaki and R.J.Cvetanovic,
a) J.Chem.Phys., 39, 1902 (1963)
b) J.Chem.Phys., 40, 582 (1964)
c) J.Chem,Phys., 41, 3703 (1964)
13. N.Basco and R.G.W. Norrish,
Can.J.Chem., 38, 1769 (1960)
14. M.C.Lin,
J.Phys. Chem., 76, 1425 (1972)
15. A.B.Callear and H.E. Van den Bergh
Chem.Phys. Lett., 8, 17 (1971)

16. C.J.Howard and K.M.Evenson,
a) J.Chem.Phys., 61, 1943 (1974)
b) J.Chem.Phys., 64, 197 (1976)
17. J.G. Anderson and F.Kaufman,
Chem.Phys.Lett., 16, 375 (1972)
18. F.Stuhl and H.Niki,
J.Chem.Phys., 57, 3671, 3677 (1972)
19. M.A.A.Clyne and P.M.Hoit,
J.C.S. Faraday Trans. 2, 75, 570 (1979)
20. M.J. Kurylo,
Chem.Phys. Lett., 23, 467 (1973)
21. C.Morley and I.W.M. Smith,
J.C.S. Faraday Trans. 2, 68, 1076 (1972)
22. R.P.Overend, G.Paraskevopoulos and R.J.Cvetanovic,
Can.J.Chem., 53, 3374 (1975)
23. S.Gordon and W.A.Mulac,
Int.J.Chem.Kinet.Symp. No.1. 289 (1975)
24. R.H.Garstang,
Mon.Notic.Roy.Astron.Soc., 3, 115 (1951)
25. D.C. Baulch and W.H.Breckenridge,
Trans. Faraday Soc., 62, 2768 (1966)
26. D.W.McCullough and W.D.McGrath,
J.Photochem., 1, 241 (1973)
27. M.C. Lin and J.E.Butler
Faraday Discussions, 67, 346 (1979)
28. J.C.Tully,
J.Chem. Phys., 62, 1893 (1975)
29. W.B.De More and O.F.Raper,
J.Chem.Phys., 46, 2500 (1967)
30. G.Paraskevopoulos and R.J.Cvetanovic,
a) J.Chem.Phys., 50, 590 (1969)
b) J.Chem.Phys., 52, 5821 (1970)
31. P.Michand and R.J.Cvetanovic,
J.Phys.Chem., 76, 1375 (1972)
32. G.Paraskevopoulos and R.J.Cvetanovic,
J,Amer.Chem.Soc., 19, 7572 (1967)

33. C.L.Lin and W.V.De More,
J.Phys. Chem., 77, 863 (1973)
34. W.Marx, F.Bahe and U.Schurath,
Ber. Buns.Physik. Chem., 83, 225 (1979)
and references therein.
35. R.Overend, G.Paraskevopoulos, J.R. Crawford and H.A.Wieke,
Can.J.Chem., 53, 1915 (1975).
36. I.W.M. Smith and R.Zellner,
J.C.S. Faraday Trans. 2, 70, 1045 (1974)
37. R.Atkinson, R.A.Perry and J.N.Pitts,
J.Chem Phys., 66, 1197 (1977)
38. C.Anastasi and I.W.M. Smith,
J.C.S. Faraday Trans. 2, 72, 1459 (1976)
39. D.H.Jaffer and I.W.M. Smith,
Faraday Discussions 67, 212 (1979)
40. H.W.Bierman, C.Zetzsch and F.Stuhl
Ber.Buns.Physik Chem., 82, 633 (1978)
41. M.J.Kurylo,
a) Chem. Phys.Lett., 58, 238 (1978)
b) J.Photochem., 9, 124 (1978)
42. A.R. Curtis and E.M. Chance,
A.E.R.E. (Harwell) - R.7345 H.M.S.O. (1974)
43. R.G.W.Norrish and G.Porter,
Nature, 164, 658 (1949)
44. G.Porter and M.A. West,
'Investigations of rates and mechanisms of reactions'
(2nd edition) part 2, edited by G.G.Hames. Wiley Interscience.
London 1973
45. N.Basco, D.G.L.James and R.D. Stuart,
Internat. J.Chem.Kinet, 2, 215 (1970)
46. H.M.Gillespie and R.J.Donovan,
Chem.Phys.Letts., 37, 468 (1976)
47. T.Carrington and H.P.Broida,
J.Mol.Spec., 2, 215 (1970)
48. F.S.Rowland and M.J.Molina,
Nature, 249, 810 (1974)
49. J.E.Lovelock,
Nature, 241, 194 (1973)
50. R.K.M.Jayanty, R.Simonaitis and J.Heicklen,
J.Photochem., 4, 381 (1975)

51. R.E.Robbert and P.J.Ausloos,
J.Photochem., 4, 419 (1975)
52. R.J.Donovan, H.M. Gillespie and J.Garraway,
J.Photochem, 7, 29 (1977)
53. J.A.N.A.F. Thermochemical Tables, 2nd ed.
Nat .Bur.Stand,Washington D.C. (1971)
54. C.J.Schack and W.Maya,
J.Amer. Chem.Soc., 91, 2902 (1969)
55. M.C. Addison, R.J.Donovan and J.Garraway,
Faraday Discussions 67, 286 (1979)
56. R.K.Jayanty, R.Simonaitis and J.Heicklen,
J.Photochem., 4, 202, 381 (1975)
57. J.N.Pitts, H.L. Sandoval and R.Atkinson,
Chem.Phys.Letts, 29, 31 (1974)
58. K.Kaufmann, R.J.Donovan and J.Wolfrum,
Nature,262, 304 (1976)
59. M.C.Lin,
J.Phys. Chem., 75, 3642 (1971)
60. M.C.Lin,
J.Phys.Chem., 76, 711, 1425 (1972)
61. M.Griggs,
J.Chem.Phys., 49, 857 (1968)
62. W.B. De More and O.F.Roper,
J.Chem.Phys., 44, 1780 (1966)
63. E.Lissi and J.Heicklen
J.Photochem., 1, 39 (1970)
64. P.W.Fairchild and E.K.C.Lee,
Chem.Phys.Letts., 60, 36 (1978)
65. R.F.Hampson,
J.Phys. Chem., Ref.Data 2, 27 (1973)
66. C.E.Fairchild, E.J.Stone and G.M. Lawrence
J.Chem. Phys., 69, 3632 (1978)
67. M.A.A.Clyne and J.A. Coxon
Proc.Roy.Soc.London Ser.A, 303, 207 (1968)
68. N.Basco and S.K.Dogra,
Proc.Roy.Soc.,London, Ser.A. 323, 29 (1971)
69. M.Mandelman and R.W.Nichols,
J.Quant.Spectry.Radioactive transfer (1977)
70. P.Rigand, B.Leroy, G.Le Bras, G.Poulet,
J.L.Jourdain and J.Combourieu,
Chem.Phys. letts. 46, 161 (1977)
57. 109 (1978)

71. M.A.A. Clyne and J.A. Coxon,
Trans. Faraday Soc., 62, 1175 (1966)
72. D.D.Davis, W.Braun and A.M.Bass,
Internat.J.Chem.Kinet, 2, 107 (1972)
73. N.R.Greiner,
J.Chem.Phys., 53, 1285 (1970)
74. M.A.A.Clyne and Wing.S.Nip,
J.C.S. Faraday Trans.2, 72, 838 (1976)
75. M.A.A.Clyne and Wing S.Nip,
J.C.S. Faraday Trans.1, 72, 2211 (1976)
76. J.Heicklen,
Advance in Photochemistry 1, 51, (1969)
77. P.B.Ayscough, J.C.Polanyi and E.W.R. Skacie,
Can.J.Chem, 33, 743 (1955)
78. J.R.Mayer, C.Olaveson and K.C. Robb,
Trans.Faraday Soc., 65, 2988 (1968)
79. N.Basco and J.E.Hunt ,
Internat.J.Chem.Kinet, 11, 649 (1979)
80. H.S.Johnston, E.D.Morris and J.Van den Bogaerde
J.Amer.Chem.Soc., 91, 7712 (1969)
81. a) R.A. Cox and R.G.Derwent ,
J.C.S. Faraday Trans. 1, 75, 1635 (1979)
b) R.A.Cox, R.G. Derwent, A.E.J.Eggleton and H.J.Reid,
J.C.S. Faraday Trans.1, 75, 1648 (1979)
82. M.A.A. Clyne, D.J.McKenney and R.I.Watson,
J.C.S. Faraday Trans, 2, 71, 322 (1975)
83. Von H.G.Wagner, C.Zetsch and J.Warnatz,
Ber.Buns.Physik.Chem. 76, 526 (1972)
84. G.C.Fettis, J.H.Knox, and A.F. Trotman - Dickenson,
Can.J.Chem., 38, 1643 (1960)
85. E.H.Appelman and M.A.A. Clyne ,
J.C.S. Faraday Trans.1, 71, 2075 (1975)
86. K.Kaufmann and J.Wolfrum , personal communication.
87. M.A.A. Clyne and R.T.Watson ,
J.C.S. Faraday Trans, 1, 73, 1169 (1977)
88. N.Basco and S.K.Dogra ,
Proc.Roy.Soc.London. Ser.A, 323, 417 (1971)

89. C.R.Parent and M.C.L.Gerry,
J.Mol.Spec. 49, 343 (1974)
90. H.Schmutz and H.J.Schumacher,
Z.Anorg. Allgem.Chem., 249, 238 (1942)
91. T.G.Ogawa, G.A. Carlson and G.C.Pimental ,
J.Phys. Chem. 74, 2090 (1970)
92. C.W. Mathews,
Can.J.Phys. 45, 2355 (1967)
93. W.J.R.Tyerman,
Trans.Faraday Soc., 65, 1188 (1969)
94. R.Simoniatis and J.Heicklen,
J.Phys. Chem. 77, 1096 (1973)
95. G.O. Pritchard and M.J.Perona,
Internat. J.Chem.Kinet., 1, 509, (1969)
96. F.W. Dalby,
J.Chem. Phys., 41, 2297 (1964)
97. G.R.Barnes, R.A.Cox and R.F. Simmons
J.Chem.Soc.B, 1176 (1971)
98. W.J.R.Tyerman,
Trans.Faraday Soc., 65, 163 (1969)
99. M.C.Lin,
Int.J.Chem.Kinet., 5, 173 (1973)
100. F.W.Dalby,
J,Chem.Phys., 41, 2297 (1964)
101. T.L.Bucks and M.C.Lin,
J.Chem.Phys., 64, 4235 (1976)
102. J.E. Nicholas and R.G.W.Norrish,
Proc. Roy.Scot.London, Ser.A, 307, 391 (1968)
103. M.A.A.Clyne and R.T. Watson,
J.C.S. Faraday Trans. 1, 71, 336 (1975)
104. M.A.A.Clyne and H.W.Cruse
Trans.Faraday Soc. 66, 2214 (1970)
105. W.G.Clark, D.W. Setser and E.E.Siefert,
J.Chem. Phys., 74, 1670 (1970) and refs., therein.
106. M.Martin, personal communication
107. D.Naumann, L.Deneken and E.Renk,
J.Fluor. Chem, 5, 509 (1975)

108. P.A.Gorry, C.V.Nowikow, and R.Grice,
Chem.Phys.Letts, 55, 24 (1978)
109. D.St.A.G.Radleir, J.C. Whitehead and R.Grice,
Mol.Phys. 29, 1813 (1975)
110. D.P.Parish and D.R.Herschbach,
J.Amer.Chem.Soc., 95, 6133 (1973)
111. C.F.Carter, M.R.Levy, K.B. Woodall and R.Grice,
Faraday Discussions, 55, 381 (1973)
112. L.Andrews, F.K.Chi and A.Arkell,
J.Amer.Chem.Soc., 96, 1997 (1974)
113. F.K.Chi and L.Andrews
J.Phys.Chem., 77, 3062 (1973)
114. T.C.Frankiewicz, F.W.Williams and R.G.Gann
J.Chem.Phys., 61, 402 (1974)
115. S.D.Worley, R.N. Colthorp and A.E.Potter
J.Chem.Phys., 76, 1511 (1972)
116. I.W.M. Smith and R.Zellner,
J.C.S. Faraday Trans., 2, 70, 1045 (1974)
117. F.Stuhl,
J.Chem.Phys., 59, 535 (1973)
118. I.W.M.Smith and R.Zellner
Int.J,Chem.Kinet., Symp., No.1. 341 (1975)
119. D.D.Davis, 'Absolute rate constants for elementary reactions
of atmospheric importance', Results from the University of
Maryland gas kinetics laboratory. Report 3 (University of
Maryland, 20742, 1976).
120. F.H.Westheimer,
Chem.Rev., 61, 265 (1961)
121. D.D.Davis, G.Machada, B.Conway, Y.Oh and R.Watson
J,Chem.Phys., 65, 1268 (1976)
122. R.A.Perry, R.Atkinson and J.N.Pitts
J.Chem.Phys., 64, 1618 (1976)
123. G.Herzberg,
'Infra-red and Raman Spectra of Polatomic Molecules',
Van Nostrand, N.Y. 1945.
124. R.P.Bell,
Faraday Soc., Disc., 39, 16 (1965)
125. W.J.Albery
Trans.Faraday Soc., 63, 200 (1967)

126. S.W.Benson,
'Foundations of Chemical Kinetics'
McGraw-Hill, N.Y. 1960.

127. M.A.A.Clyne and Wing S.Nip
Int.J.Chem.Kinet., 10, 367 (1978)

128. R.G.W. Norrish and R.P.Wayne,
Proc.Roy.Soc.,London Ser.A, 288, 361 (1965)

129. K.J.Olszyna, R.G.De Pena, M.Luria and J.Heicklen
J.Aerosol Sci., 5, 421 (1974)

130. J.A. Davidson, H.I.Schiff, G.E. Streit, J.R.McAfee,
A.L.Schmeltekopf and C.J.Howard
J.Chem.Phys., 67, 5021 (1977)

131. R.F.Hampson
J.Phys.Chem.Ref. Data 2, 267 (1973)

132. W.Hack, A.W.Preuss and H.Gg.Wagner
Ber.Bunsenges, Phys.Chem., 82, 1167 (1978)

133. D.W.Trainor and C.W.von Rosenberg
J.Chem.Phys., 61, 1010 (1974)

134. J.Caldwell and R.Black,
Trans.Faraday Soc., 61, 1939 (1965)

135. S.G.Cheskis and O.M. Sarkison
Chem.Phys.,Lett., 62, 72 (1979)

136. M.Gehring, J.Hoyerman, H.Schacke and J.Wolfrum,
Symp.Combus.14th (Combusion Institute, Pittsburgh) 99, (1973)

137. J.W.Bozzelli and M.Kaufman,
J.Phys.Chem., 77, 1748 (1973)

138. J.M.Farrar and Y.T.Lee,
J.Chem.Phys. 63, 3639 (1975)

139. E.N.Okafo and E.Whittle,
Int.J.Chem.Kinet., 7, 273, 287 (1975)

140. D.M.Golden and S.W.Benson,
Chem.Rev., 69, 125 (1968)

141. R.Hiatt and S.W.Benson,
Int.J.Chem.Kinet., 4, 479 (1972)

142. J.M.Farrar and Y.T.Lee,
J.Amer. Chem.Soc., 96, 7570, (1974)

143. J.D.McDonald, P.R.le Breton, Y.T.Lee and D.R.Herschbach
J.Chem.Phys. 65, 769 (1972)

144. Y.T.Lee, J.D.McDonald, P.R.Le Breton and D.R.Herschbach,
J.Chem.Phys., 49, 2447 (1968)
51, 455 (1969)
145. J.B.Cross and N.C.Blais,
J.Chem.Phys., 52, 3580 (1970)
55, 3970 (1971)
146. C.F.Carter, M.R.Levy and R.Grice,
Faraday Disc., 55, 357 (1973)
147. J.Barassin and J.Combourieu
Bull.Soc. Chem. Fr. 1, (1974)
148. A.A.Westenbergh and N.de Haas,
J.Chem.Phys., 62, 4477 (1975)
149. J.T.Herron and R.E.Huie,
J.Phys.Chem., 73, 1326 (1969)
150. V.I.Vedeneyev, L.V. Garvich, V.N.Kondrat' yev
V.A.Medvedev and Ye.L.Frankevich
'Bond Energies, Ionisation Potentials and Electron Affinities'
Edward Arnold, London (1966)
151. M.A.A.Clyne, P.B.Monkhouse and L.W.Townsend,
Internat.J.Chem.Kinet., 8, 425 (1976)
and refs., therein.
152. R.Foon and G.P.Reid,
Trans.Faraday Soc., 67, 3513 (1971)
153. M.C. Addison, R.J.Donovan, and H.M.Gillespie,
Chem.Phys.Lett., 44, 602, (1976)
154. I.W.M.Smith and R.Zellner,
J.C.S. Faraday Trans., 2, 70, 1045 (1974)
155. M.T.Leu and C.L.Lin
Geophys.Res.Letts. 6, 425 (1979)
156. M.J.Kurylo,
Chem.Phys., Lett., 23, 467 (1973)
157. W.B.De More
Internat.J.Chem.Kinet., Symp. No.1. 273 (1975)
158. J.G. Anderson and F.Kaufman,
Chem.Phys.Lett., 19, 483 (1973)
159. R.P.Mariella, B.Lantzsch, V.T.Maxsin and A.C.Luntz
J.Chem.Phys., 69, 5411 (1978)
160. B.Reimann and F.Kaufman
J.Phys.Chem., 69, 2925 (1978)

161. R.Overend and G.Paraskevopoulos,
Chem.Phys.Lett., 49, 109 (1977) and refs. therein.
162. H.W.Bierman, C.Zetzsch and F.Stuhl, Ber, Buns.
Phys.Chem., 82, 633 (1978)
163. I.W.M.Smith,
Chem.Phys.Lett., 49, 112 (1977)
164. D.E.Milligan and M.E.Jacox,
J.Chem.Phys., 54, 927 (1971)
165. A.M.Mearns and R.A.Back,
Can.J.Chem., 41, 1197 (1963)
166. R.J.Morrissey and C.C.Schubert,
Combustion Flame, 7, 263 (1963)
167. P.N.Clough and B.A.Thrush,
Chem. and Ind. 1971 (1966)
168. G.A. Cook, A.D.Kiffer, C.V.Klump, A.H.Malik and L.A.Spence
Adv.in Chem.Ser., Am.Chem.Soc., 21, 44 (1957)
169. K.N.Becker, W.Groth and W.Schurath
Chem.Phys. Lett.14 489 (1972)
170. M.A.A.Clyne and H.W. Cruse,
J.C.S.Faraday Trans., 2, 68 1377 (1970)
171. P.P.Bemand, M.A.A.Clyne and R.I.Watson,
J.C.S.Faraday Trans.1. 69, 1356 (1973).
172. A.A.Westenberg and N.De Haas,
J.Chem.Phys. 62, 4477 (1975)
173. A.C.Luntz
J.Chem.Phys. 73 , 1143 , (1980)
174. C.T.Rettner , J.F.Cordova and J.L.Kinsey ,
J.Chem.Phys. 79 , 5280 (1980)
175. R.K.Sparks , L.R.Carlson , K.Shobatake , M.L.Kowalczyk and Y.T.Lee
J.Chem.Phys . 72 , 1401 (1980) .
176. S.D.Worley, R.N. Coltharp and A.E.Potter,Jr.,
J.Phys., Chem., 76, 1511 (1972)

ADDENDUM

Luntz¹⁷³ has recently investigated the reaction of $O(2^1D)$ with alkanes using laser photolysis of O_3 with laser induced fluorescence of OH. He concluded that there were two distinct modes of reaction leading to the formation of OH, which he termed 'insertion' and 'abstraction'. The first predominated for small alkanes, the latter for the larger alkanes.

Insertion as its name implies, proceeds by the insertion of $O(2^1D)$ into the RH bond to give ROH^* . This may undergo prompt fission to yield $R + OH$ before equipartition of the excess energy occurs. If equipartition of the excess energy occurs, and this is favoured by increasing size of the alkane, then the breakdown of the alkane occurs as predicted by RRKM theory with C-C bond fission being favoured.

Luntz also concluded that the distinct 'abstraction' reaction initially proceeded along the same singlet potential surface as the reaction leading to ROH^* but crossed to the triplet surface corresponding to the $O(2^3P) + RH$ reaction.

It can be seen that this mechanism is essentially similar to that proposed in this work (chapter 5) for the reaction of $O(2^1D)$ with halomethanes. The reaction initially proceeds along a singlet surface leading to ROH or $RCIO$ and may continue along this singlet surface to products. However in both cases crossing to a triplet surface is readily possible. For $O(2^1D) + RH$ this reaction accounts for about 20% of the reaction cross section, a similar figure is observed in the reaction of $O(2^1D)$ with halomethanes.

PUBLISHED WORK

References

- 1 P. M. Rentzepis, *Chem. Phys. Lett.*, **2** (1976) 117.
- 2 M. Mourou and M. M. Malley, *Opt. Commun.*, **11** (3) (1974) 283; **10** (4) (1974) 323.
- 3 D. Madge and M. Windsor, *Chem. Phys. Lett.*, **24** (1974) 144.
- 4 R. Hochstrasser, H. Lutz and G. W. Scott, *Chem. Phys. Lett.*, **24** (1974) 162; **28** (1974) 153.
- 5 P. P. Sorokin, W. H. Culver, E. C. Hammond and J. R. Lankard, *IBM J. Res. Dev.*, **10** (1966) 401.
- 6 P. P. Sorokin, J. J. Luzzi, J. R. Lankard and G. D. Pettit, *IBM J. Res. Dev.*, **8** (1964) 182.
- 7 B. B. Snavely, *Proc. IEEE*, **57** (1969) 1374.
- 8 F. P. Schaeffer and W. Schmidt, *Z. Naturforsch.*, **22** (1977) 1563.
- 9 E. G. Arthurs, D. J. Bradley and A. G. Roddie, *Opt. Commun.*, **8** (1973) 118; *Chem. Phys. Lett.*, **22** (1973) 230.
- 10 C. Rullière, J. P. Morand and J. Jousset-Dubien, *Opt. Commun.*, **15** (1975) 263.
- 11 J. P. Fouassier, D. J. Lougnot and J. Faure, *J. Chim. Phys. Phys. Chim. Biol.*, in the press.
- 12 I. Wieder, *Appl. Phys. Lett.*, **21** (1972) 318.
- 13 J. P. Fouassier, D. J. Lougnot and J. Faure, *Chem. Phys. Lett.*, **35** (2) (1975) 189.
- 14 J. P. Fouassier, D. J. Lougnot and J. Faure, *C. R. Acad. Sci.*, **281** (1975) 161.
- 15 J. P. Fouassier, D. J. Lougnot and J. Faure, *Opt. Commun.*, **18** (1976) 263.
- 16 M. Maeda and Y. Miyazoe, *Jpn. J. Appl. Phys.*, **11** (1972) 692.
- 17 H. Furumoto and H. Ceccon, *J. Appl. Phys.*, **40** (1969) 4204.
- 18 M. Maeda and Y. Miyazoe, *Jpn. J. Appl. Phys.*, **13** (1974) 369.
- 19 E. Wilhelm and R. Battino, *Chem. Rev.*, **73** (1973) 1.
- 20 W. R. Ware, *J. Phys. Chem.*, **66** (1962) 455.
- 21 H. Lami, J. Gresset and G. Laustriat, *Int. Luminescenz Symp.*, Verlag Karl Thieme KG, München, 1965.
- 22 D. N. Dempster, T. Morrow and M. F. Quinn, *J. Photochem.*, **2** (1973) 329.
- 23 T. G. Pavlopoulos and P. R. Hammond, *J. Am. Chem. Soc.*, **96** (1974) 6568.

REACTION OF O(2¹D₂) WITH HALOMETHANES

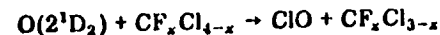
H. M. GILLESPIE, J. GARRAWAY and R. J. DONOVAN

Department of Chemistry, University of Edinburgh, West Mains Road, Edinburgh, EH19 3JJ (Gt. Britain)

(Received December 2, 1976)

Summary

The reactions of O(2¹D₂) with the halomethanes CFCl₃, CF₂Cl₂, CF₂Cl, CF₂HCl, CFHCl₂ and CF₃Br have been studied using flash photolysis with kinetic spectroscopy (O(2¹D₂) atoms were generated by photolysis of O₃ or N₂O in the ultraviolet). Formation of ClO has been observed and lower limits for the branching ratio into the channel



relative to the total cross section for removal of O(2¹D₂) were determined as 0.39, 0.47, 0.39, 0.27 and 0.36 for the molecules CF₃Cl, CF₂Cl₂, CFCl₃, CF₂HCl and CFHCl₂, respectively. The secondary yields of ClO following the reaction of CF_xCl_{3-x} radicals with O₂ are also reported.

The reaction of O(2¹D₂) with CF₃Br is shown to yield BrO as a primary product. The photolysis of CCl₃Br in the presence of O₂ is also shown to yield BrO, but in this case via secondary reactions.

1. Introduction

There is considerable current interest [1, 2] in the ClO_x cycle which is one of the catalytic processes leading to removal of odd oxygen (O₃ and O) in the stratosphere:

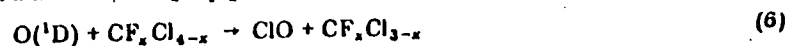


($k_1 = 1.25 \times 10^{-11} \text{ cm}^3 \text{ molecule}^{-1} \text{ s}^{-1}$ [3, 4], $k_2 = 5.3 \times 10^{-11} \text{ cm}^3 \text{ molecule}^{-1} \text{ s}^{-1}$ [5] at 300 K). Injection of ClO_x into the stratosphere by reactions of both naturally occurring and synthetic halogenated alkanes (the latter including in particular the commercially important CF₂Cl₂ and CFCl₃) has been considered [1, 2]. Photolysis by solar UV radiation and reaction with electronically excited oxygen atoms O(2¹D₂) may each release ClO_x:



There may be further release of ClO_x in subsequent reactions of the fragment R and in photolysis or reactions of products of other channels (5). Several studies of the photo-oxidation of haloalkanes employing end product analysis [6 - 8] indicate that a carbonyl halide is the main and possibly the only oxidation product; however, the complete mechanism has not been established unambiguously and there is a clear need for more direct studies of the reactions of halomethyl radicals with O₂ and of the contribution of the various possible channels in the reaction of O(¹D) atoms with halomethanes.

The complexity of the reaction of O(¹D) atoms with CH₄ is now reasonably well understood [9] and studies by Lin [10] of HCl and HF chemical laser emission following the reaction of O(¹D) atoms with various hydrogen-containing chlorofluoromethanes have provided some information on the occurrence of insertion-elimination reactions with these molecules. Given this background, a number of possible channels in the reaction of O(¹D) with a molecule CF_xCl_{4-x} merit consideration:

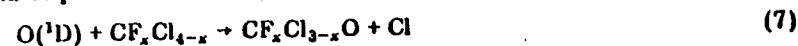


There is no reason to discount reaction (7) *a priori*, although its analogue has not been observed for O(¹D) + CH₄. Equation (7) is more exothermic than eqn. (6) (with CF₃Cl, ΔH₂₉₈^o (eqn. (6)) = -98 kJ mol⁻¹ and ΔH₂₉₈^o (eqn. (7)) = -239 kJ mol⁻¹)*. Since it appears that certain reactions of O(¹D) atoms occur by insertion followed by fragmentation in a statistical manner governed by the volume of phase space available for different channels [13], reaction (7) appears quite plausible. It should be noted that the molecule CF₃OCl is well characterised [14] and might be stabilised at very high pressures if the reaction proceeds via CF₃OCl. Furthermore, hypochlorites are known to be useful reagents for producing alkoxy radicals and the photolysis and thermal reactions of CF₃OCl are thought to proceed through the formation of CF₃O, thus supporting our suggestion that channel (7) deserves serious consideration. Direct abstraction, on the other hand, would favour reaction (6). Evidence for reactions of the type shown in

*Thermochemical data have been taken from ref. 11, with the exceptions of CF₃O [6] and ClO [12].

eqns. (9) and (10) has been obtained [15] by employing flash photolysis in a fast flow system with nozzle beam mass spectrometric sampling. Heicklen and coworkers [7] have concluded from steady photolysis experiments that deactivation of O(¹D) to O(³P) by CCl₄, CFCl₃ and CF₂Cl₂ is negligible. Pitts *et al.* [16] have come to a similar conclusion but no direct measure of any contribution from this channel has been reported.

In a preliminary report [17] we described measurements of a lower limit to the branching ratio for ClO formation in the reaction of O(¹D) with CF₃Cl, CF₂Cl₂ and CFCl₃, employing O₃ as the source of O(¹D) atoms. However, these experiments are open to the possible objection that ClO could be produced indirectly via



The possible involvement of reaction (7) has been mentioned; under the conditions of our experiments [17] the half-life of a Cl atom with respect to reaction (1) is about 5 μs, so that a large contribution from reactions (7) and (1) would not be readily distinguishable from the occurrence of reaction (6) alone. For this reason we have carried out further studies employing N₂O as the source of O(¹D). We also describe some experiments on the oxidation of halomethyl radicals.

2. Experimental

The apparatus for flash photolysis with time-resolved absorption spectroscopy in the ultraviolet (λ > 200 nm) has been described [17]. During work where measurements were made on the NO γ(0,0) and δ(0,4) bands it was found that the spectral intensity in the region below 230 nm fell quite rapidly owing to the deposition of powdered silica on the window of the spectroscopic flashlamp when this was discharged at 15 kV as in previous experiments. Reducing the voltage to 13 kV did not significantly alter the output of the lamp but greatly prolonged the useful life of the window.

The concentration of ozone in mixtures was measured by recording the UV absorption around 250 nm on a spectrophotometer (Perkin-Elmer model 402); absorption coefficients were taken from the work of Griggs [18]. Pressures of other gases were measured with a glass spiral gauge backed by a mercury manometer. Gases were handled in a conventional greaseless glass vacuum system.

Photographic plates were developed under standard conditions and optical density tracings obtained using a Joyce-Loebl double beam recording microdensitometer. The concentration of ClO was determined from the optical density in the (8,0) or (11,0) bands of the A²Π ← X²Π system. The contrast at the wavelength of these bands was determined for the

majority of plates and remained constant throughout this work at about 1.2. Extinction coefficients (base 10) of $\epsilon(11,0) = 3 \times 10^{-18} \text{ cm}^2 \text{ molecule}^{-1}$ and $\epsilon(8,0) = 2.5 \times 10^{-18} \text{ cm}^2 \text{ molecule}^{-1}$ were employed (see below). The Beer-Lambert law was obeyed in the concentration range of these experiments ($[\text{ClO}] < 5 \times 10^{14} \text{ molecule cm}^{-3}$). The concentration of $\text{NO}(v'' = 0)$ was calibrated directly using standard mixtures of NO in the presence of the same pressure of N_2O or $\text{N}_2\text{O} + \text{CF}_3\text{Cl}$, as used in kinetic experiments. Because of the low plate density at the wavelengths of the various $\text{NO}(v'' \leq 4)$ transitions employed, the contrast was not constant and was determined for the wavelength of each band; plots of D versus $\log E$ were approximately linear for small optical density changes in this region, the contrast falling to about 0.6 at 227 nm. Concentrations of vibrationally excited NO were normalised to the $\text{NO}(v'' = 0)$ calibration using Franck-Condon factors from the compilations of Jain and Sahni [19] (γ bands) and Ory [20] (δ bands) together with a value for the relative oscillator strength $f_{00}^v/f_{00}^0 = 0.08$ calculated as the mean of several reported values for these two quantities [21 - 25].

2.1. Materials

O_3 was prepared by passing dried O_2 through an ozonizer and trapping the product on silica gel at 195 K. After pumping to remove O_2 , the O_3 was allowed to expand into a large blackened bulb. N_2O of B.O.C. medical grade ($\geq 99\%$) was thoroughly degassed and used directly. NO (Matheson) was fractionally distilled several times from 90 K to a trap held at 77 K, retaining the middle fraction. CF_2Cl_2 and CFCl_3 (given by I.C.I.) were degassed and used without further purification. CF_3Cl , CF_3Br (Matheson) and CF_2HCl , CFHCl_2 (I.C.I. Arcton) were taken from cylinders, degassed by repeated freeze-pump-thaw cycles and used directly.

3. Results and discussion

3.1. Branching ratio for ClO formation using O_3

The determination of a lower limit to the branching ratio for ClO formation, $k_4/(k_4 + k_5)$, for CF_3Cl , CF_2Cl_2 and CFCl_3 has been described [17]. In these experiments, O_3 was photolysed in the presence of a large excess (10.7 kN m^{-2}) of chlorofluoromethane. Under such conditions the half-life for removal of $\text{O}(^1\text{D})$ is about 1 ns, so that the early appearance of ClO followed the integrated profile of the photolysis flash. Branching ratios for ClO formation were estimated by comparison of the extent of O_3 removal at $10 \mu\text{s}$ with the amount of ClO produced. An improved measurement of the relative extinction coefficients of $\text{ClO}(A^2\Pi \leftarrow X^2\Pi)$ bands and continuum has now been carried out, using the photolysis of N_2O in the presence of CF_3Cl to produce ClO in the absence of other absorbers in the spectral region of interest (250 - 290 nm). Extinction coefficients relative to the ClO continuum at 257.7 nm, which was taken as unity, in the (8,0)

TABLE 1

Lower limits to the branching ratio for ClO formation in removal of $\text{O}(^2\text{D})$ atoms by chlorofluoromethanes using O_3

Molecule	$k_4/(k_4 + k_5)$
CF_3Cl	> 0.39
CF_2Cl_2	> 0.47
CFCl_3	> 0.39
CF_2HCl	> 0.27
CFHCl_2	> 0.36

and (11,0) bands were found to be 1.25 and 1.46, respectively. Clyne and Coxon [26] determined absolute extinction coefficients at 298 K of $\epsilon(257.7 \text{ nm}) = (2.11 \pm 0.07) \times 10^{-18} \text{ cm}^2 \text{ molecule}^{-1}$ and $\epsilon(11,0) = (3.15 \pm 0.10) \times 10^{-18} \text{ cm}^2 \text{ molecule}^{-1}$; Basco and Dogra [27] have obtained $\epsilon(257.7 \text{ nm}) = 1.91 \times 10^{-18} \text{ cm}^2 \text{ molecule}^{-1}$ and $\epsilon(11,0) = 2.82 \times 10^{-18} \text{ cm}^2 \text{ molecule}^{-1}$. Combining these results, we have used $\epsilon(11,0) = 3 \times 10^{-18} \text{ cm}^2 \text{ molecule}^{-1}$ and $\epsilon(8,0) = 2.5 \times 10^{-18} \text{ cm}^2 \text{ molecule}^{-1}$. The (11,0) band was employed for concentration measurements in experiments using N_2O as the source of excited atoms, while the (8,0) band was used in experiments with O_3 , the intensity of absorption by O_3 being less at the wavelength of the latter band, 285.2 nm.

Results for CF_3Cl , CF_2Cl_2 and CFCl_3 , modified in the light of the above determination of the ClO extinction coefficient and of a small systematic error in O_3 concentration measurement, are listed in Table 1. Also included are lower limits for the ClO formation branching ratio for CF_2HCl and CFHCl_2 . It is emphasised that these results represent lower limits only, since it appears that removal of ClO may be important even at a very early stage of the reaction. In contrast, secondary formation of ClO is fairly slow in the cases where it is possible. Since these experiments involved a rather imprecise measurement of reduction in O_3 concentration using plate photometry, it was not possible to circumvent this problem by calculating ClO formation and O_3 removal for delays less than $10 \mu\text{s}$.

3.2. Secondary reactions in the presence of O_3 and O_2

The kinetic behaviour of ClO subsequent to the initial rapid formation is of interest; results for CF_3Cl , CF_2Cl_2 and CFCl_3 appear in Fig. 1. For CF_3Cl , the disappearance of ClO may be divided into two distinct regions. Immediately after the photolysis flash, ClO removal is rapid and cannot be explained solely by the bimolecular reaction of ClO

*The vibrational numbering in the A state has recently been revised [28] and differs from that given in refs. 26 and 27; the revised values are lower by unity.

Calculation in this manner is made difficult by the fact that the reaction of $O(^1D)$ with N_2O releases a substantial part of the available excess energy in channel (15b) as vibrational excitation of $NO(v'' < 6)$ [37]. In the present work the (0,0), (0,1) and (0,2) bands in the γ system could be monitored, together with the (0,4) δ band, but measurement by plate photometry of the very small concentrations of $NO(v'' > 0)$ near $t = 0$ was imprecise. The ratio of vibrationally excited to ground vibrational state NO in the early stages of reaction of the N_2O/CF_3Cl system was estimated to be 0.3 and the branching ratio for ClO formation to be greater than 0.27. This does not improve upon the limit determined using O_3 (Section 3.1) which is therefore to be preferred. While these results confirm that formation of ClO is by the direct reaction of $O(^1D)$ with CF_3Cl , this does not appear to be a promising method for precise determination of the branching ratio into reaction (4) because of the relatively imprecise nature of plate photometry measurements and the difficulty of making due allowance for the contribution of vibrationally excited NO formation.

The production of ClO in a primary step suggests that the reaction proceeds via direct dynamics; one would expect the product CF_3O to be favoured if the insertion complex CF_3OCl were formed (see Section 1). There is, however, an alternative structure for the collision complex which has the geometry CF_3ClO (analogous to iodoso compounds). This type of complex, while probably less stable than the hypochlorite (CF_3OCl) structure, would be more likely to yield ClO and CF_3 . Observations on the energy distribution in ClO are needed before more detailed conclusions can be drawn about the dynamics of this reaction.

3.4. Reaction of $O(^1D)$ with CF_3Br

Formation of BrO has been observed from the reaction



using both N_2O and O_3 as the source of $O(^1D)$ atoms. Concentrations were measured at the (4,0) band head at 316.9 nm in the $A^2\Pi + X^2\Pi$ system. When O_3 was employed, the photolysis radiation was filtered ($\lambda > 240$ nm) so that no appreciable photolysis of the CF_3Br occurred. The reaction



is slower than that of the chlorine analogue ($k_{19} = (1.2 \pm 0.2) \times 10^{-12} \text{ cm}^3 \text{ molecule}^{-1} \text{ s}^{-1}$ [38]) so that in this case all the initial rapid BrO formation must be due to reaction (18). This conclusion is confirmed by the observation of BrO following the photolysis of N_2O in the presence of CF_3Br . Rapid disappearance of BrO was observed during the tail of the flash (Fig. 2) so that no useful estimate of the branching ratio for reaction (18) could be made. This disappearance might be attributable to the occurrence of an appreciable degree of quenching of $O(^1D)$ to $O(^3P)$, followed by the rapid reaction ($k_{20} = (5 \pm 2) \times 10^{-11} \text{ cm}^3 \text{ molecule}^{-1} \text{ s}^{-1}$ [38])

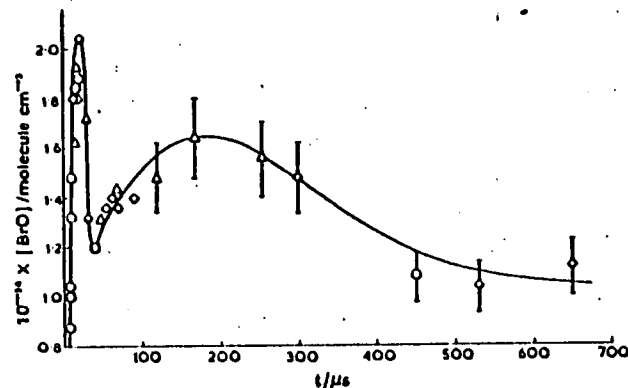


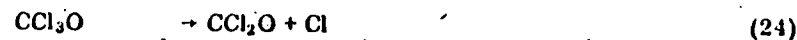
Fig. 2. Formation and decay of BrO after the photolysis of O_3 in the presence of CF_3Br . The various symbols used indicate the scatter in data obtained from three independent experimental runs. The same experimental conditions were used for all three runs: $P_{O_3} = 40.0 \text{ N m}^{-2}$; $P_{CF_3Br} = 0.56 \text{ kN m}^{-2}$; $P_{He} = 2.27 \text{ kN m}^{-2}$.

until the $O(^3P)$ atoms are substantially depleted. The rise in BrO concentration in the range 40 - 100 μs is consistent with the known rate of reaction (19). At longer times, when most of the O_3 has been removed, the BrO decay was found to be second order in $[BrO]$; using the extinction coefficient $\epsilon(4,0) = (8.0 \pm 0.3) \times 10^{-18} \text{ cm}^2 \text{ molecule}^{-1}$ obtained by Clyne and Cruse [39], a second order rate constant for BrO disappearance, $k_{21} = (4 \pm 2) \times 10^{-12} \text{ cm}^3 \text{ molecule}^{-1} \text{ s}^{-1}$, was obtained. Clyne and Watson [38] have determined $k_{21} = (6.4 \pm 1.3) \times 10^{-12} \text{ cm}^3 \text{ molecule}^{-1} \text{ s}^{-1}$ for the reaction

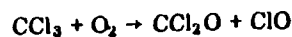


3.5. Oxidation of halomethyl radicals

Reactions of radicals CF_xCl_{3-x} with other species which are present in systems where photo-oxidation is occurring are not well understood. Milstein and Rowland [8] have photolysed CF_2Cl_2 in the presence of O_2 and deduced a quantum yield of 2 for the formation of ($Cl + ClO$). Heicklen and coworkers [7] have investigated the photolysis of CCl_4 and chlorofluoromethanes in the presence of O_2 and O_3 using static photolysis with end product analysis. The points of interest for the present discussion are that the following mechanism of oxidation of the radical CCl_3 by O_2 was proposed:



Also it was concluded that the contribution of the following reaction, earlier favoured by Heicklen [6], is negligible:



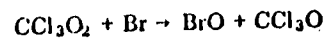
Reactions analogous to eqns. (22) - (24) were proposed for CF_2Cl and CFCl_2 .

We have observed ClO formation following photolysis of CFCl_3 (5.33 kN m^{-2}) in the presence of O_2 (4.67 kN m^{-2}). However, this might arise solely from the Cl/O_2 reaction and provides no definitive information on the reaction of CFCl_2 with O_2 . Studies of the reaction $\text{CCl}_3 + \text{O}_2$, using photolysis of CCl_3Br to produce the CCl_3 radical, are more revealing. Our observations are consistent with dissociation to give $\text{CCl}_3 + \text{Br}$ in the first continuum ($\lambda_{\text{max}} \approx 236 \text{ nm}$) with dissociation giving Cl atoms at shorter wavelength. Photolysis of CCl_3Br (133 N m^{-2}) in the presence of O_2 (3.87 kN m^{-2}) using unfiltered radiation ($\lambda > 200 \text{ nm}$) gave both BrO and ClO. BrO, which has a larger rate constant for removal, passed through a maximum concentration at about $50 \mu\text{s}$; ClO continued to increase until about $300 \mu\text{s}$. The reaction of Br with O_2 is very slow [39] and cannot be responsible for the observed rapid formation of BrO. Nevertheless, Br and Cl atoms are responsible for the production of BrO and ClO, as the following observations indicate.

(1) With photolysis down to 200 nm , the addition of 4.2 kN m^{-2} of C_2H_6 to intercept Cl atoms reduced the ClO yield to an undetectable level, while the BrO yield was only slightly reduced.

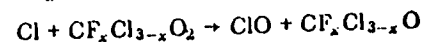
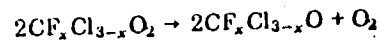
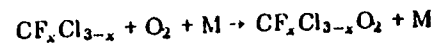
(2) With filtered photolysis radiation ($\lambda > 223 \text{ nm}$), so that the formation of Cl atoms in photolysis of CCl_3Br was reduced, the ratio BrO/ClO increased fivefold.

These observations demonstrate that reaction (25) is indeed negligible, but that reactions (22) - (24), while they may occur, do not constitute a complete mechanism since OX radicals are also present as intermediates. Reaction (22) is expected to be rapid (by analogy with $\text{ClI}_3 + \text{O}_2$) and might be followed by abstraction reactions such as



The inclusion of such reactions is consistent with the end products which have been observed.

The secondary formation of ClO from reaction of CF_2Cl and CFCl_2 with O_2 , referred to in Section 3.2, can now be accounted for by the sequence of reactions



Further study of these systems is clearly warranted.

Acknowledgments

We thank Professor C. Kemball for his support and encouragement and the S.R.C. for the award of a Research Fellowship to H.G. We also thank Dr. D. Leaver for helpful discussions concerning the stability of hypochlorite and iodoso structures.

References

- 1 F. S. Rowland and M. J. Molina, *Rev. Geophys. Space Phys.*, **13** (1975) 1.
- 2 R. S. Stolarski and R. J. Cicerone, *Can. J. Chem.*, **52** (1974) 1610.
- 3 M. J. Kurylo and W. Braun, *Chem. Phys. Lett.*, **37** (1976) 232.
- 4 M. S. Zahniser, F. Kaufman and J. G. Anderson, *Chem. Phys. Lett.*, **37** (1976) 226.
- 5 P. Bemand, M. A. A. Clyne and R. T. Watson, *J. Chem. Soc. Faraday Trans. 1*, **69** (1973) 1356.
- 6 J. Heicklen, *Adv. Photochem.*, **7** (1970) 57.
- 7 R. K. M. Jayanty, R. Simonaitis and J. Heicklen, *J. Photochem.*, **4** (1975) 203; 381.
- 8 R. Milstein and F. S. Rowland, *J. Phys. Chem.*, **79** (1975) 669.
- 9 C.-L. Lin and W. B. DeMore, *J. Phys. Chem.*, **77** (1973) 863.
- 10 M. C. Lin, *J. Phys. Chem.*, **76** (1972) 1425.
- 11 JANAF Thermochemical Tables, 2nd edn., Natl. Bur. Stand., Washington D.C., 1971.
- 12 M. A. A. Clyne, D. J. McKenney and R. T. Watson, *J. Chem. Soc. Faraday Trans. 1*, **71** (1975) 322.
- 13 J. C. Tully, *J. Chem. Phys.*, **62** (1975) 1893.
- 14 C. J. Schack and W. Maya, *J. Am. Chem. Soc.*, **91** (1969) 2902.
- 15 R. J. Donovan, K. Kaufman and J. Wolfrum, *Nature (London)*, **262** (1976) 204.
- 16 J. N. Pitts, H. L. Sandoval and R. Atkinson, *Chem. Phys. Lett.*, **29** (1974) 31.
- 17 H. M. Gillespie and R. J. Donovan, *Chem. Phys. Lett.*, **37** (1976) 468.
- 18 M. Griggs, *J. Chem. Phys.*, **49** (1968) 857.
- 19 D. C. Jain and R. C. Sahni, *Trans. Faraday Soc.*, **64** (1968) 3169.
- 20 H. A. Ory, *J. Chem. Phys.*, **40** (1964) 562.
- 21 A. Pery-Thorne and F. P. Banfield, *J. Phys. B*, **3** (1970) 1011.
- 22 A. J. D. Farmer, V. Hasson and R. W. Nicholls, *J. Quant. Spectrosc. Radiat. Transfer*, **12** (1972) 627.
- 23 V. Hasson, A. J. D. Farmer, R. W. Nicholls and J. Anketell, *J. Phys. B*, **5** (1972) 627.
- 24 A. B. Callear and M. Pilling, *Trans. Faraday Soc.*, **66** (1970) 1886.
- 25 M. Mandelman, T. Carrington and R. A. Young, *J. Chem. Phys.*, **58** (1973) 84.
- 26 M. A. A. Clyne and J. A. Coxon, *Proc. R. Soc. London, Ser. A*, **303** (1968) 207.
- 27 N. Basco and S. K. Dogra, *Proc. R. Soc. London, Ser. A*, **323** (1971) 29.
- 28 J. A. Coxon, W. E. Jones and E. G. Skolnik, *Can. J. Phys.*, **54** (1976) 1043.
- 29 H. S. Johnston, E. D. Morris and J. Van Der Bogaerde, *J. Am. Chem. Soc.*, **91** (1969) 7712.
- 30 S. Jaffe and W. B. DeMore, Abstract of paper presented at 12th Informal Conf. on Photochemistry, Washington, D.C., 1976.
- 31 F. Kaufman, N. J. Gerri and D. A. Pascale, *J. Chem. Phys.*, **24** (1956) 32.
- 32 J. A. Ghormley, R. L. Ellsworth and C. J. Hochanadel, *J. Phys. Chem.*, **77** (1973) 1341.
- 33 R. Simonaitis, R. I. Greenberg and J. Heicklen, *Int. J. Chem. Kinet.*, **4** (1972) 497.
- 34 P. M. Scott, K. F. Preston, R. J. Anderson and L. M. Quick, *Can. J. Chem.*, **49** (1971) 1808.
- 35 H. A. Wiebe and G. Paraskevopoulos, *Can. J. Chem.*, **52** (1974) 2165.
- 36 I. S. Fletcher and D. Husain, *J. Phys. Chem.*, **60** (1976) 1837.
- 37 G. A. Chamberlain and J. P. Simons, *J. Chem. Soc. Faraday Trans. 2*, **71** (1975) 402.
- 38 M. A. A. Clyne and R. T. Watson, *J. Chem. Soc. Faraday Trans. 1*, **71** (1975) 336.
- 39 G. Burns and R. G. W. Norrish, *Proc. R. Soc. London, Ser. A*, **271** (1963) 289.

Reactions of $O(2^1D_2)$ and $O(2^3P_j)$ with Halogenomethanes

BY MICHAEL C. ADDISON, ROBERT J. DONOVAN
AND JOHN GARRAWAY

Department of Chemistry, University of Edinburgh,
West Mains Road, Edinburgh EH9 3JJ

Received 20th December, 1978

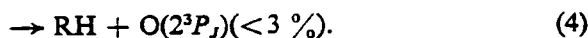
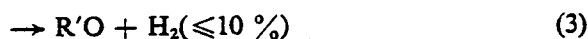
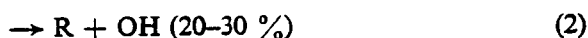
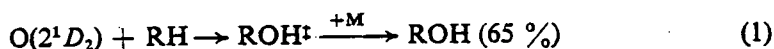
Product branching ratios for the reaction of $O(2^1D_2)$ with the halogenomethanes CF_3Cl , CF_3Br , CF_3I and CF_2HCl are presented. The dominant channel is shown to be abstraction yielding a halogen oxide. This contrasts with the behaviour observed with hydrocarbons, where insertion into C-H bonds dominates. Quenching of $O(2^1D_2)$ to the ground state is also observed with the halogenomethanes and accounts for $\approx 30\%$ of the total removal cross-section.

Reaction of $O(2^1D_2)$ with CF_2HCl leads to the formation of ClO (55%) and to the elimination of HCl (40%). The latter process is accompanied by the formation of CF_2 and $O(2^3P_j)$.

The reactions of $O(2^1D_2)$ are compared with those for $O(2^3P_j)$, where these are known, and the absolute rate for reaction of $O(2^3P_j)$ with CF_3I is determined as $(1.1 \pm 0.3) \times 10^{-11} \text{ cm}^3 \text{ molecule}^{-1} \text{ s}^{-1}$ at 300 K.

The results are discussed in terms of the main topological features on the potential surfaces involved.

Reactions of $O(2^1D_2)$ with hydrocarbons have been studied extensively.¹⁻³ The reaction cross-sections are large and the main reaction channel involves insertion into C-H bonds. Insertion has been shown to proceed indiscriminately and the total reaction cross-section found to be proportional to the number of C-H bonds in the molecule.³ A number of other reaction channels have also been recognised and may be summarised as follows,



It is clear that quenching is negligible and that a *direct* abstraction reaction, leading to OH formation, plays an appreciable role.

By comparison the reactions of $O(2^1D_2)$ with halogen-containing molecules have been little studied, although it is known that the reaction cross-sections are again large.^{4,5} The formation of halogen oxide products has been observed and lower limits for branching into this channel presented.^{6,7}

In the present work we have made a detailed study of the branching ratios into different reaction channels for a number of halogen-containing molecules. The dominant channel is shown to be *abstraction* of a halogen atom. Quenching to the ground state is also an important process.

We also present data for the reaction of $O(2^3P_j)$ with CF_3I and compare these, together with data for the other halogenomethanes, with those for the analogous reactions involving $O(2^1D_2)$.

EXPERIMENTAL

Three separate experimental arrangements were employed for this work, all of them based on the flash photolysis technique.

(i) FLASH SPECTROSCOPY

A conventional arrangement, suitable for photographing transient spectra in the visible and ultraviolet regions, was used to obtain kinetic data on the halogen oxides and CF_2 . Spectra were dispersed on a Hilger-Watts medium quartz spectrograph and recorded on Kodak Panchro-Royal film. A more detailed description of this technique and the data processing has been given in ref. (6) and (7).

(ii) TIME-RESOLVED PHOTOMETRY IN THE VACUUM ULTRAVIOLET

This apparatus employed a conventional flash photolysis unit coupled to a vacuum ultraviolet monochromator and fast photometric recording system. It was used to monitor the formation and decay of $O(2^3P_1)$ (via the resonance lines at $\lambda \approx 130$ nm), following quenching of $O(2D_2)$ by the halogenomethanes, and also to obtain absolute rate data for reaction of $O(2^3P_1)$ with CF_3I . The experimental arrangement was similar to one described previously⁸ for work on $S(3^3P_1)$, however, for the present work an EMR542 solar blind photomultiplier was used. The use of this photomultiplier eliminated the effect of scattered light from the flash lamp and allowed kinetic measurements to commence during the flash. A flow system was used for the atomic lamp and the best results were obtained when very low (<0.1%) oxygen/helium ratios were passed through the microwave discharge. An extensive series of experiments were carried out to establish that this new arrangement gave a linear photometric response with stable molecules such as O_3 . Curves of growth for $O(2^3P_1)$ were then determined by photolysing O_3 under optically thin conditions [in the presence of excess N_2 to quench $O(2^1D_2)$ to $O(2^3P_1)$] over a range of pressures (fig. 1). As a final check the rate of the reaction between $O(2^3P_1)$ and NO_2 was determined* as $k = (1.1 \pm 0.3) \times 10^{-11}$ cm³ molecule⁻¹ s⁻¹, in excellent agreement with the accepted result obtained by resonance fluorescence⁹ [$k = (9.12 \pm 0.44) \times 10^{-12}$ cm³ molecule⁻¹ s⁻¹ at 295 K].

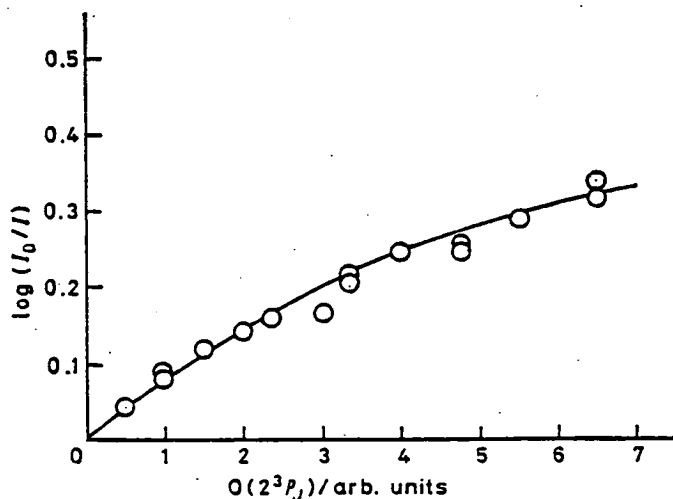


FIG. 1.—Curve of growth for $O(2^3P_1)$ using the three resonance lines at 130.2, 130.5, 130.6 nm. The $O(2^3P_1)$ concentration was taken to be proportional to that of O_3 , which was varied over the range 0.4–6.1 N m⁻².

* In these experiments $O(2^3P_1)$ was formed by photolysis of NO_2 ($\approx 1\%$) in the visible and near u.v. regions.

In all of these experiments the output from the photomultiplier was fed to a fast analogue-to-digital converter (Datalab DL905) and data were processed in the standard way.

(iii) TIME-RESOLVED PHOTOMETRY IN THE NEAR-ULTRAVIOLET

The yield of OH from reaction of $O(2^1D_2)$ with CF_2HCl was determined using an arrangement similar to that described by Morley and Smith.¹⁰ The intense OH emission produced by a microwave discharge through a flowing mixture of water vapour in argon carrier gas was focused through the reaction vessel and onto the slit of a McKee-Peterson (MP1018B) monochromator which selected¹⁰ the $Q_{1,3}$ line at 308.15 nm. A chlorine gas filter surrounded the reaction vessel and reduced scattered light from the flash to a negligible level. The output from the photomultiplier was fed to a transient recorder (Datalab DL905) and data were processed as in section (ii) above.

For all experiments $O(2^1D_2)$ was produced by the ultraviolet photolysis of O_3 ($\lambda = 200$ – 300 nm) and, where required, $O(2^3P_1)$ was formed by adding an excess of N_2 , to quench $O(2^1D_2)$ to $O(2^3P_1)$. The experimental conditions used with the three different techniques varied significantly and will be described in the appropriate section dealing with results.

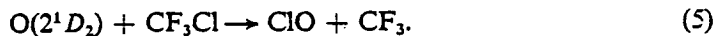
RESULTS

ABSOLUTE CONCENTRATIONS OF $O(2^1D_2)$ PRODUCED BY THE FLASH

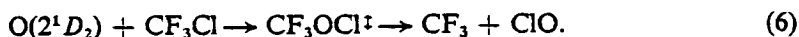
Photolysis of O_3 in the ultraviolet (200–300 nm) is known to produce almost exclusively $O(2^1D_2)$ and thus the absolute yield of this atomic state can be determined by observing the amount of O_3 removed by the flash. In pure O_3 (or $O_3 + SF_6$ and $O_3 + He$ mixtures) $O(2^1D_2)$ reacts rapidly with a second O_3 molecule, and under our conditions the amount of O_3 removed immediately after the flash will in fact be twice the amount photolysed in the primary photochemical step. However, by adding excess CO_2 to the ozone, the effect of the secondary reaction can be eliminated, as $O(2^1D_2)$ is quenched to the ground state. We, therefore, carried out experiments to determine the amount of O_3 removed after the flash ($30 \mu s$) both in the presence and absence of CO_2 . The depletion in the presence of CO_2 was found to be $12 \pm 1\%$ ($P_{O_3} = 26.6 \text{ N m}^{-2}$) and in the absence of CO_2 $24 \pm 2\%$, this gives a yield of $O(2^1D_2)$ of 8×10^{14} atoms cm^{-3} per flash. These results confirm that the yield of $O(2^3P_1)$ in the ultraviolet photolysis of O_3 is negligible ($< 10\%$) and that $O(2^1D_2)$ is removed entirely by reaction with O_3 , physical quenching being unimportant. The decay of O_3 at times greater than $30 \mu s$ was observed to be very slow, as expected from the known slow rates for reactions involving $O(2^3P_1)$ and $O_2(a^1\Delta_g)$ with O_3 .

REACTION OF $O(2^1D_2)$ WITH CF_3Cl

When O_3 is photolysed in the presence of excess CF_3Cl ($P_{CF_3Cl} = 2.7 \text{ kN m}^{-2}$) a strong spectrum of ClO is observed *via* the ($A^2\Pi \leftarrow X^2\Pi$) system, and its rate of formation closely follows the integrated form of the flash. No ClO is observed when CO_2 or N_2 is added to quench $O(2^1D_2)$ and it is clear from these, as well as earlier experiments,^{6,7} that ClO results from a fast reaction between $O(2^1D_2)$ and CF_3Cl . There are however three possible mechanisms for ClO formation. The first and most obvious is the direct formation of ClO in a primary abstraction step

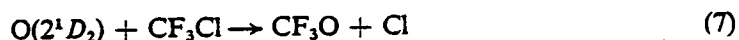


A second possibility is insertion into the C–Cl bond followed by fragmentation to yield ClO



444 REACTIONS OF $O(2^1D_2)$ AND $O(2^3P_J)$ WITH HALOGENOMETHANES

The third possibility is that Cl atoms are produced by a displacement reaction, followed by the fast reaction of Cl with O_3 , *i.e.*,



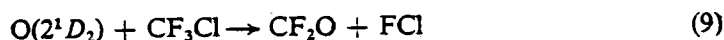
Under the conditions of our experiment it would be difficult to distinguish between these three mechanisms simply by observing the rate of formation of ClO as they are all very rapid. We can, however, use a chemical method to distinguish between the first two and the third mechanisms. By adding a small amount of ethane to mixtures of O_3 and CF_3Cl ($P_{C_2H_6} = 67 \text{ N m}^{-2}$), any Cl atoms formed in the primary step can be removed before reacting with O_3 ; the yield of ClO will then be reduced by an amount which depends on the yield of free chlorine atoms in the primary step. As the pressure of C_2H_6 used is very much lower than that of CF_3Cl it will not interfere by reacting with $O(2^1D_2)$ (>95 % of the excited oxygen atoms react with CF_3Cl). Our results show that the yield of ClO is only slightly reduced by addition of C_2H_6 and Cl atom formation accounts for ≤ 20 % of the total $O(2^1D_2)$ removal by CF_3Cl .

Quantitative yields of ClO were determined *via* the (5, 0) band of the $A^2\Pi \leftarrow X^2\Pi$ system¹¹ [see ref. (7) for a detailed discussion], and when these are compared with the amount of $O(2^1D_2)$ produced by the flash we find that 65 % of the excited oxygen gives rise to ClO formation in a primary step.

Measuring the yield of $O(2^3P_J)$ by time resolved photometry in the vacuum ultraviolet proved more difficult than first envisaged. Absorption by CF_3Cl reduced the intensity of the oxygen resonance line reaching the photomultiplier (the 130.6 nm line was used), as expected, however we also observed a change in the sensitivity with which $O(2^3P_J)$ could be detected; as the extent of absorption by CF_3Cl increased, the sensitivity for detecting $O(2^3P_J)$ decreased. Thus in order to measure the yield of $O(2^3P_J)$ quantitatively, new curves of growth were determined over a range of conditions under which the oxygen resonance lines were attenuated by an absorbing gas such as CF_3Cl .

For the present work relative $O(2^3P_J)$ concentrations were read directly from the appropriate curve of growth and the yield of $O(2^3P_J)$ formed by the quenching of $O(2^1D_2)$ by CF_3Cl was determined by comparing the concentrations produced in the absence and presence of excess N_2 [the N_2 quenches a large and calculable fraction of the $O(2^1D_2)$ directly to the ground state]. By this means the branching ratio for $O(2^3P_J)$ formation was determined as $30 \times \pm 19$ %. Typical conditions in these experiments were $P_{O_3} = 0.5 \text{ N m}^{-2}$, $P_{CF_3Cl} = 4.0 \text{ N m}^{-2}$, with a flash energy of 180 J.

The branching ratios for all the channels determined in this work are summarised in table 1. We also include a recent estimate^{12b} for the elimination channel^{12b}



which is seen to have a small branching ratio.

REACTION OF $O(2^1D_2)$ WITH CF_3Br AND CF_3I

Reaction of $O(2^1D_2)$ with CF_3Br results in the rapid formation of BrO; however the decay is also rapid and this makes the absolute determination of the BrO yield extremely difficult.⁷ Nevertheless we can obtain a useful lower limit for the yield of BrO and using the extinction coefficient given by Clyne *et al.*¹³ for the (4, 0) band of the $A^2\Pi-X^2\Pi$ system we find a branching ratio for BrO formation of >25 %. It should be noted that reaction between Br and O_3 is much slower than the corre-

sponding reaction for Cl atoms, and that we can therefore distinguish between BrO formed in a primary step and that formed by secondary reaction of Br with O₃.

Experiments to determine the yield of IO from reaction of O(2¹D₂) with CF₃I are considerably more difficult than the corresponding experiments with CF₃Cl and CF₃Br. A strong spectrum of IO is observed, however some photolysis of CF₃I occurs, (it absorbs in the same region as O₃) and it is known that iodine atoms react rapidly with O₃ to yield IO. Preliminary results from our laboratory show that spin-orbit excited

TABLE 1.—BRANCHING RATIOS FOR PRODUCT CHANNELS IN THE REMOVAL OF O(2¹D₂) BY HALOGENOMETHANES

reactant	products/%			
	quenching to O(2 ³ P ₁)	halogen oxide	halogen atom	other products
CF ₃ Cl	30 ± 10 %	65 ± 10 %	≤ 20 %	FCI (≈ 10 %)
CF ₂ HCl	28 ± 10 %*	55 ± 10 %	≤ 10 %	OH (5 %)
CF ₃ Br		> 25 %		

* Yield of O(2³P₁) based on CF₂ formation (*i.e.*, via the dissociative excitation channel yielding CF₂ + HCl + O) is 45 ± 10 %.

iodine atoms, I(5²P₁), react more rapidly with O₃ than ground state I(5²P_{3/2}) atoms; the rate constant for the ground state iodine atom reaction has been determined¹⁴ as $k = 0.8 \times 10^{-12} \text{ cm}^3 \text{ molecule}^{-1} \text{ s}^{-1}$. Thus IO can be formed by more than one reaction and detailed experiments are required to distinguish between the various possibilities. Our present results indicate that the yield of IO from reaction of O(2¹D₂) with CF₃I is substantial and we hope to report a quantitative measure for the branching ratio into this channel at the Discussion.

REACTION OF O(2¹D₂) WITH CF₂HCl

Strong transient spectra of ClO and CF₂ were observed following the photolysis of O₃ or N₂O in the presence of CF₂HCl ($P_{\text{O}_3} = 13.3 \text{ N m}^{-2}$; $P_{\text{CF}_2\text{HCl}} = 2.7 \text{ kN m}^{-2}$). Both spectra were completely suppressed by addition of excess N₂, showing that they resulted from reaction of O(2¹D₂) with CF₂HCl. Photolysis of CF₂HCl in the far-ultraviolet is known to produce CF₂, however this region is not transmitted by our equipment and CF₂ was not observed when CF₂HCl ($P_{\text{CF}_2\text{HCl}} = 2.7 \text{ kN m}^{-2}$) alone was flashed in the reaction vessel. The yield of ClO was measured as described for CF₃Cl and found to be 55 × 10 % of the initial O(2¹D₂) yield. Addition of small amounts of ethane to the system had no significant effect on the ClO yield, showing that Cl atom formation is of little importance (≤ 10 %) in the removal of O(2¹D₂) by CF₂HCl.

The yield of CF₂ was determined using the known extinction coefficient for the $\nu_2 = 6$ band (249 nm) of the $A^1B_1 \leftarrow X^1A_1$ system, given by Tyerman.¹⁵ The branching ratio into this channel was determined as 45 × 10 %.

The branching ratio for O(2³P₁) formation was measured using the method described above for CF₃Cl and found to be 28 ± 10 %, which suggests that both CF₂ and O(2³P₁) must be formed in the same process.

The formation of OH radicals was not observed using plate photometry, however we would expect OH to react rapidly with CF₂HCl under the conditions employed. Using the more sensitive technique of time resolved spectrophotometry at 308 nm

666 REACTIONS OF $O(2^1D_2)$ AND $O(3^3P_J)$ WITH HALOGENOMETHANES

($P_{CF_2HCl} = 2.0 \text{ kN m}^{-2}$, $P_{O_3} = 40 \text{ N m}^{-2}$) formation of OH was detected but in very low yield. A careful calibration of the system was achieved using the reactions of $O(2^1D_2)$ with H_2O and CH_4 . Assuming that H_2O gives two OH radicals for each $O(2^1D_2)$ atom reacting, the yield of OH from CH_4 was found to be 80 %, in good agreement with previous work.¹⁶ The yield of OH from CF_2HCl , based on the same method, was found to be only 5 %.

REACTION OF $O(2^3P_J)$ WITH CF_3I

The kinetics of $O(2^3P_J)$ removal by CF_3I were investigated using time-resolved spectrophotometry at 130 nm (the slit width used was $800 \mu\text{m}$ and thus the three atomic lines at 130.2, 130.5 and 130.6 nm were transmitted by the monochromator). By photolysing O_3 ($P_{O_3} = 1.33 \text{ N m}^{-2}$) in the presence of excess N_2 ($P_{N_2} = 800 \text{ N m}^{-2}$), suitable concentrations of $O(2^3P_J)$ could be generated ($\approx 3\%$ photolysis of O_3 occurred). The decay of the ground state oxygen atom under these conditions was found to be very slow, as expected. Addition of small partial pressures of CF_3I ($0.13\text{--}0.6 \text{ N m}^{-2}$) resulted in a marked increase in the rate of decay and by measuring the pseudo first-order rate coefficients for removal of $O(2^3P_J)$ over a range of CF_3I pressures (data are shown in fig. 2) the second order rate constant was determined as,

$$k_{O(2^3P_J) + CF_3I} = (1.1 \times 0.3) \times 10^{-11} \text{ cm}^3 \text{ molecule}^{-1} \text{ s}^{-1}.$$

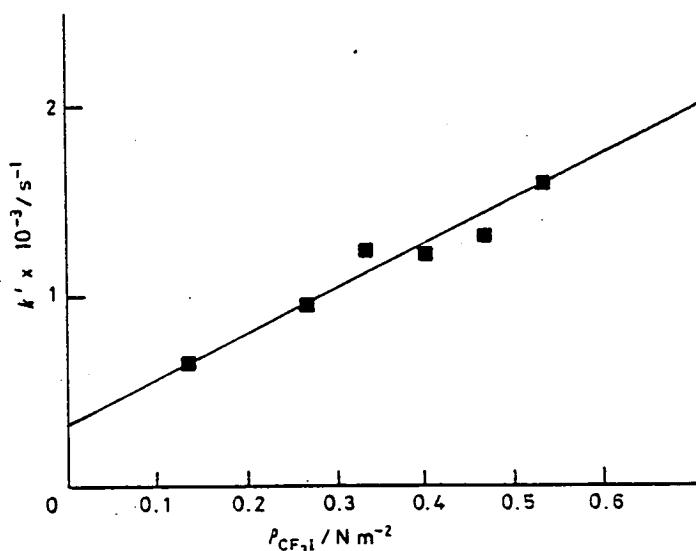


FIG. 2.—Plot of the first-order rate coefficients for removal of $O(2^3P_J)$ against partial pressure of CF_3I . ($P_{O_3} = 1.3 \text{ N m}^{-2}$; $P_{N_2} = 800 \text{ N m}^{-2}$).

A small correction¹⁷ was made for departure from Beer-Lambert behaviour and the slope of fig. 2 should be multiplied by 1.3 ($\gamma = 0.76$ based on the data in fig. 1) to obtain the rate constant given above.

Some photolysis of CF_3I will inevitably occur under the conditions used, however the percentage photolysis will be much less than that for O_3 (*i.e.*, $\ll 33\%$), due to the lower extinction coefficient for CF_3I , and should have no effect on the kinetics of the oxygen atom decay. As a check, further experiments were carried out over a range of flash energies (180–320 J). No significant difference in the decay rate for $O(2^3P_J)$

could be detected and we conclude that radical-radical reactions do not influence the observed kinetics and that photolysis of CF_3I is unimportant.

Some slow regeneration of $\text{O}(2^3P_j)$ will occur via the reaction of $\text{O}_2(a^1\Delta_g)$ with O_3 , but this is entirely negligible on the time scale used here.

DISCUSSION

REACTION OF $\text{O}(2^1D_2)$ WITH CF_3Cl , CF_3Br AND CF_3I

A major channel in the reactions of $\text{O}(2^1D_2)$ with halogenomethanes (excepting attack on C-F bonds)*, is clearly the formation of a halogen oxide molecule. We shall concentrate our discussion on the reaction with CF_3Cl , as the data for this molecule are most complete, but we expect the same general points to apply for CF_3Br and CF_3I .

Formation of ClO from CF_3Cl can in principle occur by two mechanisms, the more direct being abstraction of a chlorine atom. The second possible mechanism involves insertion of $\text{O}(2^1D_2)$ into the C-Cl bond, to form a vibrationally excited hypochlorite $\text{CF}_3\text{OCl}^\ddagger$, followed by fragmentation. CF_3OCl is a stable molecular species and its thermal and photochemical reactions have been examined. The results suggest that the favoured primary dissociation channel is formation of CF_3O and Cl (thermochemically this is the most favourable dissociation process). Thus if insertion of $\text{O}(2^1D_2)$ into C-Cl bonds was important, we would expect a high yield of Cl and not ClO , contrary to observations. Our results therefore suggest that ClO formation occurs by a direct abstraction mechanism. Similar behaviour has been reported previously for reactions of singlet methylene (CH_2), which is isoelectronic with $\text{O}(2^1D_2)$, with halomethanes.¹⁹⁻²² Thus, while both singlet methylene and $\text{O}(2^1D_2)$ undergo fast insertion reactions into C-H bonds, the main reaction channel with halogenomethanes involves direct abstraction.¹⁹⁻²²

The above behaviour can be understood when we consider the strong interaction that will occur between the vacant *p*-orbital of $\text{O}(2^1D_2)$ (or CH_2) and the lone pairs on the halogen atom. Thus the potential surface contains an attractive basin which surrounds the halogen atom and facilitates attack at this point in the molecule. A further attractive region must exist on the potential surface, corresponding to insertion of $\text{O}(2^1D_2)$ into the C-Cl bond (the minimum corresponding to the ground state configuration for CF_3OCl), however it appears that this region is less accessible, possibly due to inertial effects; both Cl and CF_3 are relatively heavy and need to move a substantial distance for insertion to occur (contrast this with the situation for C-H insertion where the much lighter H atom can move rapidly to accommodate the insertion process).

Our data also provide information on another aspect of the singlet potential surface discussed above. Thus the singlet surface must be sufficiently attractive to be crossed by one or more triplet surfaces correlating with $\text{O}(2^3P_j) + \text{CF}_3\text{Cl}$ and non-adiabatic transitions at these crossings must be favourable, as evidenced by the relatively high branching ratio for $\text{O}(2^3P_j)$ formation.

For $\text{O}(2^1D_2)$ interacting with CF_3I the singlet surface may pass below the asymptote for $\text{O}(2^3P_j) + \text{CF}_3\text{I}$ (fig. 3) and could therefore influence the dynamics of the reaction between $\text{O}(2^3P_j)$ with CF_3I (see below). Stable compounds with the structure RIO can be prepared (e.g., iodoxybenzene, $\text{C}_6\text{H}_5\text{IO}$) showing that the singlet surface has a very deep minimum in the region occupied by the lone pair electrons of iodine.

* Removal of $\text{O}(2^1D_2)$ is much slower by CF_x groups^{4,5} and appears to proceed entirely by quenching.¹⁸

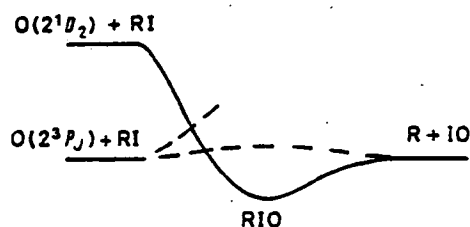
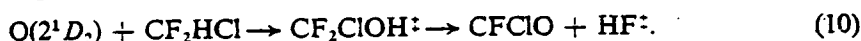


FIG. 3.—Section through the proposed potential surfaces for $O(2^3P_J)$ and $O(2^1D_2)$ interacting with an iodide. The lowest singlet surface is shown by the continuous line and the triplet surfaces by dashed lines.

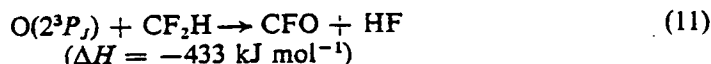
REACTION OF $O(2^1D_2)$ WITH CF_2HCl

Lin²³ has studied the photolysis of O_3 in the presence of a number of hydrogen containing halomethanes, including CF_2HCl , and observed stimulated emission from vibrationally excited hydrogen halide molecules formed in these systems. He proposed that this resulted from the insertion of $O(2^1D_2)$ into C—H bonds followed by the elimination of a vibrationally excited hydrogen halide molecule from the hot intermediate, *e.g.*,



With CF_2HCl , only HF emission was observed, although the formation of HCl is more exothermic. The present results clearly show that HF elimination cannot account for more than 10–20 %* of the total reaction cross-section and that elimination of ground state HCl is a more important process.

It seems unlikely that chemical laser emission would result from a minor reaction channel and an alternative explanation for Lin's result is that excited HF is produced by secondary radical reactions. In a separate series of studies, Lin²⁴ has suggested that the reaction,



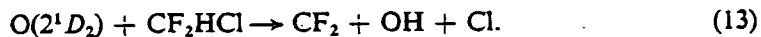
can give rise to HF laser emission. Our results show that both $O(2^3P_J)$ and CF_2H are major products of the interaction of $O(2^1D_2)$ with CF_2HCl and we therefore suggest that reaction (11) could account for Lin's observations in the $O_3 + CF_2HCl$ photochemical laser system.²³

The dominant channel in the interaction of $O(2^1D_2)$ with CF_2HCl is clearly that leading to the formation of ClO (55 %) and as the branching ratio is similar to that for CF_3Cl , we infer that the mechanism is the same.

The second most important channel involves dissociative excitation *viz.*,



This channel is thermoneutral within the bounds of current thermodynamic data ($\Delta H = 17 \times 19 \text{ kJ mol}^{-1}$) and it is surprising that it competes so effectively with the other highly exothermic channels. However, the observed rapid formation of CF_2 and $O(2^3P_J)$ cannot be accounted for by any other process. We have shown that Cl atom formation is unimportant (≤ 10 % of the total cross-section) which rules out reactions such as



* This is an upper limit based on the error bounds for the products which are directly observed.

This is further confirmed by the very low yield of OH(5 %) observed. CF_2 is known to be formed by the disproportionation reaction



however, this could only account at most for 10 % of the CF_2 observed as the dominant removal channel for two CF_2H radicals is dimerisation. We, therefore, conclude that dissociative excitation [reaction (12)] accounts for ≈ 40 % of the total cross-section. It is interesting to note that both the thermal and infrared multiphoton dissociation²⁵ of CF_2HCl lead to the formation of CF_2 and HCl. The other surprising feature is that $\text{O}(2^3P_J)$ escapes from the force field of CF_2 , as CF_2O is a very strongly bound molecule. This can however be understood when it is realised that $\text{CF}_2(X^1A_1)$ and $\text{O}(2^3P_J)$ do *not* correlate directly with the ground state of CF_2O , but with an excited triplet state which may not allow efficient combination.

The branching ratio for OH formation (5 %) is surprisingly low. From the bond additivity relationships suggested by Cvetanovic *et al.*³ and by Davidson *et al.*,⁵ we would expect OH formation to account for ≈ 30 % of the total cross section. This is clearly not the case and it appears that the distribution in the product channels does not follow the simple additivity relationship suggested for the total removal rates. The low yield of OH is in fact similar to the situation previously encountered with singlet methylene reactions where it was found that attack at C-H bonds was reduced to a very low level when a chlorine atom is present on the same, or adjacent, carbon atom.²⁶

REACTION OF $\text{O}(2^3P_J)$ WITH CF_3Br AND CF_3I

Reaction of $\text{O}(2^3P_J)$ with CF_3Br , to yield BrO , is strongly endothermic ($\Delta H = +65 \pm 5 \text{ kJ mol}^{-1}$) and negligibly slow at 300 K. However, the reaction has been studied at elevated temperatures (800-1200 K) and Arrhenius parameters determined²⁷ as $A = (1.5 \pm 0.5) \times 10^{-11} \text{ cm}^3 \text{ molecule}^{-1} \text{ s}^{-1}$ and $E_a = 57 \pm 4 \text{ kJ mol}^{-1}$. The activation energy for reaction is thus close to the endothermicity and the pre-exponential factor (A) is low when compared with reactions involving $\text{O}(2^1D_2)$. We shall return to the latter point after discussing the corresponding reaction with CF_3I .

The reaction of $\text{O}(2^3P_J)$ with CF_3I has been studied in some detail by Gorry *et al.*²⁸ using the molecular beam technique and has been shown to involve the formation of a weakly bound collision complex. The product scattering (IO) changes from a mainly backward, to a near isotropic distribution as the kinetic energy of the incident $\text{O}(2^3P_J)$ is increased. It was suggested²⁸ that at low collision energies the lifetime of the complex is shorter than its rotational period (as it is probably formed in low impact parameter collisions with low angular momentum). At higher collision energies the rotational period is reduced (higher angular momentum) and this leads to an increase in the forward scattering.

The total cross-section for reaction was not determined in the molecular beam work but a thermally averaged (300 K) cross-section can be obtained from the present data as $\sigma \approx 2 \text{ \AA}^2$. It is clear that the reaction must be close to thermoneutral and our results provide an upper limit for the activation energy of $E_a \leq 6 \text{ kJ mol}^{-1}$. When this is combined with the bond strength of CF_3I ,²⁹ $D(\text{CF}_3\text{-I}) = 221 \times 5 \text{ kJ mol}^{-1}$, we obtain a lower limit for the bond strength of IO as, $D_0(\text{IO}) \geq 210 \text{ kJ mol}^{-1}$, which is consistent with the value given earlier by Radlein *et al.*³⁰

We might expect the Arrhenius pre-exponential factor for reaction of $\text{O}(2^3P_J)$ with CF_3I to be similar to that for the analogous reaction with CF_3Br , and the fact that the rate constant (at 300 K) for $\text{O}(2^3P_J) + \text{CF}_3\text{I}$ is close to the pre-exponential factor for

000 REACTIONS OF $O(2^1D_2)$ AND $O(2^3P_J)$ WITH HALOGENOMETHANES

$O(2^3P_J) + CF_3Br$, suggests that this is probably the case. These values are surprisingly low when compared with the analogous reactions for $O(2^1D_2)$ (where any kinematic constraints should be the same), but appear to be characteristic of reactions involving $O(2^3P_J)$ with halogen, or halogen-containing molecules. As these reactions involve attractive potential surfaces and a bound collision complex we would normally expect a substantial reaction cross-section or large pre-exponential factor. It has been suggested that the low values observed result from a very restrictive reaction geometry and that a near collinear collision is required before reaction can occur.^{28,31} This was rationalized in terms of the molecular orbital structure for the collision intermediate which favours a linear O-X-Y structure for lowest energy on the triplet potential surface. However, the above discussion on the quenching of $O(2^1D_2)$ by halomethanes leads us to suggest an alternative explanation. We have seen that crossings between triplet and singlet surfaces must occur and that for iodoxy compounds one of these may be close to the dissociation asymptote for $O(2^3P_J) + RI$ (fig. 3). Thus the low reaction cross-section could result from a "low" triplet-singlet transition probability, while the scattering dynamics would be determined by the potential minimum in the singlet surface.

CONCLUSIONS

Reactions of $O(2^1D_2)$ with halomethanes proceed with a large total cross-section, the dominant channel being abstraction to yield a halogen oxide. The singlet potential surface, on which these reactions occur, is strongly attractive and is crossed by lower lying triplet surfaces correlating with $O(2^3P_J)$. This provides an efficient mechanism by which $O(2^1D_2)$ is quenched to the ground state.

The reactions of $O(2^1D_2)$ closely parallel those of singlet methylene.

Reactions of $O(2^3P_J)$ with halogenomethanes have relatively low total cross-sections (and Arrhenius pre-exponential factors) and may involve a triplet-singlet surface crossing.

- ¹ H. Yamazaki and R. J. Cvetanovic, *J. Chem. Phys.*, 1964, 41, 3703.
- ² A. J. Colussi and R. J. Cvetanovic, *J. Phys. Chem.*, 1975, 79, 1891.
- ³ P. Michaud, G. Paraskevopoulos and R. J. Cvetanovic, *J. Phys. Chem.*, 1974, 78, 1457.
- ⁴ I. S. Fletcher and D. Husain, *J. Phys. Chem.*, 1976, 80, 1837.
- ⁵ J. A. Davidson and H. I. Schiff, *J. Chem. Phys.*, 1978, 69, 4277.
- ⁶ H. M. Gillespie and R. J. Donovan, *Chem. Phys. Letters*, 1976, 37, 468.
- ⁷ H. M. Gillespie, J. Garraway and R. J. Donovan, *J. Photochem.*, 1977, 7, 29.
- ⁸ R. J. Donovan and D. J. Little, *Chem. Phys. Letters*, 1972, 13, 488.
- ⁹ D. D. Davis, J. T. Herron and R. E. Huie, *J. Chem. Phys.*, 1973, 58, 530.
- ¹⁰ C. Morley and I. W. M. Smith, *J.C.S. Faraday II*, 1972, 68, 1016.
- ¹¹ M. A. A. Clyne and J. A. Coxon, *Proc. Roy. Soc. A*, 1968, 303, 207.
- ¹² (a) J. Wolfrum and K. Kaufmann, personal communication; (b) R. J. Donovan, K. Kaufmann and J. Wolfrum, *Nature*, 1976, 262, 204.
- ¹³ M. A. A. Clyne and H. W. Cruse, *Trans. Faraday Soc.*, 1970, 66, 2214.
- ¹⁴ M. A. A. Clyne and H. W. Cruse, *Trans. Faraday Soc.*, 1970, 66, 2227.
- ¹⁵ W. J. R. Tyerman, *Trans. Faraday Soc.*, 1969, 65, 1188.
- ¹⁶ C-L Lin and W. B. DeMore, *J. Phys. Chem.*, 1973, 77, 863.
- ¹⁷ R. J. Donovan and H. M. Gillespie, *Reaction Kinetics* (Specialist Periodical Report, Chemical Society, London, 1975), 1, 14.
- ¹⁸ R. G. Green and R. P. Wayne, *J. Photochem.*, 1977, 6, 371.
- ¹⁹ D. W. Setser, R. Littrell and J. C. Hassler, *J. Amer. Chem. Soc.*, 1965, 87, 2062.
- ²⁰ C. H. Bamford, J. E. Casson and R. P. Wayne, *Proc. Roy. Soc. A*, 1966, 289, 287.
- ²¹ C. H. Bamford, J. E. Casson and A. N. Hughes, *Proc. Roy. Soc. A*, 1968, 306, 135.
- ²² R. L. Johnson and D. W. Setser, *J. Phys. Chem.*, 1967, 71, 4366.
- ²³ M. C. Lin, *J. Phys. Chem.*, 1972, 76, 1425.
- ²⁴ M. C. Lin, *Int. J. Chem. Kinetics*, 1973, 5, 173.

- ²⁵ J. C. Stephenson and D. S. King, *J. Chem. Phys.*, 1978, **69**, 1485.
- ²⁶ C. H. Bamford and J. E. Casson, *Proc. Roy. Soc. A*, 1969, **312**, 163.
- ²⁷ T. C. Frankiewicz, F. W. Williams and R. G. Gann, *J. Chem. Phys.*, 1974, **61**, 402.
- ²⁸ P. A. Gorry, C. V. Nowikow and R. Grice, *Chem. Phys. Letters*, 1978, **55**, 19.
- ²⁹ E. N. Okafo and E. Whittle, *Int. J. Chem. Kinetics*, 1975, **7**, 273.
- ³⁰ D. St. A. G. Radlein, J. C. Whitehead and R. Grice, *Nature*, 1975, **253**, 37.
- ³¹ D. D. Parrish and D. R. Herschbach, *J. Amer. Chem. Soc.*, 1973, **95**, 6133.